Genome-wide association study and functional characterisation identifies candidate genes for insulin-stimulated glucose uptake

Alice Williamson[1,2], Dougall M Norris[3], Xianyong Yin[4,5,6], K. Alaine Broadaway[7], Anne H Moxley[7], Swarooparani Vadlamudi[7], Emma P Wilson[7], Anne U Jackson[4,5], Vasudha Ahuja[8], Mette K Andersen[9], Zorayr Arzumanyan[10], Lori L Bonnycastle[11], Stefan R Bornstein[12,13,14], Maxi P. Bretschneider[12,13,14], Thomas A Buchanan[15], Yi-Cheng Chang[16,17,18], Lee-Ming Chuang[19], Ren-Hua Chung[20], Tine D Clausen[21,22], Peter Damm[22,23,24], Graciela E Delgado[25], Vanessa D de Mello[26], Josée Dupuis[27,28], Om P Dwivedi[8], Michael R Erdos[11], Lilian Fernandes Silva[29], Timothy M Frayling[30], Christian Gieger[31,14], Mark O Goodarzi[32], Xiuqing Guo[10], Stefan Gustafsson[33], Liisa Hakaste[8], Ulf Hammar[34], Gad Hatem[35], Sandra Herrmann[36,13], Kurt Højlund[37], Katrin Horn[38,39], Willa A Hsueh[40], Yi-Jen Hung[41], Chii-Min Hwu[42], Anna Jonsson[9], Line L Kårhus[43], Marcus E Kleber[44,45], Peter Kovacs[46], Timo A Lakka[47,48,49], Marie Lauzon[50], I-Te Lee[51,52,53], Cecilia M Lindgren[54,55,56,57], Jaana Lindström[58], Allan Linneberg[43,22], Ching-Ti Liu[27], Jian'an Luan[1], Dina Mansour Aly[35], Elisabeth Mathiesen[22,23,59], Angela P Moissl[60,61,44], Andrew P Morris[62], Narisu Narisu[11], Nikolaos Perakakis[12,13,14], Annette Peters[31,14], Rashmi B Prasad[35,8], Roman N Rodionov[63,64], Kathryn Roll[65], Carsten F Rundsten[9], Chloé Sarnowski[66], Kai Savonen[49], Markus Scholz[38,39], Sapna Sharma[67,68], Sara E Stinson[9], Sufyan Suleman[9], Jingyi Tan[10], Kent D Taylor[10], Matti Uusitupa[69], Dorte Vistisen[70,71], Daniel R Witte[72,73], Romy Walther[74,13], Peitao Wu[75], Anny H Xiang[76], Björn Zethelius[77], **The Meta-Analysis of Glucose and Insulin-related Traits Consortium (MAGIC)**, Emma Ahlqvist[35], Richard N Bergman[78], Yii-Der Ida Chen[50], Francis S Collins[11], Tove Fall[34], Jose C Florez[79,80,81], Andreas Fritsche[82], Harald Grallert[67,31,14], Leif Groop[83,8], Torben Hansen[9], Heikki A Koistinen[84,85,86], Pirjo Komulainen[49], Markku Laakso[29], Lars Lind[33], Markus Loeffler[38,39], Winfried März[87,25], James B Meigs[88,89,90], Leslie J Raffel[91], Rainer Rauramaa[49], Jerome I Rotter[92], Peter E. H. Schwarz[36,13,14], Michael Stumvoll[46], Johan Sundström[33], Anke Tönjes[46], Tiinamaija Tuomi[93,8], Jaakko Tuomilehto[94,95,96], Robert Wagner[82], Inês Barroso[97], Mark Walker[98], Niels Grarup[9], Michael Boehnke[4,5], Nicholas J Wareham[1], Karen L Mohlke*#[7], Eleanor Wheeler*#[1], Stephen O'Rahilly*#[3], Daniel J Fazakerley*#[3], Claudia Langenberg*#[1,99,100]

[1]MRC Epidemiology Unit, Institute of Metabolic Science, University of Cambridge School of Clinical Medicine, Cambridge, UK, [2]Metabolic Research Laboratories, Wellcome Trust-MRC Institute of Metabolic Science, Department of Clincial Biochemistry, University of Cambridge, Cambridge, UK, [3]Metabolic Research Laboratories, Wellcome Trust-MRC Institute of Metabolic Science, Department of Clinical Biochemistry, University of Cambridge, Cambridge, UK, [4]Department of Biostatistics, University of Michigan, Ann Arbor, MI, USA, [5]Center for Statistical Genetics, University of Michigan, Ann Arbor, MI, USA, [6]Department of Epidemiology, School of Public Health, Nanjing Medical University, Nanjing, Jiangsu 211166, China, [7]Department of Genetics, University of North Carolina, Chapel Hill, NC, USA, [8]Institute for Molecular Medicine Finland (FIMM), University of Helsinki, Helsinki, Finland, [9]Novo Nordisk Foundation Center for Basic Metabolic Research, Faculty of Health and Medical Sciences, University of Copenhagen, Copenhagen, Denmark, [10]Department of Pediatrics, Genomic Outcomes, The Institute for Translational Genomics and Population Sciences, The Lundquist Institute for Biomedical Innovation at Harbor-UCLA Medical Center, Torrance, CA, USA, [11]Center for Precision Health research, National Human Genome Research Institute,

National Institutes of Health, Bethesda, MD, USA, [12]Department of Internal Medicine III, Metabolic and Vascular Medicine, Medical Faculty Carl Gustav Carus, Dresden, Germany, [13]Helmholtz Zentrum München, Paul Langerhans Institute Dresden (PLID), University Hospital and Faculty of Medicine, TU Dresden, Dresden, Germany, [14]German Center for Diabetes Research (DZD e.V.), Neuherberg, Germany, [15]Department of Medicine, Division of Endocrinology and Diabetes, Keck School of Medicine USC, Los Angeles, CA, USA, [16]Graduate Institute of Medical Genomics and Proteomics, National Taiwan University, Taipei City, Taiwan, [17]Internal Medicine, National Taiwan University Hospital, Taipei City, Taiwan, [18]Institute of Biomedical Sciences, Academia Sinica, Taipei City, Taiwan, [19]Department of Internal Medicine, Division of Endocrinology and Metabolism, National Taiwan University Hospital, Taipei City, Taiwan, [20]Institute of Population Health Sciences, National Health Research Institutes, Miaoli County, Taiwan, [21]Department of Gynecology and Obstetrics, Nordsjaellands Hospital, Hilleroed, Denmark, [22]Department of Clinical Medicine, Faculty of Health and Medical Sciences, University of Copenhagen, Copenhagen, Denmark, [23]Center for Pregnant Women with Diabetes, Rigshospitalet, Copenhagen, Denmark, [24]Department of Obstetrics, Rigshospitalet, Copenhagen, Denmark, [25]Vth Department of Medicine, Medical Faculty Mannheim, Heidelberg University, Mannheim, BW, Germany, [26]Institute of Public Health and Clinical Nutrition, University of Eastern Finland, Kuopio, Finland, [27]Department of Biostatistics, Boston University School of Public Health, Boston, MA, USA, [28]Department of Epidemiology, Biostatistics and Occupational Health, McGill University, Montréal, Quebec, Canada, [29]Institute of Clinical Medicine, University of Eastern Finland, Kuopio, Finland, [30]University of Exeter Medical School, University of Exeter, Exeter, UK, [31]Institute of Epidemiology II, Helmholtz Zentrum München-German Research Center for Environmental Health, Neuherberg, Germany, [32]Department of Medicine, Division of Endocrinology, Diabetes & Metabolism, Cedars-Sinai Medical Center, Los Angeles, CA, USA, [33]Department of Medical Sciences, Clinical Epidemiology, Uppsala University, Uppsala, Sweden, [34]Department of Medical Sciences, Molecular Epidemiology, Uppsala University, Uppsala, Sweden, [35]Clinical Sciences Malmö, Genomics, Diabetes and Endocrinology, Lund University, Malmö, Sweden, [36]Department of Internal Medicine III, Prevention and Care of Diabetes, Medical Faculty Carl Gustav Carus, Dresden, Germany, [37]Steno Diabetes Center Odense, Odense University Hospital, Odense, Denmark, [38]Medical Faculty, Institute for Medical Informatics, Statistics and Epidemiology, Leipzig, Germany, [39]LIFE Research Center for Civilization Diseases, Medical Faculty, Leipzig, Germany, [40]Internal Medicine, Endocrinology, Diabetes & Metabolism, The Ohio State University Wexner Medical Center, Columbus, OH, USA, [41]Institute of Preventive Medicine, National Defense Medical Center, New Taipei City, Taiwan, [42]Department of Medicine, Section of Endocrinology and Metabolism, Taipei Veterans General Hospital, Taipei City, Taiwan, [43]Center for Clinical Research and Prevention, Copenhagen University Hospital – Bispebjerg and Frederiksberg, Copenhagen, Denmark, [44]Vth Department of Medicine, Medical Faculty Mannheim, Heidelberg University, Mannheim, Germany, [45]SYNLAB MVZ Humangenetik Mannheim, Mannheim, Germany, [46]Medical Department III-Endocrinology, Nephrology, Rheumatology, University of Leipzig Medical Center, Leipzig, Germany, [47]Institute of Biomedicine, School of Medicine, University of Eastern Finland, Kuopio, Finland, [48]Department of Clinical Physiology and Nuclear Medicine, Kuopio University Hospital, Kuopio, Finland, [49]Foundation for Research in Health Exercise and Nutrition, Kuopio Research Institute of Exercise Medicine, Kuopio, Finland, [50]Department of Pediatrics, Genomic Outcomes, The Institute for Translational Genomics and Population Sciences, The Lundquist Institute at Harbor-UCLA Medical Center, Torrance, CA, USA, [51]Department of Internal

Medicine, Division of Endocrinology and Metabolism, Taichung Veterans General Hospital, Taichung City, Taiwan, [52]School of Medicine, National Yang Ming Chiao Tung University, Taipei City, Taiwan, [53]School of Medicine, Chung Shan Medical University, Taichung City, Taiwan, [54]Big Data Institute, Li Ka Shing Centre for Health Information and Discovery, University of Oxford, Oxford, UK, [55]Nuffield Department of Population Health, University of Oxford, Oxford, UK, [56]Wellcome Trust Centre Human Genetics, University of Oxford, Oxford, UK, [57]Broad Institute, Cambridge, MA, USA, [58]Finnish Institute for Health and Welfare, Helsinki, Finland, [59]Department of Endocrinology, Rigshospitalet, Copenhagen, Denmark, [60]Institute of Nutritional Sciences, Friedrich-Schiller-University, Jena, Germany, [61]Competence Cluster for Nutrition and Cardiovascular Health (nutriCARD) Halle-Jena, Jena, Germany, [62]Centre for Genetics and Genomics Versus Arthritis, Centre for Musculoskeletal Research, The University of Manchester, Manchester, UK, [63]Department of Internal Medicine III, University Center for Vascular Medicine, Medical Faculty Carl Gustav Carus, Dresden, Germany, [64]College of Medicine and Public Health, Flinders University and Flinders Medical Centre,, Adelaide, Australia, [65]Pediatrics, Genomic Outcomes, The Institute for Translational Genomics and Population Sciences, The Lundquist Institute for Biomedical Innovation at Harbor-UCLA Medical Center, Torrance, CA, USA, [66]Epidemiology, Human Genetics & Environmental Sciences, The University of Texas Health Science Center, Houston, TX, USA, [67]Research Unit of Molecular Epidemiology, Helmholtz Zentrum München-German Research Center for Environmental Health, Neuherberg, Germany, [68]Chair of Food Chemistry and Molecular and Sensory Science, Technical University of Munich, Freising-Weihenstephan, Germany, [69]Department of Public Health and Clinical Nutrition, University of Eastern Finland, Kuopio, Finland, [70]Clinical Research, Steno Diabetes Center Copenhagen, Herlev, Denmark, [71]Department of Public Health, University of Copenhagen, Copenhagen, Denmark, [72]Steno Diabetes Center Aarhus, Aarhus, Denmark, [73]Department of Public Health, Aarhus University, Aarhus, Denmark, [74]Department of Internal Medicine III, Pathobiochemistry, Medical Faculty Carl Gustav Carus, Dresden, Germany, [75]Department of Biostatistics, Boston University School of Public Health, Boston, MA, 2118, [76]Research & Evaluation, Division of Biostatistics, Kaiser Permanente Southern California, Pasadena, CA, USA, [77]Public Health and Caring Sciences, Geriatrics, Uppsala University, Uppsala, Sweden, [78]Diabetes and Obesity Research Institute, Cedars-Sinai Medical Center, Los Angeles, CA, USA, [79]Diabetes Unit and Center for Genomic Medicine, Massachusetts General Hospital, Boston, MA, USA, [80]Programs in Metabolism and Medical & Population Genetics, Broad Institute, Cambridge, MA, USA, [81]Department of Medicine, Harvard Medical School, Harvard Medical School, Boston, MA, USA, [82]Department of Internal Medicine IV, University Hospital Tübingen, Tübingen, Germany, [83]Clinical Sciences Malmö, Genomics, Diabetes and Endocrinology, Lund University, Lund, Sweden, [84]Department of Public Health and Welfare, Finnish Institute for Health and Welfare, Helsinki, Finland, [85]Department of Medicine, University of Helsinki and Helsinki University Hospital, Helsinki, Finland, [86]Minerva Foundation Institute for Medical Research, Helsinki, Finland, [87]Synlab Academy, SYNLAB Holding Deutschland GmbH, Mannheim, BW, Germany, [88]Department of Medicine, Division of General Internal Medicine, Massachusetts General Hospital, Boston, MA, USA, [89]Department of Medicine, Harvard Medical School, Boston, MA, USA, [90]Programs in Metabolism and Medical & Population Genetics, The Broad Institute, Cambridge, MA, USA, [91]Department of Pediatrics, Genetic and Genomic Medicine, University of California, Irvine, CA, USA, [92]The Institute for Translational Genomics and Population Sciences, Department of Pediatrics, The Lundquist Institute for Biomedical Innovation at Harbor-UCLA Medical Center, Torrance, CA, USA, [93]Folkhälsan Research Center, Helsinki,

Finland, [94]Department of Public Health, University of Helsinki, Helsinki, Finland, [95]Population Health Unit, Finnish Institute for Health and Welfare, Helsinki, Finland, [96]Diabetes Research Group, King Abdulaziz University, Jeddah, Saudi Arabia, [97]Exeter Centre of Excellence for Diabetes Research (EXCEED), Genetics of Complex Traits, University of Exeter Medical School, University of Exeter, Exeter, UK, [98]Faculty of Medical Sciences, Newcastle University, Newcastle upon Tyne, UK, [99]Computational Medicine, Berlin Institute of Health at Charité–Universitätsmedizin, Berlin, Germany, [100]Precision Healthcare University Research Institute, Queen Mary University of London, London, UK.
# corresponding author * contributed equally.

Corresponding Authors:
Claudia Langenberg: claudia.langenberg@qmul.ac.uk
Stephen O'Rahilly: so104@medschl.cam.ac.uk
Daniel J Fazakerley: djf72@cam.ac.uk
Eleanor Wheeler: eleanor.wheeler@mrc-epid.cam.ac.uk
Karen L Mohlke: karen_mohlke@med.unc.edu

Abstract

Distinct tissue-specific mechanisms mediate insulin action in fasting and postprandial states. Previous genetic studies have largely focused on insulin resistance in the fasting state, where hepatic insulin action dominates. Here we studied genetic variants influencing insulin levels measured 2 hours after a glucose challenge in >55,000 participants from three ancestry groups. We identified 10 novel loci ($P<5x10^{-8}$) not previously associated with post-challenge insulin resistance, 8 of which were shown to share their genetic architecture with type 2 diabetes in colocalization analyses. We investigated candidate genes at a subset of associated loci in cultured cells and identified 9 candidate genes newly implicated in the expression or trafficking of GLUT4, the key glucose transporter in postprandial glucose uptake in muscle and fat. By focusing on post-prandial insulin resistance, we highlight mechanisms of action at T2D loci that are not adequately captured by studies of fasting glycaemic traits.

Introduction

Insulin resistance is a state in which higher than normal levels of circulating insulin are required to maintain glucose homeostasis and compensate for decreased insulin sensitivity of key organs involved in metabolic control – liver, muscle, and fat[1]. If the pancreas fails to maintain the elevated insulin supply and glucose uptake into these tissues becomes insufficient, hyperglycaemia and impaired glucose tolerance can subsequently lead to the development of T2D[2] and related cardiometabolic disorders[1].

The mechanisms and tissues of action of insulin action are distinct in the fasting and postprandial state and therefore the aetiology of insulin resistance in the fasting and fed state differs across tissues. Most genetic studies of common forms of insulin resistance have focused on the fasting state, which largely reflects hepatic insulin sensitivity .[3–5]In the liver, insulin controls the expression and post translational modification of genes controlling glycogenolysis and gluconeogenesis, thereby supressing hepatic glucose output and the promotion of glycogen synthesis.[6–8] Postprandially, insulin rapidly stimulates the translocation of an intracellular pool of the glucose transporter GLUT4 (encoded by *SLC2A4*) to the cell surface in muscle and fat [9–11] Insulin resistance is associated with lower GLUT4 expression and translocation in adipose tissue[12], and impaired GLUT4 translocation in muscle . [13] This postprandial distrubance in insulin action has been identified to be one of the key initating steps to onset of T2D[14], however the genetic underprinnings of this have been understudied.

There are currently only a few examples of loss of function coding variants that contribute to tissue-specific changes in postprandial insulin action. A loss of function mutation in *TBC1D4*, encoding a Rab-GTPase activating protein involved in control of GLUT4 translocation[15], was first reported to co-segregate with severe isolated post-prandial hyperinsulinaemia in a single family[16]. Subsequently a different loss of function mutation in a muscle specific isoform of *TBC1D4* was found to be common in Inuit populations with carriers having selective postprandial hyperglycaemia and hyperinsulinemia[17,18]. Thus, deeper understanding of the genetic architecture of tissue-specific insulin resistance in the fed state is needed to further the understanding of this process in T2D aetiology.

The gold standard method of measuring insulin resistance in these GLUT4-expressing tissues is the hyperinsulinemic-euglycaemic clamp combined with isotope-based measurement of glucose clearance. Such measures are not readily available at the scale required for robust genome-wide analyses[19,20]. Proxy measures derived from insulin and glucose measured during an oral glucose tolerance test (OGTT) have been developed[21,22], and are available in much greater numbers.

Here, we studied two OGTT-derived measures of insulin resistance after a glucose challenge (subsequently referred to as post-challenge insulin resistance) to identify genetic variants underlying these traits in a genome-wide meta-analysis (GWAS) of >55,000 participants without diabetes from 3 ancestry groups across 28 studies. These measures were the Modified Stumvoll Insulin Sensitivity Index (ISI) and the fold-change in insulin concentration (insulin fold-change; IFC) following an OGTT.

IFC reflects the relationship between fasting and post challenge plasma insulin Higher IFC values suggest more insulin is required to lower blood glucose after a standard glucose load and is therefore indicative of post-challenge insulin resistance This is dramatically increased in carriers of loss of function mutations in *TBC1D4* that impair glucose transporter translocation[16–18]. IFC therefore can be leveraged as an index of post-challenge, rather than fasting, insulin resistance.

ISI incorporates measures of insulin and glucose during an OGTT and has been demonstrated to approximate hyperinsulinemic-euglycaemic measures of whole-body insulin sensitivity[22]. Lower values of ISI reflect greater insulin resistance. Previous meta-analysis efforts have examined the genetic architecture of ISI[23,24]. Whilst no genome wide significant loci were identified by Dimas *et al* (2014)[24], Walford *et al* (2016) identified 3 loci significantly associated with ISI ($P < 5x10^{-8}$; N = 16,753) [23]. These include *BCL2* (rs12454712) and *NYAP2* (rs13422522; in Linkage Disequilibrium (LD) with previously known *IRS1* locus rs2943641). The *FAM19A2* locus (rs10506418) was identified to be significantly associated only in an interaction model testing the effect of genotype on ISI by body mass index (BMI), which we have not explored

in this present study.[23] Our expanded meta-analysis is >3x increased in sample size from this previous meta-analysis [23].

Using a genetically driven approach, we identified 9 novel genetic loci specifically implicated in post-challenge insulin resistance in cohorts of European ancestry. This includes 4 novel loci for post-challenge insulin resistance significantly ($P < 5x10^{-8}$) associated with IFC and 6 novel loci for post-challenge insulin resistance associated with ISI, with one locus associated with both traits. We systematically selected 36 genes from each locus associated with IFC and assessed the functional impact of reducing the expression of candidate genes from each locus in an insulin responsive cell-based reporter system that examines the translocation and abundance of GLUT4 protein (**Extended Data Figure 1**). This approach identified 9 candidate genes not previously implicated in insulin-regulated glucose uptake.

Results

Overview

Modified Stumvoll Insulin Sensitivity Index (ISI) and insulin fold change (IFC) were highly correlated with post-challenge measures of glucose and insulin during an OGTT in the Fenland study but were shown to capture different aspects of post-challenge insulin resistance suggesting value in studying both traits in parallel (See **Supplementary Note, Extended Data Figure 2, Supplementary Table 4).** In the RISC study we assessed the correlation of OGTT derived ISI and IFC with the clamp-based measure of insulin sensitivity M/I, which represents the amount of glucose metabolized per unit of plasma insulin during the clamp[25]. We identified significant observational correlations of both OGTT-derived traits with this clamp-derived measure of insulin sensitivity (ISI vs M/I Spearman's rho = 0.522, P = 5.10×10^{-76}; IFC vs M/I rho = -0.180, P = 3.29×10^{-9}; **Extended Data Figure 3, Supplementary Note; Supplementary Table 5**). Therefore, we can approximate clamp-based measures with OGTT indices available in a greater number of studies. The weaker correlations with IFC and M/I is expected, with M/I being reflective of whole-body insulin sensitivity and not specifically post-challenge insulin sensitivity which IFC captures more explicitly. ISI and IFC were moderately correlated in the Fenland (IFC vs ISI Spearman's rho = -0.375, P < 1×10^{-300}) and RISC studies (IFC vs ISI Spearman's rho = -0.458, P = 3.14×10^{-57}). Therefore, ISI and IFC capture similar phenotypes, but also differing aspects of post-challenge insulin resistance, suggesting there is value in studying both traits in parallel.

In this study we assessed the genetic architecture of post-challenge insulin resistance through meta-analysis of GWAS from a total of 28 studies of European, Hispanic American, and East Asian ancestry (**Extended Data Figure 4; Supplementary Tables 1- 3**). We conducted ancestry specific fixed effect meta-analysis, with the primary analysis presented being the meta-analysis only of cohorts of European ancestry for IFC and ISI, adjusted for BMI. We additionally conducted random effects multi-ancestry meta-analysis across all ancestries as well as the 3 cohorts of East Asian and Hispanic American ancestry without cohorts of European ancestry.

Genetic discovery of post-challenge insulin resistance

We identified 11 genome-wide significant loci ($P < 5x10^{-8}$) across both ISI and IFC in analyses adjusted for BMI in individuals without diabetes from 25 studies of European ancestry (**See methods, Table 1, Supplementary Figures 1-4**). Nine of these associations were not previously reported for post-challenge insulin resistance. Four of these loci, all not previously implicated in post-challenge insulin resistance, were significantly associated with IFC (N = 52,474; *SLC2A4, PPP1R3B, C2CD4A* and *MTNR1B;* **Figure 1; Table 1; Supplementary Figures 3, 4 and 6; Supplementary Table 6 and 7**). The remaining loci were associated with ISI, including 6 loci not previously implicated in post-challenge insulin resistance: *MTOR, COBLL1, PPARG, C5orf67, FAM101A, SLC2A4*. We replicated 2 previously-identified ISI loci at *IRS1* and *BCL2* (**Figure 1; Table 1; Supplementary Figures 1, 2 and 5; Supplementary Table 6 and 7**).[23] Exact conditional analysis revealed 2 distinct signals at *PPP1R3B* for IFC*,* with no additional signals identified at other loci for either trait (**Table 1; Extended Data Figure 5 ; Supplementary Tables 6 and 7**). The *SLC2A4* (rs117643180) locus was the only locus significantly associated with both ISI and IFC (**Supplementary Table 6 and 7)**.

We conducted fine mapping to define 99% credible sets that accounted for ≥99% of the posterior probability of association (PPA) for each of the 12 independent association signals (**Supplementary Tables 8 and 9**). At *SLC2A4* the 99% credible set included a single variant for ISI and 2 variants for IFC, with high confidence that rs117643180 is the candidate causal variant (IFC PPA for rs117643180 = 0.938; ISI PPA for rs117643180 = 0.985).

To fully assess the effect of adiposity, we repeated analyses without adjusting for BMI. IFC associations were largely unaffected by BMI adjustment (effect size R^2 BMI adjusted vs BMI unadjusted = 0.98; **Supplementary Figure 3 and 4, Supplementary Table 6 and 7**). In contrast, for ISI, adjusted and unadjusted beta estimates were moderately correlated (Pearson correlation between betas = 0.78**,** but significance levels were weaker in BMI unadjusted models, as previously reported for other glycaemic traits[3], with only *IRS1* and *SLC2A4* remaining significant at $P < 5x10^{-8}$ (**Supplementary Figure 1 and 2, Supplementary Table 6 and 7)**.

With 25 of 28 studies recruited being of European ancestry, 97% of total sample size, we did not identify additional loci in our multi-ancestry meta-analysis including all cohorts

(**Supplementary Table 7; Supplementary Figures 7-10**). All 11 loci identified in the European only analyses remained genome wide significant ($P < 5x10^{-8}$) (**Supplementary Figures 7-10**). Further, no loci were identified at genome wide significance in ancestry-specific analyses of cohorts of Hispanic American or East Asian ancestry for IFC or ISI. Therefore, to increase power, we conducted a random effects meta-analysis of studies of Hispanic American and East Asian ancestry (**Supplementary Figures 11-14; Supplementary Table 6**). This identified *BICC1* (rs60453193, beta = 0.43, SE = 0.08, $P = 4.06x10^{-8}$, N = 1,837) as a signal associated with IFC **(see Methods; Supplementary Note, Supplementary Table 7; Extended Data 6 and 7).** This locus has not been implicated in post-challenge insulin resistance previously and no significant association was seen in cohorts of European ancestry (beta = -0.0026, SE = 0.01, p = 0.80, N = 50,671), despite the lead variant being common in all three ancestry groups (**Supplementary Note**). Ancestry-specific loci with such effects have been identified previously for glycaemic traits, and it is possible that heterogeneous effect sizes despite similar EAF may be due to genotype-by-environment interactions or other epistatic effects (Supplementary Note).[3] Further, the variants detected here may be in LD with ancestry specific causal variants that were not investigated in this study and differ in frequency across ancestries.[3]

Genetic colocalisation with type 2 diabetes

We identified strong evidence of a shared genetic signal between post-challenge insulin resistance and T2D[26] for 10 of the 11 loci identified through meta-analysis of GWAS from studies of European ancestry, using statistical colocalisation methods (posterior probability of colocalisation > 0.7; **Supplementary Table 10**), providing strong evidence of a shared genetic signal underlying both post-challenge insulin resistance and T2D at each of these loci. Of the 11 loci, 8 loci were associated with T2D at genome wide significance and 2 loci at the suggestive significance threshold of $P < 1x10^{-4}$ (**Supplementary Table 6**)[26]. Even though the *SLC2A4* lead variant (rs117643180) was associated with an increased risk of T2D at nominal significance (beta = 0.046, SE = 0.015, P = 0.0018, N = 1,041,200, OR = 1.047) [26], this was the only post-challenge insulin resistance locus identified in European ancestry cohorts without evidence of a shared signal with T2D using formal colocalisation testing. rs117643180 is in perfect linkage disequilibrium (LD; D' = 1) with lead SNPs at T2D loci identified in East Asian

and Hispanic American ancestries. Several reasons may contribute to lack of colocalisation for example differences in the allele frequency and ancestry composition considered in the respective GWAS efforts (discussed further in **Supplementary Note, Supplementary Figures 15 and 16, Supplementary Table 11**). Further, it is possible that rs117643180 is the causal variant underlying differences in post-challenge insulin resistance but is not sufficient to cause T2D unless accompanied by beta cell dysfunction. The IFC *BICC1* locus identified in our meta-analysis of Hispanic American and East Asian ancestry cohorts also showed no evidence of a shared signal with T2D.

Using LD score regression and genetic risk score analyses, we identified significant associations between an increased genetic risk for post-challenge insulin resistance and a range of biochemical and cardiometabolic traits (**Supplementary Note; Supplementary Tables 13-16**). Using LDSC-SEG we further identified tissue-specific enrichment of IFC and ISI loci in regulatory regions in T2D relevant tissues (muscle, adipose, pancreas and liver) (**Supplementary Note, Supplementary Tables 21-24**)

rs117643180 (*SLC2A4*) affects transcriptional regulation in muscle

The only locus we identified at genome-wide significance for both ISI and IFC was *SLC2A4* (rs117643180). *SLC2A4* encodes GLUT4, the insulin-dependent glucose transporter responsible for postprandial glucose uptake into muscle and adipose tissues. rs117643180 was associated with post-challenge insulin resistance and was previously reported to be associated with higher 2 h glucose (Beta = 0.19, SE = 0.025, P = 7.31×10^{-14}, N = 38,302)[3] but not fasting insulin (P = 0.22)[3] or fasting glucose (P = 0.14)[3] suggesting the effect of this locus is specific to the postprandial state (**Figure 2**). This is, to our knowledge, the first time a post-challenge insulin resistance trait association has been reported at this locus.

rs117643180 is additionally in a region of accessible muscle chromatin since it overlaps with enhancer or promoter annotations in skeletal muscle, and adipose tissues (**Figure 2c**) and lies within a region of high conservation within intron 1 of *SLC2A4*. Together, these features suggest that rs117643180 is in a region of importance for *SLC2A4* gene regulation. In humans, *SLC2A4* expression is high in skeletal muscle relative to other tissues.[27,28] rs117643180 is the

lead SNP at a primary expression quantitative trait locus (eQTL) for *SLC2A4* expression in skeletal muscle, with the effect allele (A) associated with lower expression of *SLC2A4* mRNA (GTEx v8, European ancestry samples (EUR); NES (normalised effect size) = -0.50, SE = 0.073, $P = 2.51x10^{-11}$).[29]

These data suggested altered GLUT4 levels in muscle tissue may underlie the associations of rs117643180 with post-challenge insulin resistance and its post-challenge specific glycaemic effect is due to impact on expression of *SLC2A4* mRNA [27,30].

We identified perfect colocalisation of the *SLC2A4* eQTL signal at rs117643180 in skeletal muscle with both IFC and ISI when conditioning on a secondary eQTL signal (rs222849) at this locus (posterior probability of colocalisation IFC/eQTL = 1.00, posterior probability of colocalisation ISI/eQTL = 1.00; **Supplementary Table 17, Supplementary Figure 17**). This colocalisation is specific to the primary eQTL signal for *SLC2A4* at rs117643180, the same genetic signal associated with IFC and ISI (**Supplementary Table 17**).

To determine whether rs117643180 exhibits allelic differences in transcriptional activity, we performed transcriptional reporter assays in murine C2C12 and human LHCN-M2 muscle cell lines using 229-bp fragments in forward and reverse orientations with respect to a minimal promoter. In all cell types, the fragment showed higher transcriptional activity than an empty vector control, especially in the forward orientation, consistent with a role as a promoter or enhancer (**Figure 2D-E, Supplementary Figure 18**). In mouse C2C12 myoblasts, the rs117643180-A effect allele showed half the transcriptional activity as the reference C allele in both orientations ($P < 0.002$) (**Figure 2D**). Similar results were observed in human LHCN-M2 myoblasts and myotubes (**Figure 2E, Supplementary Figure 18)**. The lower transcriptional activity observed for the rs117643180-A allele is consistent with the GTEx v8 eQTL analysis of *SLC2A4* in skeletal muscle tissue.[29] In addition, we carried out electrophoretic mobility shift assays using LHCN-M2 nuclear extract and probes spanning the rs117643180 alleles. These assays provided supporting evidence for allelic differences in transcription factor binding (**Extended Data Figure 8**). Taken together, these data suggest that rs117643180 may contribute to allele-specific differences in *SLC2A4* transcriptional activity in skeletal muscle.

Genes implicated in insulin-stimulated glucose transport

IFC was identified to be associated with 4 loci at genome wide significance in our meta-analysis of studies of European ancestry. This included the *SLC2A4* locus directly implicating the encoded protein GLUT4. IFC further appears more specific to the post-challenge insulin resistance observationally, with IFC being more strongly correlated than ISI with 2 h measures of insulin and glucose in the Fenland Study (**Supplementary Table 2, Extended Data Figure 2**). Therefore, we reasoned that further study of genes at genetic loci associated with IFC, may identify additional novel genes involved in insulin-stimulated glucose disposal.

Since no such systematic follow up of genes at genetic loci associated with post-challenge insulin resistance has been reported previously, we used an inclusive approach to prioritise genes for screening their effects on GLUT4 and glucose transport in cultured cells (**Extended Data Figure 1**). In addition to selecting 12 genes at the 4 genome-wide IFC loci, we prioritised a further 24 genes at 4 'subthreshold' loci at $5x10^{-8} < P < 5x10^{-5}$) that displayed a clear post-challenge specific insulin resistance association signature (**See methods; Supplementary Note; Supplementary Table 19 and 20, Supplementary Figure 19 and 20**). A total of 36 genes were selected following this strategy and we assessed the impact of siRNA gene knockdown on insulin-stimulated GLUT4 translocation in two 3T3-L1 adipocyte cell lines (**Methods, Supplementary Figure 21 and 22, Supplementary Table 26**).

This approach identified 4 of the 36 genes-of-interest already implicated in insulin signalling and GLUT4 trafficking significantly altered cell surface GLUT4 abundance (FDR < 5%): *Irs1*[31], *Lnpep*[32], *Tnks*[33,34] and *Vps13c*[35], as well as GLUT4 itself (*Slc2a4*) (**Supplementary Tables 28 and 29**). We identified a further 9 genes (*Alkbh5, Cmpk1, Drg2, Flii, Llgl1, Pdzk1ip1, Slc36a4, Toml12, Tvp23b*) whose siRNA knockdown significantly (FDR < 5%) altered absolute cell surface GLUT4 abundance and/or the ratio of cell surface GLUT4-to-total GLUT4 protein upon insulin stimulation, indicative of dysfunctional insulin-stimulated GLUT4 translocation (**Supplementary Tables 28 and 29**). To our knowledge, these genes have not been previously implicated in insulin action or GLUT4 trafficking and warrant further mechanistic investigation. The 14 genes identified to be implicated in GLUT4 trafficking are located across

8 IFC loci. Three of these genes were located at genome-wide loci and 11 from prioritised subthreshold loci. (**Supplementary Table 30**).

siRNA knockdown of 7 of the 9 novel genes also altered insulin-stimulated 2-deoxyglucose (2DOG) uptake in a directionally consistent manner to their observed effects on cell surface GLUT4 (**Supplementary Figure 21 and 24; Supplementary Table 33)**. For example, knockdown of *Alkbh5, Cmpk1, Drg2, Ppp1r11, Slc36a4, Tom1l2,* and *Tvp23b* decreased cell surface GLUT4 and 2DOG uptake (**Figure 3a, c**) Conversely, *Pdzk1ip1* knockdown increased cell surface GLUT4 and 2DOG uptake (**Figure 3a, d)**. Only *Flii* and *Llgl1* knockdown resulted in inconsistent effects on cell surface GLUT4 and 2DOG uptake, with increased cell surface GLUT4 but lower 2DOG uptake (**Figure 3a**).

Discussion

The impairment of insulin's ability to control glucose metabolism, or insulin resistance, is a major contributor to a range of metabolic and endocrine disorders including T2D. Previous studies of the genetic determinants of insulin resistance in humans without diabetes have predominantly used fasting samples of glucose and insulin, levels of which are largely determined by hepatic insulin sensitivity. Here, we used measures that reflect, at least in part, insulin's important postprandial action on glucose uptake into muscle and adipose tissue. These traits act as valuable proxies of postprandial insulin resistance which are more readily scalable to population-based genetic studies than gold standard measures. Using this approach, we identified 9 loci not previously associated with post-challenge insulin resistance in studies of European ancestry, including *SLC2A4*, which encodes the glucose transporter implicated in insulin-stimulated glucose disposal. We further identified *BICC1* associated with IFC in a meta-analysis of cohorts of Hispanic American and East Asian ancestries.

The glucose transporter GLUT4 (encoded by *SLC2A4*) is enriched in muscle and fat but not present in liver. In response to insulin (and exercise in skeletal muscle), GLUT4 rapidly translocates from an intracellular pool to the cell surface to facilitate glucose uptake.[36] Genetic ablation of GLUT4 in mice results in severe postprandial insulin resistance, hyperinsulinemia, and hyperglycaemia.[37] Our results demonstrate that genetic variation directly influencing *SLC2A4* expression has a significant impact on human postprandial insulin action.

We also identified loci near genes directly implicated in insulin signalling including *IRS1 (reviewed in*[38]*)* and others near genes known to be involved more broadly in insulin sensitivity including *PPARG*[39]*, PPP1R3B*[40,41]*,* and *MTOR*[42]. The observation that 10 of the 11 loci we identified in European ancestry populations are additionally associated with increased T2D risk highlights the importance of insulin resistance in T2D pathogenesis and provides evidence of potential mechanisms behind the T2D association at these loci.

Notably, we identified genes such as *MTNR1B* and *C2CD4A* that have been implicated in T2D through an impact on pancreatic beta-cell function.[43,44] As we used indirect measures of post-

challenge insulin resistance that include measurements of circulating insulin, it is not surprising that some genetic variants regulating insulin secretion are also captured by our approach. However, at the *MTNR1B* locus, we identified a neighbouring gene *SLC36A4*, encoding a non-ionic amino acid transporter, the depletion of which resulted in a marked impairment of GLUT4 trafficking in 3T3-L1 adipocytes. Further investigations are warranted to identify possible additional effects of this locus on insulin resistance, possibly via impact on *SLC36A4*, as well as insulin secretion through *MTNR1B*.

The *BICC1* locus was the only locus associated with post-challenge insulin resistance at genome wide significance in cohorts of non-European ancestry, despite similar frequency of the lead variant in all 3 ancestry groups. We hypothesise that the identified lead variant may not be the causal variant at this locus and differences in frequency of the causal variant across ancestries may underlie the observed differences in associations.

Using technology that incorporated two complementary methods of detecting GLUT4 at the cell surface (see **Methods**), as well as direct measures of glucose uptake, we examined the impact of reducing the expression of 36 genes identified at genetic loci associated with IFC. We revealed 9 novel candidate genes implicated in insulin-stimulated glucose uptake and GLUT4 translocation from 4 IFC-associated loci. Although muscle is the major site of insulin-stimulated glucose uptake *in vivo,* the molecular mechanisms of insulin-stimulated glucose uptake are largely shared with adipocytes.[45] To date, no skeletal muscle-based model to assess GLUT4 trafficking with insulin-responsiveness comparable to that of the mouse 3T3-L1 adipocyte has been developed.

Of the genes found to influence insulin stimulated glucose uptake, most did not affect total GLUT4 cellular content but are likely to be involved in its trafficking. These include *Llgl1*, (known to interact with Rab10[46]) and genes involved in the control of membrane traffic via the Golgi (*Drg2*[47,48]*, Tvp23b*[49]) and endosomes (*Pdzk1ip1*[50]*, Toml12*[51]), both key sites of GLUT4 traffic. In contrast interference with the expression of Alkbh5, a M6A RNA demethylase, which has previously been implicated in post-transcriptional regulation of GLUT4 expression in a breast cancer model[52], also reduced total GLUT4 cellular content in our studies. Additional processes involved in the maintenance of the cellular GLUT4 pool, including transcription,

stable intracellular localisation, or protein degradation may be involved in the case of other genes.

To conclude, here we report a total of 10 genome-wide loci not previously associated with post-challenge insulin resistance. We show that 8 of these share their genetic architecture with T2D and hence identify the likely mechanism of action that leads to T2D pathogenesis for these loci, and identify one locus, *BICC1*, to be specific to cohorts of Hispanic American and East Asian ancestries, despite much smaller sample size.

We identify a common intronic variant (rs117643180) in *SLC2A4* to be associated with post-challenge insulin resistance and demonstrate it's *in silico* and *in vitro* effect on *SLC2A4* expression in skeletal muscle. *SLC2A4* encodes GLUT4 - a critical player in postprandial glucose disposal, and together this provides evidence for *the* mechanism underlying the post-challenge specific glycaemic signature seen for *SLC2A4* in individuals without diabetes. Finally, through the employment of cell-based screening methods, we identified 9 putative novel genes involved in GLUT4 trafficking. This study highlights the importance of characterising refined dynamic measures of insulin resistance to further the understanding of physiological mechanisms in T2D that are not sufficiently captured by more readily obtainable measures at a single timepoint.

Acknowledgements

We are grateful to investigators, staff members and study participants for their contribution to all participating studies. A full list of individual and study acknowledgments appears in the **Supplementary Note**. The funders had no role in study design, data collection and analysis, decision to publish or preparation of the manuscript.

Author contributions:

Central analysis group: A.W., X.Y., K.A.B., E.P.W., N.G., M.B., N.J.W., K.L.M., E.W., S.O'R, C.Langenberg. **Follow up analyses and interpretation:** A.W., X.Y., K.A.B., A.U.J, M.W., N.J.W. ,K.L.M., E.W., S.O'R, C.Langenberg ***SLC2A4*** **in vitro follow up:** A.H.M., S.V., K.L.M. **siRNA knockdown screen:** A.W., D.M.N., D.J.F.**Study-level GWAS: analysis, phenotyping, genotyping:** A.W., X.Y., K.A.B., A.U.J, V.A., M.K.A. ,Z.A. ,L.L.B. ,S.R.B., M.P.B., T.A.B., Y-C.C., L-M.C., R-H.C., T.D.C., P.D., G.E.D., V.D.dM., J.D., O.P.D., M.R.E, L.F., T.M.F., C.G., M.O.G., X.G., S.G., L.H., U.H., G.H., S.H., K.Højlund, K.Horn, W.A.H., Y-J.H., C-M.H., A.J., L.L.K., M.E.K., P.K., T.A.L., M.L., I-T.L., C.Lindgren., J.L., A.L., C-T.L. ,J'an.L. ,D.M. ,E.M., A.P.Moissl, A.P.Morris, N.N., N.P., A.Peters, R.B.P., R.N.R., K.R., C.R., C.S., K.S., M.Scholz, S.Sharma, S.E.S., S.Suleman, J.Tan, K.T., M.U., D.V., P.W., D.R.W., R.W., A.H.X., B.Z. ,E.A., M.Laakso, L.L., J.B.M., R.R., J.S., M.W., N.G., N.J.W. **Study-level oversight/PI:** E.A., R.N.B., Y.C., F.S.C., T.F., J.C.F., A.F., H.G., L.G., T.H., H.A.K., P.K., M.Laakso, L.L., M.Loeffler, W.M., J.B.M., L.J.R., R.R., J.I.R., P.E.H.S., M.Stumvoll, J.S., A.T., T.T., J.Tuomilehto, R.W., M.W., N.G., M.B., N.J.W., K.L.M., C.Langenberg. **Writing group:** A.W., D.M.N., A.H.M., I.B., K.L.M., E.W., S.O'R, D.J.F., C.Langenberg

All authors read, edited, and approved the final version of the manuscript.

The Meta-Analysis of Glucose and Insulin-related Traits Consortium (MAGIC)

Alice Williamson[1,2], Xianyong Yin[4,5,6], K. Alaine Broadaway[7], Emma P Wilson[7], Anne U Jackson[4,5], Vasudha Ahuja[8], Mette K Andersen[9], Zorayr Arzumanyan[10], Lori L Bonnycastle[11], Stefan R Bornstein[12,13,14], Maxi P. Bretschneider[12,13,14], Thomas A Buchanan[15], Yi-Cheng Chang[16,17,18], Lee-Ming Chuang[19], Ren-Hua Chung[20], Tine D Clausen[21,22], Peter Damm[22,23,24], Graciela E Delgado[25], Vanessa D de Mello[26], Josée Dupuis[27,28], Om P Dwivedi[8], Michael R Erdos[11], Lilian Fernandes Silva[29], Timothy M Frayling[30], Christian Gieger[31,14], Mark O Goodarzi[32], Xiuqing Guo[10], Stefan Gustafsson[33], Liisa Hakaste[8], Ulf Hammar[34], Gad Hatem[35], Sandra Herrmann[36,13], Kurt Højlund[37], Katrin Horn[38,39], Willa A Hsueh[40], Yi-Jen Hung[41], Chii-Min Hwu[42], Anna Jonsson[9], Line L Kårhus[43], Marcus E Kleber[44,45], Peter Kovacs[46], Timo A Lakka[47,48,49], Marie Lauzon[50], I-Te Lee[51,52,53], Cecilia M Lindgren[54,55,56,57], Jaana Lindström[58],

Allan Linneberg[43,22], Ching-Ti Liu[27], Jian'an Luan[1], Dina Mansour Aly[35], Elisabeth Mathiesen[22,23,59], Angela P Moissl[60,61,44], Andrew P Morris[62], Narisu Narisu[11], Nikolaos Perakakis[12,13,14], Annette Peters[31,14], Rashmi B Prasad[35,8], Roman N Rodionov[63,64], Kathryn Roll[65], Carsten F Rundsten[9], Chloé Sarnowski[66], Kai Savonen[49], Markus Scholz[38,39], Sapna Sharma[67,68], Sara E Stinson[9], Sufyan Suleman[9], Jingyi Tan[10], Kent D Taylor[10], Matti Uusitupa[69], Dorte Vistisen[70,71], Daniel R Witte[72,73], Romy Walther[74,13], Peitao Wu[75], Anny H Xiang[76], Björn Zethelius[77],Emma Ahlqvist[35], Richard N Bergman[78], Yii-Der Ida Chen[50], Francis S Collins[11], Tove Fall[34], Jose C Florez[79,80,81], Andreas Fritsche[82], Harald Grallert[67,31,14], Leif Groop[83,8], Torben Hansen[9], Heikki A Koistinen[84,85,86], Pirjo Komulainen[49], Markku Laakso[29], Lars Lind[33], Markus Loeffler[38,39], Winfried März[87,25], James B Meigs[88,89,90], Leslie J Raffel[91], Rainer Rauramaa[49], Jerome I Rotter[92], Peter E. H. Schwarz[36,13,14], Michael Stumvoll[46], Johan Sundström[33], Anke Tönjes[46], Tiinamaija Tuomi[93,8], Jaakko Tuomilehto[94,95,96], Robert Wagner[82], Inês Barroso[97], Mark Walker[98], Niels Grarup[9], Michael Boehnke[4,5], Nicholas J Wareham[1], Karen L Mohlke*#[7], Eleanor Wheeler*#[1], Stephen O'Rahilly*#[3], Claudia Langenberg*#[1,99,100]

Affiliations are as provided for the manuscript author list. Consortium Representative: Inês Barroso: ines.barroso@exeter.ac.uk

Competing Interests

I Barroso: IB and spouse declare stock ownership in GlaxoSmithkline, Incyte Ltd and Inivata Ltd. J.C. Florez: Consulting honoraria from Goldfinch Bio and AstraZeneca; speaker honoraria from Novo Nordisk, AstraZeneca and Merck for research lectures over which I had full control on content. M.E. Kleber: Employed by SYNLAB Holding Deutschland GmbH. C. Lindgren: CL receives grants from Bayer Ag & Novo Nordisk and her Husband works for Vertex. W. März: reports grants and personal fees from Siemens Diagnostics, grants and personal fees from Aegerion Pharmaceuticals, grants and personal fees from AMGEN, grants and personal fees from Astrazeneca, grants and personal fees from Danone Research, grants and personal fees from Sanofi, personal fees from Hoffmann LaRoche, personal fees from MSD, grants and personal fees from Pfizer, personal fees from Synageva, grants and personal fees from BASF, grants from Abbott Diagnostics, grants and personal fees from Numares, outside the submitted work. W. März is employed by Synlab Holding Deutschland GmbH. J.B. Meigs: Academic Associate for Quest Diagnostics. S. O'Rahilly: S.O. has undertaken remunerated consultancy work for Pfizer, AstraZeneca, GSK and ERX Pharmaceuticals.N. Parakakis: Nikolaos Perakakis reports consulting honoraria from Bayer Vital GmbH and speaker honoraria from Novo Nordisk. J. Sundström: Shareholder in Anagram kommunikation AB and Symptoms Europe AB, outside of the present study. D. Vistisen: DV has received research

grants from Bayer A/S, Sanofi, Novo Nordisk A/S and Boehringer Ingelheim. DV holds shares in Novo Nordisk A/S. E. Wheeler: EW is now an employee of AstraZeneca. B. Zethelius: Björn Zethelius is employed at the Swedish Medical Products Agency, SE-751 03 Uppsala, Sweden. The views expressed in this paper are the personal views of the authors and not necessarily the views of the Swedish government agency. All other authors declare no competing interests.

Main text Tables and Figures

Table 1: Genome wide significant loci for Insulin fold change and Modified Stumvoll ISI, adjusted for BMI in meta-analysis of cohorts of European ancestry.

Trait	Locus	CHR:POS	rsid	EA	OA	EAF	Beta	SE	P-value	N
Insulin Fold Change	*MTN1RB*	11:92673828	rs1387153	T	C	0.3023	0.0438	0.0069	2.25E-10	52698
	PPP1R3B (primary)	8:9173358	rs7012814	A	G	0.4796	0.0481	0.0065	1.35E-13	52458
	PPP1R3B (secondary)	8:9185146	rs2126259	T	C	0.1265	-0.0688	0.0099	2.86E-12	52698
	C2CD4A	15:62396189	rs7167878	A	C	0.4606	-0.0426	0.0064	2.76E-11	53287
	SLC2A4	17:7185779	rs117643180	A	C	0.0231	0.1428	0.0221	1.11E-10	50671
Modified Stumvoll ISI	*IRS1*	2:227101411	rs2972144	A	G	0.366	0.0644	0.0067	1.10E-21	50511
	COBLL1	2:165558252	rs12692738	T	C	0.7724	-0.0568	0.0075	5.24E-14	53657
	PPARG	3:12385828	rs11128603	A	G	0.8595	-0.0635	0.0091	2.64E-12	53657
	SLC2A4	17:7185779	rs117643180	A	C	0.0231	-0.1416	0.0221	1.58E-10	51187
	C5orf67	5:55806751	rs459193	A	G	0.2816	0.0409	0.007	6.18E-09	53657
	MTOR	1:11322628	rs2295080	T	G	0.6961	-0.0394	0.0069	1.34E-08	53657
	BCL2	18:60845884	rs12454712	T	C	0.5858	-0.0374	0.0068	4.42E-08	52701
	FAM101A	12:124539537	rs1906937	A	C	0.2894	-0.0384	0.007	4.86E-08	53657

EA – effect allele, OA – other allele, EAF – effect allele frequency, SE – standard error. CHR:POS – chromosome:position GRCh37 (hg19).

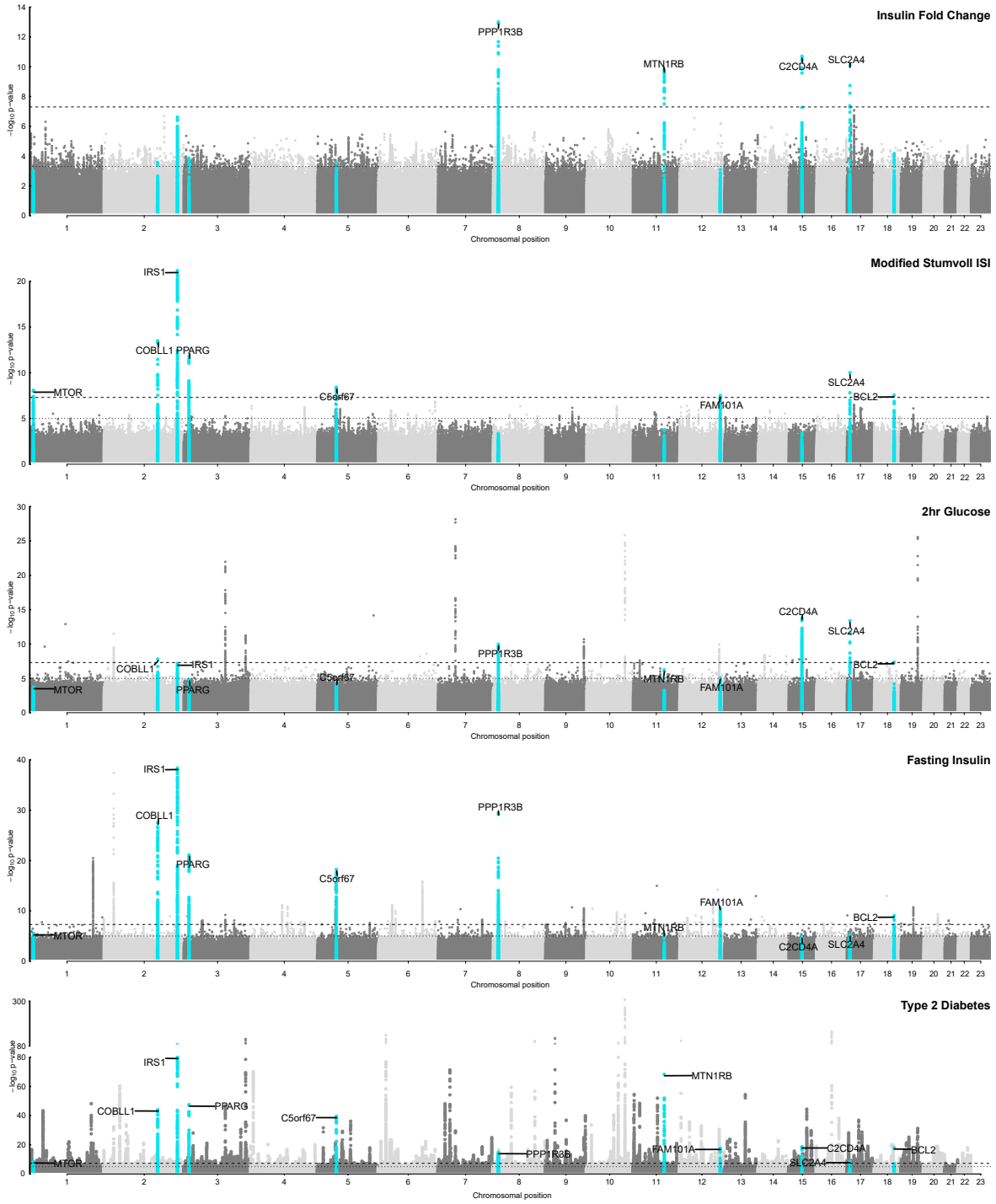

Figure 1: Loci associated with post-challenge insulin resistance overlap with associations with other glycaemic traits and T2D

Manhattan plot of results for IFC, ISI and relative association with key glycaemic traits of interest. Y-axis denotes the -$\log_{10}$(p-value) of association for each trait. X-axis outlines the chromosomal position, with alternate chromosomes represented in light and dark grey. The dashed line defines genome-wide significance threshold ($P = 5x10^{-8}$), and the dotted line denotes $P = 1x10^{-5}$. Points highlighted in blue on each plot represent those that

meet genome-wide significance for either IFC and ISI ($P < 5x10^{-8}$). Labels for indicate the nearest gene at a locus defined at genome-wide significance for either IFC and ISI, and their relative association with other traits. Published GWAS were used for fasting insulin and 2 h glucose[3],, and T2D[26]. For T2D y axis is cut at $1x10^{-80}$ for clarity, with the minimum p value truncated to $P = 1x10^{-300}$. Uncorrected p-values are shown. All GWAS are in cohorts of European ancestry and adjusted for BMI, except T2D which is unadjusted for BMI.

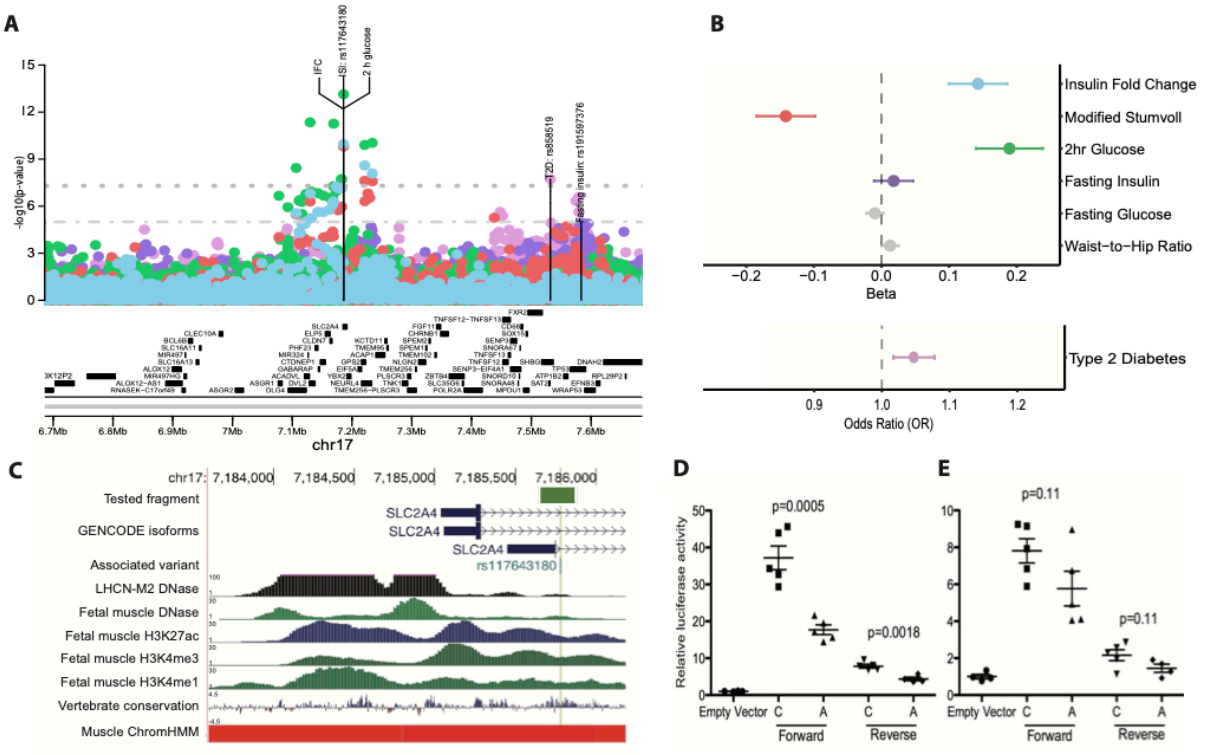

Figure 2: rs117643180 at *SLC2A4* affects GLUT4 expression and transcription regulation.

A) Regional association plot showing ± 500kb around rs117643180 (SLC2A4) : insulin fold change (IFC) - blue, Modified Stumvoll (ISI) – red, and 2 h glucose[3] – green, fasting insulin[3] – purple, type 2 diabetes[26] – pink . Y-axis denotes the unadjusted $\log_{10}$(p-value) of association. The dashed lines and dotted line indicate genome-wide ($P = 5x10^{-8}$) and suggestive ($P = 1x10^{-5}$) significance threshold, respectively. All association statistics are from BMI adjusted analyses in studies of European ancestry, except T2D which is unadjusted for BMI**.** Labels indicate the lead variant for each trait, with location indicating position. **B)** Association of rs117643180 with key metabolic traits of interest. Plot shows beta estimate or odds ratio of association for rs117643180 with traits outlined in (A) and fasting glucose[3] and waist-to-hip ratio[53] in grey. Point represents effect size and error bars indicate 95% CI. **C)** rs117643180 overlaps a transcriptionally active region in muscle tissues. rs117643180 is located ~730 bp downstream of the main *SLC2A4* transcription start site (TSS) and ~330 bp downstream of an alternate *SLC2A4* TSS. A 229-bp region flanking the variant, as shown by the orange bar, overlaps with accessible chromatin in LHCN-M2 (DNAase)[54], chromatin marks of regulatory activity in fetal muscle leg tissue [55], a region conserved across species (vertebrate conservation), and a skeletal muscle ChromHMM[56] (red = ActiveTSS). Created using http://genome.ucsc.edu[57]

D-E) rs117643180 exhibits allelic differences in transcriptional activity**.** Values represent fold-change of firefly luciferase/*Renilla* activity normalized to empty pGL4.23 vector in C2C12 cells, for the A (effect) and C (non-effect) alleles clones in forward and reverse orientation (See **Methods**) (D) and LHCN-M2 myotubes (E). Error bars represent the SEM of 4 to 5 independent clones tested in duplicate wells; points represent individual biological replicates. P-values are calculated from two-sided t-tests.

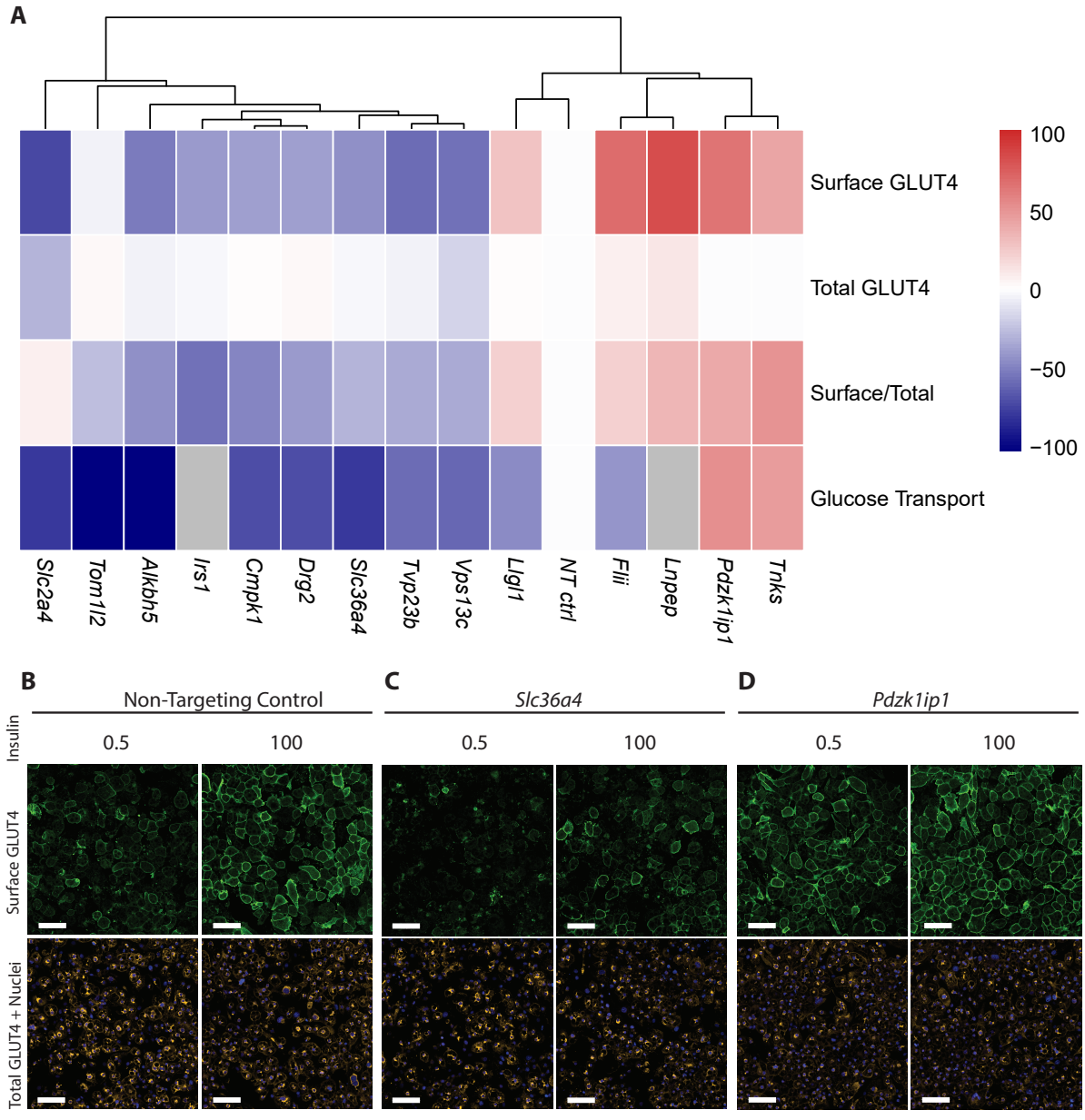

Figure 3: 15 genes at loci associated with insulin fold change were identified to significantly impact GLUT4 trafficking in adipocytes

a) Effect of gene knockdown on GLUT4 trafficking and glucose transport at 0.5 nM insulin stimulation in WT 3T3-L1 adipocytes (N = 3 biologically independent replicates, 2 technical replicates per N). Genes are clustered using

hierarchical clustering. All results are normalised to non-targeting (NT) control. Grey represents genes for which glucose transport data was not collected as their role is established in the literature. Scale represents relative effect of gene knockdown compared to NT control for given measures – red positive, and blue negative, with the maximal scale representing the maximum absolute response relative to NT (0) across all measures, expressed as a percentage, to allow direct comparison across measures.-. B-D) Representative fluorescence microscopy images of example siRNA knockdown in WT 3T3-L1 adipocytes (N = 3 biologically independent replicates, 2 technical replicates per N) at 0.5 and 100nM insulin stimulation. Green represents the surface GLUT4 signal, orange the total GLUT4 signal and blue indicates individual nuclei. Scale bars indicate 100 μm. Quantification of *Slc36a4* and *Pdzk1ip1* compared to NT control and images at 0 nM are shown in **Supplementary Figure 25**. b) shows non-targeting control, c) Slc36a4 and d) Pdzk1ip1.

Main Text References

1. James, D. E., Stöckli, J. & Birnbaum, M. J. The aetiology and molecular landscape of insulin resistance. *Nat. Rev. Mol. Cell Biol. 2021 2211* **22**, 751–771 (2021).
2. Defronzo, R. A. From the Triumvirate to the Ominous Octet: A New Paradigm for the Treatment of Type 2 Diabetes Mellitus. *Diabetes* **58**, 773–795 (2009).
3. Chen, J. *et al.* The trans-ancestral genomic architecture of glycemic traits. *Nat. Genet. 2021 536* **53**, 840–860 (2021).
4. Scott, R. A. *et al.* Large-scale association analyses identify new loci influencing glycemic traits and provide insight into the underlying biological pathways. *Nat. Genet.* **44**, 991–1005 (2012).
5. Lagou, V. *et al.* Sex-dimorphic genetic effects and novel loci for fasting glucose and insulin variability. *Nat. Commun. 2021 121* **12**, 1–18 (2021).
6. Taylor, R. *et al.* Direct assessment of liver glycogen storage by 13C nuclear magnetic resonance spectroscopy and regulation of glucose homeostasis after a mixed meal in normal subjects. *J. Clin. Invest.* **97**, 126–132 (1996).
7. Jue, T., Rothman, D. L., Tavitian, B. A. & Shulman, R. G. Natural-abundance 13C NMR study of glycogen repletion in human liver and muscle. *Proc. Natl. Acad. Sci. U. S. A.* **86**, 1439–1442 (1989).
8. Petersen, M. C. & Shulman, G. I. Mechanisms of Insulin Action and Insulin Resistance. *Physiol. Rev.* **98**, 2133 (2018).
9. Fischer, Y. *et al.* Insulin-induced Recruitment of Glucose Transporter 4 (GLUT4) and GLUT1 in Isolated Rat Cardiac Myocytes: EVIDENCE OF THE EXISTENCE OF DIFFERENT INTRACELLULAR GLUT4 VESICLE POPULATIONS. *J. Biol. Chem.* **272**, 7085–7092 (1997).
10. Goodyear, L. J. *et al.* Glucose Ingestion Causes GLUT4 Translocation in Human Skeletal Muscle. *Diabetes* **45**, 1051–1056 (1996).
11. Kahn, B. B. Dietary Regulation of Glucose Transporter Gene Expression: Tissue Specific Effects in Adipose Cells and Muscle. *J. Nutr.* **124**, 1289S-1295S (1994).
12. Maianu, L., Keller, S. R. & Garvey, W. T. Adipocytes Exhibit Abnormal Subcellular Distribution and Translocation of Vesicles Containing Glucose Transporter 4 and Insulin-Regulated Aminopeptidase in Type 2 Diabetes Mellitus: Implications Regarding Defects in Vesicle Trafficking. *J. Clin. Endocrinol. Metab.* **86**, 5450–5456 (2001).
13. Rothman, D. L. *et al.* Decreased muscle glucose transport/phosphorylation is an early defect in the pathogenesis of non-insulin-dependent diabetes mellitus. *Proc. Natl. Acad. Sci. U. S. A.* **92**, 983–987 (1995).
14. DeFronzo, R. A. & Tripathy, D. Skeletal Muscle Insulin Resistance Is the Primary Defect in Type 2 Diabetes. *Diabetes Care* **32**, S157 (2009).
15. Sano, H. *et al.* Insulin-stimulated phosphorylation of a Rab GTPase-activating protein regulates GLUT4 translocation. *J. Biol. Chem.* **278**, 14599–14602 (2003).
16. Dash, S. *et al.* A truncation mutation in TBC1D4 in a family with acanthosis nigricans and postprandial hyperinsulinemia. *Proc. Natl. Acad. Sci. U. S. A.* **106**, 9350–9355 (2009).
17. Grarup, N. *et al.* Identification of novel high-impact recessively inherited type 2 diabetes risk variants in the Greenlandic population. *Diabetologia* **61**, 2005–2015 (2018).
18. Moltke, I. *et al.* A common Greenlandic TBC1D4 variant confers muscle insulin

resistance and type 2 diabetes. *Nature* **512**, 190–193 (2014).
19. Tam, C. S. *et al.* Defining insulin resistance from hyperinsulinemic-euglycemic clamps. *Diabetes Care* **35**, 1605–1610 (2012).
20. Reinauer, H. *et al.* Determination of glucose turnover and glucose oxidation rates in man with stable isotope tracers. *J. Clin. Chem. Clin. Biochem.* **28**, 505–512 (1990).
21. Muniyappa, R., Lee, S., Chen, H. & Quon, M. J. Current approaches for assessing insulin sensitivity and resistance in vivo: Advantages, limitations, and appropriate usage. *Am. J. Physiol. - Endocrinol. Metab.* **294**, 15–26 (2008).
22. Stumvoll, M. *et al.* Use of the oral glucose tolerance test to assess insulin release and insulin sensitivity. *Diabetes Care* **23**, 295–301 (2000).
23. Walford, G. A. *et al.* Genome-wide association study of the modified stumvoll insulin sensitivity index identifies BCL2 and FAM19A2 as novel insulin sensitivity loci. *Diabetes* **65**, 3200–3211 (2016).
24. Dimas, A. S. *et al.* Impact of Type 2 Diabetes Susceptibility Variants on Quantitative Glycemic Traits Reveals Mechanistic Heterogeneity. *Diabetes* **63**, 2158–2171 (2014).
25. DeFronzo, R. A., Tobin, J. D. & Andres, R. Glucose clamp technique: A method for quantifying insulin secretion and resistance. *Am. J. Physiol. Endocrinol. Metab. Gastrointest. Physiol.* **6**, (1979).
26. Vujkovic, M. *et al.* Discovery of 318 new risk loci for type 2 diabetes and related vascular outcomes among 1.4 million participants in a multi-ancestry meta-analysis. *Nat. Genet. 2020 527* **52**, 680–691 (2020).
27. Zhu, Y., Wang, L., Yin, Y. & Yang, E. Systematic analysis of gene expression patterns associated with postmortem interval in human tissues. *Sci. Rep.* **7**, 5435 (2017).
28. Uhlén, M. *et al.* Tissue-based map of the human proteome. *Science (80-.).* **347**, (2015).
29. Aguet, F. *et al.* The GTEx Consortium atlas of genetic regulatory effects across human tissues. *Science (80-.).* **369**, 1318–1330 (2020).
30. Lonsdale, J. *et al.* The Genotype-Tissue Expression (GTEx) project. *Nature Genetics* vol. 45 580–585 (2013).
31. Kanai, F. *et al.* Insulin-stimulated GLUT4 translocation is relevant to the phosphorylation of IRS-1 and the activity of PI3-kinase. *Biochem. Biophys. Res. Commun.* **195**, 762–768 (1993).
32. Keller, S. R., Scott, H. M., Mastick, C. C., Aebersold, R. & Lienhard, G. E. Cloning and Characterization of a Novel Insulin-regulated Membrane Aminopeptidase from Glut4 Vesicles. *J. Biol. Chem.* **270**, 23612–23618 (1995).
33. Chi, N. W. & Lodish, H. F. Tankyrase is a golgi-associated mitogen-activated protein kinase substrate that interacts with IRAP in GLUT4 vesicles. *J. Biol. Chem.* **275**, 38437–38444 (2000).
34. Guo, H. L. *et al.* The Axin/TNKS complex interacts with KIF3A and is required for insulin-stimulated GLUT4 translocation. *Cell Res.* **22**, 1246–1257 (2012).
35. Hook, S. C. *et al.* TBC1D1 interacting proteins, VPS13A and VPS13C, regulate GLUT4 homeostasis in C2C12 myotubes. *Sci. Rep.* **10**, 1–14 (2020).
36. Klip, A., McGraw, T. E. & James, D. E. Thirty sweet years of GLUT4. **294**, 11369–11381 (2019).
37. Stenbit, A. E. *et al.* GLUT4 heterozygous knockout mice develop muscle insulin resistance and diabetes. *Nat. Med.* **3**, 1096–1101 (1997).
38. Gual, P., Le Marchand-Brustel, Y. & Tanti, J. F. Positive and negative regulation of

insulin signaling through IRS-1 phosphorylation. *Biochimie* **87**, 99–109 (2005).
39. Barroso, I. Dominant negative mutations in human PPARγ associated with severe insulin resistance, diabetes mellitus and hypertension. *Nature* **402**, 880–883.
40. Li, Q. *et al.* The Protein Phosphatase 1 Complex Is a Direct Target of AKT that Links Insulin Signaling to Hepatic Glycogen Deposition. *Cell Rep.* **28**, 3406-3422.e7 (2019).
41. Agius, L. Role of glycogen phosphorylase in liver glycogen metabolism. *Mol. Aspects Med.* **46**, 34–45 (2015).
42. Yoon, M. S. The Role of Mammalian Target of Rapamycin (mTOR) in Insulin Signaling. *Nutrients* **9**, (2017).
43. Kuo, T. *et al.* Identification of C2CD4A as a human diabetes susceptibility gene with a role in β cell insulin secretion. *Proc. Natl. Acad. Sci. U. S. A.* **116**, 20033–20042 (2019).
44. Lyssenko, V. *et al.* Common variant in MTNR1B associated with increased risk of type 2 diabetes and impaired early insulin secretion. *Nat. Genet.* **41**, 82–88 (2009).
45. Huang, S. & Czech, M. P. The GLUT4 Glucose Transporter. *Cell Metab.* **5**, 237–252 (2007).
46. Degrandmaison, J. *et al.* In vivo mapping of a GPCR interactome using knockin mice. *Proc. Natl. Acad. Sci. U. S. A.* **117**, 13105–13116 (2020).
47. Mani, M. *et al.* DRG2 knockdown induces Golgi fragmentation via GSK3β phosphorylation and microtubule stabilization. *Biochim. Biophys. acta. Mol. cell Res.* **1866**, 1463–1474 (2019).
48. Mani, M. *et al.* Developmentally regulated GTP-binding protein 2 coordinates Rab5 activity and transferrin recycling. *Mol. Biol. Cell* **27**, 334–348 (2016).
49. Gendre, D. *et al.* Conserved Arabidopsis ECHIDNA protein mediates trans-Golgi-network trafficking and cell elongation. *Proc. Natl. Acad. Sci. U. S. A.* **108**, 8048–8053 (2011).
50. Gonzales, P. A. *et al.* Large-scale proteomics and phosphoproteomics of urinary exosomes. *J. Am. Soc. Nephrol.* **20**, 363–379 (2009).
51. Wang, T., Liu, N. S., Seet, L. F. & Hong, W. The emerging role of VHS domain-containing Tom1, Tom1L1 and Tom1L2 in membrane trafficking. *Traffic* **11**, 1119–1128 (2010).
52. Liu, H. *et al.* ALKBH5-mediated m6A demethylation of GLUT4 mRNA promotes glycolysis and resistance to HER2-targeted therapy in breast cancer. *Cancer Res.* (2022) doi:10.1158/0008-5472.CAN-22-0800.
53. Pulit, S. L. *et al.* Meta-analysis of genome-wide association studies for body fat distribution in 694 649 individuals of European ancestry. *Hum. Mol. Genet.* **28**, 166–174 (2019).
54. Dunham, I. *et al.* An integrated encyclopedia of DNA elements in the human genome. *Nature* **489**, 57–74 (2012).
55. Kundaje, A. *et al.* Integrative analysis of 111 reference human epigenomes. *Nature* **518**, 317–330 (2015).
56. Ernst, J. & Kellis, M. ChromHMM: automating chromatin-state discovery and characterization. *Nat. Methods* **9**, 215–6 (2012).
57. Kent, W. J. *et al.* The human genome browser at UCSC. *Genome Res.* **12**, 996–1006 (2002).

Materials and Methods

Contributing studies

All contributing studies included in this analysis were approved by the relevant Institutional Review Boards, with all participants having given informed consent. Study specific ethics statements are provided in the **Reporting Summary**.

A total of 55,535 and 55,172 participants without diabetes across 28 studies contributing to the Meta-Analyses of Glucose and Insulin-related Traits Consortium (MAGIC) contributed to the analyses of Modified Stumvoll ISI and insulin fold change, respectively (**Supplementary Tables 1-3**). Two of these studies included participants of Hispanic American ancestry (MACAD and HTN-IR; N ISI = 1095, N IFC = 1099) and 1 included participants of East Asian ancestry (TAICHI; N ISI = 730 N IFC = 739); the remaining 25 studies included individuals of European ancestry.

Ancestry group was defined at the study level as the ancestry reported by each respective study at point of data collection. Within each study, we excluded individuals with missing traits or covariates from the analyses.

Phenotype definition

Individuals were excluded from study-level analyses if they were diagnosed with type 2 diabetes, reported use of diabetes medication, or had Fasting Glucose ≥ 7mmol/L, 2hr Glucose ≥ 11.1 mmol/L or HbA1c ≥ 6.5% (**Supplementary Table 1**).

Fasting measures of plasma insulin and glucose were collected before a standard 75g oral glucose tolerance test (OGTT) with 2hr glucose and insulin measures obtained 120mins after the ingestion of the glucose challenge. Biochemical assays used to quantify insulin and glucose in individual studies are outlined in **Supplementary Table 1**.

Modified Stumvoll insulin sensitivity index (ISI) was calculated as previously described using the formula[22,58]:

$$Modified\ Stumvoll\ ISI = 0.156 - \left(0.0000456 \times insulin_{120\ \mathrm{min[pmol/L]}}\right) - \left(0.000321 \times insulin_{0\ \mathrm{min[pmol/L]}}\right) - \left(0.0054 \times glu\cos e_{120\ \mathrm{min[mmol/L]}}\right)$$

Insulin fold change (IFC) was calculated using fasting and 120 min insulin measures during OGTT using formula:

$$IFC = \ln\left(\frac{Insulin_{120mins[pmol/L]}}{Insulin_{0\ mins[pmol/L]}}\right)$$

Formulae terms: $insulin_{120min}$ – insulin levels at 120 mins post-ingestion of glucose challenge in pmol/L. $Insulin_{0min}$ – fasting insulin levels prior to glucose challenge in pmol/L. $Glucose_{120min}$ – glucose levels at 120 mins post-ingestion of glucose challenge in mmol/L.

Phenotypic correlations of ISI and IFC with relevant traits

We assessed observational correlations of relevant traits was assessed in the Fenland[59] and RISC[60] studies using Spearman's Rank correlation for pairwise complete observations. ISI and IFC were calculated as defined above and were restricted to individuals without diabetes. Those who reported use of diabetes medication or had fasting glucose ≥ 7 mmol/L, 2hr glucose ≥ 11.1 mmol/L or HbA1c ≥ 6.5% were excluded. Blood biochemistry measures were natural log transformed. In RISC and the Fenland Study, IFC was calculated using OGTT measures of insulin at 0 min and 120 min.

Genotyping, quality control, (QC), and imputation

Study-level QC, genotype imputation, and genome-wide association study (GWAS) analyses were conducted following a shared analysis plan to ensure analyses were conducted consistently across studies. Most study samples were genotyped using commercially available genome-wide genotyping arrays, with a small subset of study samples genotyped on targeted arrays such as Illumina Cardio-Metabochip (Metabochip) array (**Supplementary Table 1**).

Genotype imputation was conducted for all autosomes and the X chromosome in all contributing studies on build 37 (Hg19) on the forward strand. Most studies of European ancestry were imputed to the Human Reference Consortium (HRC) reference panel.[61] Studies of non-European ancestry were imputed to population-specific 1000 genomes (1000G) reference panel[62]. Botnia-PPP was imputed to the SISu v3 reference panel in genome build 38[63] and variants were mapped to build 37 using UCSC LiftOver, after GWAS analyses[64].

Study-level GWAS

Study-level GWAS were performed using an additive model, modelling on the inverse normal transformed residuals of each trait and adjusting for age, sex, population structure, and study-specific covariates with or without adjustment for BMI. (**Supplementary Table 1**). To control for type 1 error rate of low-frequency variants and remove trait-covariate correlations, covariate adjustment for each trait was conducted in two steps before association analysis. First, a given trait was adjusted for all covariates in a model and residuals were derived. These residuals were inverse normal transformed and then adjusted for all covariates.

Study-level GWAS QC

Each contributing study shared GWAS summary statistics for both traits and both models. Study-level GWAS QC was performed by the central analysis group using easyQC (v17.8), to assess trait transformation and exclude variants that failed QC from downstream analyses.[65] Variants were flagged if the differences of their minor allele frequency (MAF) between the study and the corresponding frequencies in the imputation reference panel were greater than 0.2. In addition, variants were excluded if they met one or more of the following criteria: monomorphic, low genotype call rate (< 95%), poor imputation quality (INFO < 0.3), duplicate variants, minor allele count (MAC) < 3 per study, or not in Hardy Weinberg Equilibrium (HWE $P < 1x10^{-5}$). Variants were additionally excluded if these had standard error of the effect size > 10 or were missing standard error, effect estimate, or p-value in the summary statistic file. For the RISC study variants were excluded where INFO < 0.8.

Single-ancestry meta-analysis

An inverse variance fixed-effect meta-analysis of the study level GWAS was done using METAL (v.2011-03-25) for each ancestry, using beta-coefficients and standard errors from each

study-level GWAS.[66] We applied genomic control correction in two stages, first to study-specific GWAS results and then to the meta-analysis. Study-specific Metabochip results were corrected by genomic control using test statistics for 4986 SNPs included on the Metabochip array associated with QT interval, a trait that is not correlated with glycaemic traits, consistent with previous analyses of other glycaemic traits.[3,67]

In each individual study variants from with a MAF < 0.005 were removed prior to meta-analysis. Genome-wide significance was considered at $P < 5x10^{-8}$, with a genomic locus considered as a 1 Mb window (± 500kb) around the lead variant at each locus. Loci were annotated with the nearest protein-coding gene where applicable or based on previously reported gene annotation in the literature. Lead variant associations were manually inspected across all individual studies to ensure consistency of association.

Conditional analysis was conducted using the –cojo-slct option in GCTA (v1.26.0) using BMI adjusted summary statistics for IFC and ISI in European studies to identify independent signals at each locus[68]. A collinearity threshold of 0.8 and conditional p-value threshold of $P < 5x10^{-8}$ were used to identify conditionally independent genetic signals at each locus. The Fenland-OMICS subset (N = 8,925) of the Fenland Study with dense genome wide genotyping was used as an LD reference panel.

Multi-ancestry meta-analysis

We conducted a multi-ancestry random-effects meta-analysis using random-metal (2017-07-24; https://github.com/explodecomputer/random-metal) to meta-analyse the European, Hispanic American (His-Amr) and East Asian (EAS) ancestry specific analyses (see above), to delineate any ancestry specific effects on these traits.[66,69] The meta-analysis strategy is summarised in **Extended Data Figure 4**.

Post meta-analysis QC.

Post-meta-analysis, variants with a total sample size less than 11,000 in the European ancestry only or multi-ancestry (EUR, HIS-AMR, and EAS) analyses were removed, ensuring that the associations observed were contributed to by at least 2 studies. In the non-European

ancestry (HIS-AMR and EAS) analysis, variants detected in < 1,000 individuals were removed, ensuring these associations were seen in at least 2 of the 3 studies.

Novel loci were defined as those loci which have not been reported to be associated with post-challenge glycaemic traits or indices reflecting post-challenge insulin resistance.

For both IFC and ISI, fixed effect meta-analyses of GWAS from BMI adjusted (adjBMI) analyses in cohorts of European ancestry were considered the primary analyses. Unless specified otherwise, the results of this primary analysis are reported.

Fine mapping

We performed fine-mapping of the 11 loci significantly associated with IFC or ISI in European ancestry meta-analysis to define 99% credible sets for each locus. We generated approximate Baye's factors (ABFs) using the method described by Wakefield (2009)[70] and calculated the posterior probability that each variant was causal. Credible sets were defined including all variants that contained cumulative posterior probability greater than 99% in each region. Credible sets were calculated using marginal summary statistics for all loci where there was identified to only be one independent signal. At *PPP1R3B* where 2 independent signals were identified for insulin fold change, conditional summary statistics were used to calculate the 99% credible set for each signal.

Statistical colocalization of IFC and ISI with T2D

Bayesian colocalisation analyses were conducted using coloc.abf from R package coloc(v 5.1.0)[71] to test for genetic colocalisation of IFC and ISI with T2D[26]. BMI adjusted summary statistics in studies of European ancestry were used except for T2D where BMI adjusted stats were not available. Colocalisation was considered at a threshold of posterior probability > 0.7 for hypothesis "PP.H4.abf": a locus is associated with both traits and there is one shared causal SNP for the pair of traits being assessed.

Phenotypic annotation of associated loci

We used gene expression data from the GTEX project to assess whether lead variants are annotated as tissue specific expression quantitative trait loci (eQTLs) at a suggestive

significance threshold of $P < 1x10^{-4}$ in tissues relevant to type 2 diabetes – skeletal muscle, adipose (subcutaneous and visceral), liver, kidney[29]. We additionally used summary statistics for relevant traits that are publicly available to further annotate the loci of interest: T2D (N control = 965,732, N case = 148,726)[26], Waist-to-hip ratio (WHR) (N = 694,649)[53], fasting insulin (N=151,000)[3], fasting glucose (N = 200,600)[3], 2hr glucose (N = 63,400)[3]. BMI adjusted summary statistics in studies of European ancestry were used for all traits except T2D where BMI adjusted statistics were not available. These were additionally used to annotate lead variants at loci identified in the integrated GWAS approach (see below). Rare variant burden association statistics were obtained from the AstraZeneca PheWAS Portal (https://azphewas.com/) which includes pheWAS analysis across exomes from ~ 450,000 individuals of European ancestry in UK Bioabank. We extracted statistics for rare damaging missense variants which were defined using the "raredmgmtr" variant mask – which includes high quality calls for missense variants that are rare (MAF < 0.005%), damaging (REVEL score >= 0.25), and fall into a region of constrained variation according to the missense tolerance score metric (MTR < 0.78 or MTR_centil < 0.5). For more information, please see the publication outlining this work.[72]

Genetic risk scores and LD Score regression

Genetic risk scores (GRS) for IFC and ISI, and LD score regression[73] were used to assess the association of IFC and ISI with other cardiometabolic traits. We constructed genetic risk scores (GRS) for IFC and ISI including lead variants at primary association signals in Europeans, weighted by their effects on IFC or ISI as appropriate, both adjusted and unadjusted for BMI (**Supplementary Note, Supplementary Table 12**). LD scores for ISI and IFC were calculated using BMI adjusted summary statistics from our analyses in cohorts of European ancestry. LDSC[73] was used to assess the genome wide correlation with other cardiometabolic traits. LDSC-SEG was additionally used to assess the genome-wide enrichment of tissue-specific and cell type specific annotations.[74] Further details can be found in the Supplementary Note.

Statistical colocalisation with relevant traits

We further assessed colocalisation of traits using hyprcoloc(v1.0)[75] to identify shared signals across the following traits: T2D[26], WHR, fasting insulin[3], 2hr glucose[3], ISI, and IFC. BMI adjusted summary statistics in studies of European ancestry, expect T2D which was

unadjusted for BMI. Loci were defined as ±500kb around the lead variant for IFC and ISI, at a significance threshold of $p < 1 \times 10^{-5}$. Additional traits assessed were dropped from the analysis at each of the selected loci where $P > 5 \times 10^{-4}$. Hyprcoloc was run across default priors (p1 = 1×10^{-4}, p2 = 0.98 and threshold = 0.5) as well as looped over a grid of priors to allow for optimisation (p1 = 1×10^{-4}; p2 = 0.95, 0.98, 0.99, 0.999; threshold = 0.5,0.6, 0.7, 0.8, 0.9). Colocalisation of traits was considered at a threshold of posterior probability of colocalisation > 0.8, the largest and most stable trait cluster using the most the most stringent set of priors at this threshold was selected. The stability of trait clusters was inspected using sensitivity plots, and pairwise colocalisation between traits at these loci, also using hyprcoloc.

Statistical colocalisation with eQTLs in relevant issues

We additionally tested for colocalisation of eQTLs in relevant tissues (skeletal muscle, adipose, liver, and pancreatic islet) with IFC/ISI at the loci of interest. We considered co-localisation significant when the colocalisation posterior probability was > 0.7. We used eQTL marginal summary statistics in individuals of European ancestry from the GTEx consortium (v8) in relevant tissues (Adipose – Subcutaneous, Adipose – Visceral Omentum, Muscle – Skeletal, Pancreas, Liver).[27,30] Bayesian colocalisation analyses were conducted using coloc.abf from R package coloc using default priors.[71]

***In vitro* assessment of rs117643180 at SLC2A4**

Cell culture

C2C12 murine myoblasts (TCF-UNC/ATCC; CRL 1772) were grown in high-glucose Dulbecco's Modified Eagle's Medium (Sigma-Aldrich, St. Louis, MO) supplemented with 10% fetal bovine serum. LHCN-M2 immortalized human myoblasts[76] (Purchased from Evercyte, Vienna, AT) were grown on dishes coated with 0.1% pigskin gelatin (Sigma-Aldrich) in a medium consisting of four parts 4.5 g/L DMEM and one-part M199 (both Gibco, Waltham MA) and supplemented with 15% FBS, 20 mM HEPES buffer, 30 ng/mL zinc sulfate, 1.4 ug/mL vitamin B12, 55 ng/mL dexamethasone, 2.5 ng/mL HFG, and 10 ng/mL basic FGF. To differentiate LHCN-M2 myoblasts to myotubes, cells were cultured on gelatin-coated dishes for seven days in 4:1 DMEM: M199 supplemented with 20 mM HEPES buffer, 30 ng/mL zinc sulfate, 1.4 ug/mL vitamin B12, 10 ug/mL insulin, and 100 ug/mL apotransferrin. All cells were maintained in a

humidified incubator at 37°C with 5% CO_2. Cells tested negative for *Mycoplasma* contamination in accordance with the MycoAlert Mycoplasma Detection Kit (Lonza, Morristown, NJ).

Transcriptional reporter assays

Dual-luciferase reporter assays were performed as previously described[77]. A 229-base pair fragment surrounding rs117643180 (chr17:7185651-7185879, GRCh37/hg19) was amplified via PCR and cloned into the firefly luciferase reporter vector pGL4.23 (Promega, Madison, WI) in both orientations with respect to the minimal promoter. This fragment is located in *SLC2A4* intron 1 and includes approximately 100 bp of an untranslated alternate first exon. Alleles for additional variants located within the insert were kept consistent across all plasmids. To create plasmids containing the rs117643180-A allele, we performed site-directed mutagenesis using QuikChange II (Agilent Technologies, Santa Clara, CA) and PAGE-purified primers (Integrated DNA Technologies, Newark, NJ). Four or five clones for each allele, in each orientation, were purified and sequence confirmed (GeneWiz, RTP, NC). Primer sequences can be found in **Supplementary Table 18**.

Duplicate wells of C2C12 cells (35,000 per 1.9 cm^2) were co-transfected with 500 ng of luciferase plasmid and 80 ng of phRL-TK *Renilla* luciferase reporter plasmid (Promega) using transfection reagent Lipofectamine 3000 (Thermo Fisher, Waltham, MA). Duplicate wells of LHCN-M2 cells (40,000 per 1.9 cm^2) were co-transfected similarly either in an undifferentiated state or on day 6 of differentiation using transfection reagent LTX (Thermo Fisher). Reporter assays were performed 30 hours (LHCN-M2) or 48 hours (C2C12) after transfection. Luciferase measures were normalized to corresponding *Renilla* measures, and mean fold-change across duplicate wells was calculated relative to two to four independent preparations of empty vector pGL4.23. Alleles were compared using two-sided unpaired t-tests ($\alpha = 0.05$). All transfections were repeated on a different day and showed consistent results.

Electrophoretic mobility shift assays

Assays were conducted as previously described using C2C12 or LHCN-M2 nuclear extracts.[78] Seventeen-bp complementary oligonucleotides centred around rs117643180-C or rs117643180-A and biotinylated at the 5’ end (IDT) were annealed (**Supplementary Table**

18).. Binding reactions were carried out with 6-10 µg of nuclear extract, 200-400 fmol of biotinylated probe, and 10- to 30-fold excess of unlabelled competing probe.

Integrated GWAS approach

We employed an integrated GWAS approach, which has been successful in identifying variants associated with insulin resistance[79], to identify genetic variants which had a similar association pattern to that of the *SLC2A4* locus, using a more permissive significance threshold. We filtered for variants which were associated with IFC and ISI ($P < 5x10^{-5}$). Those prioritised for IFC were used as a starting point for gene selection for in vitro follow up work assessing the role of candidate genes in GLUT4 trafficking (see below).

We subsequently integrated associations for IFC and ISI with the associations reported for fasting insulin[3], 2hr glucose[3], and skeletal muscle eQTLs[29]. We used BMI adjusted summary statistics from meta-analyses including studies of European ancestry for all traits. For IFC and Modified Stumvoll ISI, we used the European only BMI adjusted analyses. For 2hr glucose and fasting insulin, we utilised the largest available BMI adjusted summary statistics in European studies.[3,5] Lead variants for IFC or ISI at the loci selected to not be associated with fasting insulin (strategy 2 outlined below), were subsequently assessed for their association and statistical colocalisation (see below) with mRNA expression levels in skeletal muscle (eQTLs) in GTEx v8[29].

We used two variant selection strategies to refine loci which have the following phenotypic patterns of association:

1. Identify loci additionally associated 2hr Glucose ($P < 5x10^{-4}$)
2. Identify loci not associated with Fasting insulin ($P > 0.05$) and reported to be an eQTL in skeletal muscle (GTEx[29], $P < 5x10^{-4}$). We also annotated loci with eQTLs in skeletal muscle identified in FUSION ($P < 0.05$)[80].

Where conditions were met at a given locus for both ISI and IFC, the lead variant was selected to be that that met the threshold for both ISI and IFC.

Assessing the role of genes at IFC loci in GLUT4 trafficking

IFC is correlated with post-challenge insulin and glucose to a greater extent than fasting measures (**Supplementary Note; Extended Data Figures 2 and 3**). Therefore, following our identification of the *SLC2A4* locus directly implicating the encoding protein, GLUT4, we reasoned that studying genes at genetic loci associated with IFC may allow identification of additional novel regulators of insulin-stimulated glucose disposal. Loci for IFC identified at genome-wide significance and those prioritised through the integrated GWAS approach were used for gene selection.

We prioritised all protein-coding genes defined in UCSC genome browser[81] located ±500kb of a lead variant at a given locus. Genes were subsequently filtered based on evidence of expression in human skeletal muscle and adipose tissue (GTEx v8) – the primary tissues where insulin-stimulated GLUT4 trafficking occurs[36]. Evidence of expression was considered where transcripts per million (TPM) greater than 1 was reported at least one of these tissues for a given gene.

We further assessed the expression of these genes in differentiated 3T3-L1 adipocytes in a publicly available RNA-sequencing dataset (GEO accession: GSE129957; FPKM >1), and by qPCR (see below).[82]

36 genes at genetic loci associated with IFC were depleted using short interfering RNA (siRNA) and the effect of gene knockdown on insulin-stimulated GLUT4 translocation was assessed in 3T3-L1 adipocytes (**Supplementary Figure 21**, **Supplementary Table 26**). These experiments were conducted in 3T3-L1 adipocytes stably expressing a GLUT4 construct (HA-GLUT4-mRuby3), and complementary experiments were conducted in wild type 3T3-L1 adipocytes to ensure findings were relevant to endogenous GLUT4 (**Supplementary Figure 25 and 26, Supplementary Tables 28 and 29**). Using this approach, knockdown of the kinases *Akt1* and *Akt2* as well as the Rab protein *Rab10* impaired insulin-stimulated HA-GLUT4-mRuby and endogenous GLUT4 translocation, as expected. [83,84] *Tbc1d4* knockdown suggested an increase in cell surface GLUT4, consistent with its role as a negative regulator of GLUT4 translocation[15] but this did not reach significance threshold of FDR < 5%. Based on testing a subset of 20 siRNAs by qPCR, including all genes reaching significance, as well as other genes where siRNA

knockdown did not affect GLUT4 trafficking, the average knockdown efficiency was 85% (**Supplementary Figure 23; Supplementary Table 32**).

Cell culture

3T3-L1 preadipocytes (originally obtained from Howard Green, Harvard Medical School) were maintained in Dulbecco's modified Eagle's medium (DMEM) supplemented with 10% foetal bovine serum (FBS) and GlutaMAX in a humidified incubator at 37 °C with 10% CO_2. For 3T3-L1 stable cell lines, preadipocytes were transduced with pBABE-puro retrovirus expressing HA-GLUT4-mRuby3. Puromycin (2 µg/mL) was used to select transduced cells. 3T3-L1 preadipocytes were seeded into 6 well plates and were differentiated into adipocytes. Differentiation was initiated at 100% confluence through addition of DMEM/FBS/GlutaMAX supplemented with 350 nM insulin, 0.5 mM 3-isobutyl-1-methylxanthine (IBMX), 250 nM dexamethasone, and 400 nM biotin. After 3 d, cells were moved to DMEM/FBS/GlutaMAX supplemented with 350 nM insulin for a further 3 d. Cells were reverse transfected with control or targeting siRNAs 6 d after the initiation of differentiation.

siRNA-mediated gene knockdown in differentiated adipocytes

Dharmacon siGenome siRNA pools (Horizon Discovery) to genes-of-interest (see **Supplementary Table 23** for details) and *Akt1 and Akt2, Tbc1d4, Rab10* as positive controls were resuspended in RNAse-free water in a laminar flow hood in RNAse free environment following manufacturer specifications. The concentration of resuspended siRNA was measured using Nanodrop and standardized to 25 µM. Aliquots of diluted siRNA were stored at -80°C and thawed on ice prior to use.

For reverse transfection, 2.5 µL of TransIT-X2 transfection reagent and 1.25 µL of siRNA (25 µM) was added to 63 µL Opti-MEM and incubated at room temperature for 30 min. 3T3-L1 adipocytes 6 days post-differentiation were trypsinised in 10x trypsin-EDTA at 37°C, resuspended in DMEM/FBS media and centrifuged at 200 x *g* for 5 min at room temperature. Pelleted cells were resuspended in DMEM/FBS/GlutaMAX (13.5 mL per 6-well plate) and 563 µL of resuspended cells were added to each tube of transfection reagent. Media containing cells and siRNA complexes were reseeded into Matrigel-coated 96-well plates (95 µL per well). For seeding of cells into 24- or 48-well plates, the amounts of OptiMEM, transfection reagent,

siRNA and cells were adjusted appropriately based on well area. After 24 h, cells were washed with DMEM/FBS/GlutaMAX and media was replaced every 24 h. Cells were assayed 96 h post-knockdown.

Knockdown of positive control genes, where involvement in GLUT4 trafficking is well established, was validated at the protein level by western blot (**Extended Data Figure 9**). Knockdown of genes that were identified to be of interest following GLUT4 translocation assay were validated at the mRNA level by qPCR (**Supplementary Figure 25**). See methods below for further details.

GLUT4 translocation assay

Assay design

siRNA knockdown in each experiment was performed in technical duplicates. Non-targeting (NT) siRNA was used as the control condition in all experiments, with three sets of NT control per assay plate. Positive control siRNA targeting *Akt1 and Akt2, Tbc1d4, Rab10* mRNA were included in all experiments.

Insulin stimulation and immunofluorescence staining

96 h after transfection cells were washed 3x in serum-free DMEM and incubated in DMEM/GlutaMAX/0.2% BSA for 2 h. Cells were stimulated with 0.5 nM or 100 nM insulin for 20 min. Cells were washed by gently immersing the 96-well plates 12 times in beakers containing ice-cold PBS (6 washes in each of two 1 L beakers containing PBS; all the subsequent PBS washes were performed using this method). Plates were placed on ice and residual PBS was removed with a multichannel pipette. Cells were fixed with 4% paraformaldehyde (PFA) for 5 min on ice, and 15 min at room temperature. PFA was quenched with 50 mM glycine in PBS for 10 min. Cells were washed in PBS and blocked with 5% Normal Swine Serum (NSS, Dako, X0901) in PBS for 20 min. Cells were then incubated with primary antibody solution in 2% NSS in PBS for 1 h at room temperature. For detecting endogenous PM GLUT4 in wild type 3T3-L1 adipocytes, cells were incubated with human anti-GLUT4 antibody (1:1000; LM048; antibody kindly provided by Joseph Rucker, Integral Molecular, PA, USA)[85]. For detecting PM HA-GLUT4-mRuby3, cells were incubated with mouse anti-HA (1:500, Covance, MMS-101R). After PBS washes, cells were incubated with secondary

antibody solution in 2% NSS in PBS containing Hoechst 33342 (1:5000; Life Technologies) for 1 h at room temperature. For detecting endogenous GLUT4, we used Alexa-488-conjugted anti-human IgG antibody (1:500; Life Technologies). For HA-GLUT4-mRuby3 expressing cells, we used Alexa-488-conjugted anti-mouse IgG antibody. 1:500; (Life Technologies). Cells were washed 12 times in RT PBS and stored in PBS containing 2.5% DABCO, 10% glycerol, pH 8.5, sealed and kept at 4°C in the dark prior to imaging. Plates were equilibrated to room temperature for 30 min before imaging.

Plates were imaged on the Perkin Elmer Opera Phenix High Content Screening System and mid-section confocal images were obtained using a 20x water objective (N.A 1.0), with 2-pixel binning. Excitation wavelengths and emission filters used were as follows: endogenous surface GLUT4 and HA-tagged surface GLUT4: 488 nm, 500-550 nm; endogenous total GLUT4 and mRuby-tagged total GLUT4: 561 nm, 570-630 nm; Hoechst: 405 nm, 435-480 nm. The microscope settings were automated and pre-defined before imaging of the entire plate, meaning identical positions in each well were sampled across all wells/siRNA knockdown conditions without any human supervision. Six to eight positions in the centre of each well were selected for imaging. As knockdowns were performed in technical duplicates across two 96-well plates, for samples where 8 fields of view were captured per a well each condition represents the mean of 16 images, per biological replicate. Following acquisition, positions across each plate and well were inspected at random to ensure proper seeding/staining for quality assurance.

All targeting siRNAs were assigned numbers throughout the entire screen to preserve anonymity. The seeding order was rearranged for each biological replicate to control for any variability arising from the well position in the plate.

To quantify total endogenous GLUT4 expression, in WT 3T3-L1 adipocytes, cells were permeabilised and stained with anti-GLUT4 antibody after plates had been imaged for surface GLUT4. Cells were permeabilised in 5% NSS in PBS containing 0.1% saponin for 20 min, followed by incubation in 2% NSS in PBS containing rabbit anti-GLUT4 antibody (1:200; Courtesy of Professor David James, University of Sydney)[86]. After washing with PBS, cells were incubated with 2% NSS in PBS containing Alexa-568-conjugated goat anti-rabbit IgG antibody

(1:500; Life Technologies) for 1 h at room temperature. Plates were then re-imaged on the Perkin Elmer Opera Phenix High Content Screening System as described above.

Imaging data analysis

Imaging data were analysed using Harmony phenoLOGIC Software (v4.9; Perkin Elmer). For endogenous GLUT4 indicated by the Alexa 488 signal was quantified for surface GLUT4 prior to permeabilisation and total GLUT4 following permeabilisation and re-staining with Alexa-568 (see above). Surface GLUT4 was quantified in HA-GLUT4-mRuby cells by Alexa-488 antibody and total GLUT4 by the mRuby signal. Nuclei were quantified using the Hoechst signal, and nuclei were defined and quantified using pre-set method A. Surface and total GLUT4 staining were quantified by taking the mean intensity across the entire field of view – the fluorescence intensity across 8 fields of view were then averaged to provide a final fluorescence intensity for each well. The intensity across two technical replicates (wells on separate 96-well plates) were then averaged providing a mean intensity for 16 fields of view, per biological replicate. The surface GLUT4 levels were subsequently normalised to nuclei number. The ratio of surface to total GLUT4 levels were calculated from the surface GLUT4 levels normalised to the total GLUT4 signal.

Data processing and statistical analysis

Experimental measures per plate were normalised to the average signal of all conditions across each plate for a given parameter Differences in mean measures for a given knockdown were compared to the non-targeting control values using a two-sided t-test in R (v4.0.4) across all replicates (N biological endogenous GLUT4 = 3; N biological replicates HA-GLUT4-mRuby = 5, 2 technical replicates per N). Significance was considered at a false discovery rate of 5% (FDR < 5%). Candidate genes which were significantly different to control ($q < 0.05$) for surface/nuclei# and/or surface/total GLUT4 in at least 1 of the assayed cell lines were taken forward for Radiolabelled Glucose Transport Assays.

Radiolabelled glucose transport assay

Following siRNA-knockdown, 3T3-L1 adipocytes were serum-starved for 2 h in DMEM containing 0.2% BSA and GlutMAX media in a humidified incubator, 37°C 10% CO_2. Cells were washed three times in pre-warmed Krebs-Ringer buffer (KRP; 0.6 mM Na_2HPO_4, 0.4 mM

NaH_2PO_4, 120 mM NaCl, 6 mM KCl, 1 mM $CaCl_2$, 1.2 mM $MgSO_4$ and 12.5 mM HEPES (pH 7.4)) at 37°C. Cells were stimulated with 0.5 nM insulin for 20 min where indicated. To determine the non-specific glucose uptake 25 µM cytochalasin B (Sigma Aldrich) was added to the wells before the addition of H^3-2-deoxyglucose (2DOG). During the final 5 min of insulin stimulation, 2DOG (0.25 µCi, 50 µM unlabelled 2DOG) was added to wells to measure glucose uptake rates. Following three washes in ice-cold PBS, cells were solubilized in 1% (w/v) Triton X-100 in PBS on a shaker for 1 h. Tracer uptake was assessed by liquid scintillation counting using a β-scintillation counter. Values for all samples were normalized to protein content, as determined by bicinchoninic acid (BCA) assay (Thermo Fisher Scientific).

Confirmation of gene knockdown

Gene knockdown by siRNA was confirmed by qPCR for a subset of 20 targets, including all genes where knockdown resulted in a significant impact on GLUT4 (**Supplementary Note, Supplementary Table 31 and 32; Supplementary Figure 23**). For genes already established to be implicated in GLUT4 trafficking – Irs1, Lnpep, Tbc1d4, Slc2a4 and Akt, SDS-PAGE and immunoblotting was also used to confirm knockdown at the protein level (**Extended Data Figure 9**). Further details can be found in the **Supplementary Note**.

Data Availability

GWAS summary statistics will be made available on the MAGIC Investigators Website (https://magicinvestigators.org/downloads/) and GWAS catalog (https://www.ebi.ac.uk/gwas/home): GCST90267567, GCST90267568, GCST90267569, GCST90267570, GCST90267571, GCST90267572, GCST90267573, GCST90267574, GCST90267575, GCST90267576, GCST90267577, GCST90267578.

Data from the Fenland cohort can be requested by bona fide researchers for specified scientific purposes via the study website (https://www.mrc-epid.cam.ac.uk/research/studies/fenland/information-for-researchers/). Data will either be shared through an institutional data sharing agreement or arrangements will be made for analyses to be conducted remotely without the necessity for data transfer.

All data used in genetic risk score association analyses are available from the UK Biobank (UKBB) upon application (https://www.ukbiobank.ac.uk). All analyses in UKBB in this manuscript were conducted under application # 44448. Further details about the RISC Study and data availability can be found here: http://www.egir.org/egirrisc/ . The Genotype-Tissue Expression (GTEx) Project was supported by the Common Fund of the Office of the Director of the National Institutes of Health, and by NCI, NHGRI, NHLBI, NIDA, NIMH, and NINDS. The data used for the analyses described in this manuscript can be obtained from the GTEx Portal (https://www.gtexportal.org/home/) and dbGaP accession number phs000424.v8.p2. Genome regulatory annotations from ENCODE (https://www.encodeproject.org/) and Roadmap Epigenomics Consortium (https://egg2.wustl.edu/roadmap/web_portal/) were explored via UCSC Genome Browser (http://genome.ucsc.edu). Published differentiated 3T3-L1 RNA sequencing data used in this study is available from GEO accession GSE129957 (https://www.ncbi.nlm.nih.gov/geo/)

Code Availability

No previously unreported custom code or algorithm was used to generate results. The following software and packages were used for data analysis: METAL v.2011-03-25 (http://csg.sph.umich.edu/abecasis/Metal/download/), random-metal v2017-07-24 (https://github.com/explodecomputer/random-metal), LD score regression v.1.0.1

(https://github.com/bulik/ldsc), R v 3.6.0 and v.4.0.3 (https://www.r-project.org/). R packages coloc v 5.1.0 (https://cran.r-project.org/web/packages/coloc/), Hyprcoloc v1.0 (https://github.com/jrs95/hyprcoloc). GCTA 1.26.0 (https://yanglab.westlake.edu.cn/software/gcta/#Overview). Easy QC v17.8 (https://www.uni-regensburg.de/medizin/epidemiologie-praeventivmedizin/genetische-epidemiologie/software/index.html). Associated code and scripts used in this manuscript are available on GitHub: https://github.com/MRC-Epid/GWAS_postchallenge_insulin.[87]

Methods Only References

58. Stumvoll, M., Van Haeften, T., Fritsche, A. & Gerich, J. Oral glucose tolerance test indexes for insulin sensitivity and secretion based on various availabilities of sampling times [11]. *Diabetes Care* vol. 24 796–797 (2001).
59. Lindsay, T. *et al.* Descriptive epidemiology of physical activity energy expenditure in UK adults (The Fenland study). *Int. J. Behav. Nutr. Phys. Act.* **16**, (2019).
60. Hills, S. A. *et al.* The EGIR-RISC Study (the European group for the study of insulin resistance: Relationship between insulin sensitivity and cardiovascular disease risk): I. Methodology and Objectives. *Diabetologia* **47**, 566–570 (2004).
61. McCarthy, S. *et al.* A reference panel of 64,976 haplotypes for genotype imputation. *Nat. Genet.* **48**, 1279–1283 (2016).
62. Auton, A. *et al.* A global reference for human genetic variation. *Nature* **526**, 68–74 (2015).
63. Lim, E. T. *et al.* Distribution and Medical Impact of Loss-of-Function Variants in the Finnish Founder Population. *PLoS Genet.* **10**, e1004494 (2014).
64. FinnGen. FinnGen Documentation of R3 release. https://finngen.gitbook.io/documentation/ (2020).
65. Winkler, T. W. *et al.* Quality control and conduct of genome-wide association meta-analyses. *Tsegaselassie Work.* **12**, 1192–1212 (2014).
66. Willer, C. J., Li, Y. & Abecasis, G. R. METAL: Fast and efficient meta-analysis of genomewide association scans. *Bioinformatics* **26**, 2190–2191 (2010).
67. Scott, R. A. *et al.* Large-scale association analyses identify new loci influencing glycemic traits and provide insight into the underlying biological pathways. *Nat. Genet.* **44**, 991–1005 (2012).
68. Yang, J. *et al.* Conditional and joint multiple-SNP analysis of GWAS summary statistics identifies additional variants influencing complex traits. *Nat. Genet.* **44**, 369–75, S1-3 (2012).
69. GitHub - explodecomputer/random-metal: Adding random effects model to the METAL software. https://github.com/explodecomputer/random-metal.
70. Wakefield, J. Bayes factors for genome-wide association studies: comparison with P-values. *Genet. Epidemiol.* **33**, 79–86 (2009).
71. Giambartolomei, C. *et al.* Bayesian Test for Colocalisation between Pairs of Genetic Association Studies Using Summary Statistics. *PLOS Genet.* **10**, e1004383 (2014).
72. Wang, Q. *et al.* Rare variant contribution to human disease in 281,104 UK Biobank

exomes. *Nat. 2021 5977877* **597**, 527–532 (2021).
73. Bulik-Sullivan, B. *et al.* LD Score regression distinguishes confounding from polygenicity in genome-wide association studies. *Nat. Genet. 2015 473* **47**, 291–295 (2015).
74. Finucane, H. K. *et al.* Heritability enrichment of specifically expressed genes identifies disease-relevant tissues and cell types. *Nat. Genet.* **50**, 621 (2018).
75. Foley, C. N. *et al.* A fast and efficient colocalization algorithm for identifying shared genetic risk factors across multiple traits. *Nat. Commun. 2021 121* **12**, 1–18 (2021).
76. Zhu, C. H. *et al.* Cellular senescence in human myoblasts is overcome by human telomerase reverse transcriptase and cyclin-dependent kinase 4: Consequences in aging muscle and therapeutic strategies for muscular dystrophies. *Aging Cell* **6**, 515–523 (2007).
77. Fogarty, M. P., Cannon, M. E., Vadlamudi, S., Gaulton, K. J. & Mohlke, K. L. Identification of a Regulatory Variant That Binds FOXA1 and FOXA2 at the CDC123/CAMK1D Type 2 Diabetes GWAS Locus. *PLoS Genet.* **10**, (2014).
78. Roman, T. S. *et al.* A type 2 diabetes-associated functional regulatory variant in a pancreatic islet enhancer at the ADCY5 locus. in *Diabetes* vol. 66 2521–2530 (Diabetes, 2017).
79. Lotta, L. A. *et al.* Integrative genomic analysis implicates limited peripheral adipose storage capacity in the pathogenesis of human insulin resistance. *Nat Genet* **49**, 17–26 (2017).
80. Leland Taylor, D. *et al.* Integrative analysis of gene expression, DNA methylation, physiological traits, and genetic variation in human skeletal muscle. *Proc. Natl. Acad. Sci. U. S. A.* 10883–10888 (2019).
81. Kuhn, R. M., Haussler, D. & Kent, W. J. The UCSC genome browser and associated tools. *Brief. Bioinform.* **14**, 144–61 (2013).
82. Sun, W. *et al.* A Transcriptomic Analysis Reveals Novel Patterns of Gene Expression During 3T3-L1 Adipocyte Differentiation. *Front. Mol. Biosci.* **7**, 249 (2020).
83. Ng, Y., Ramm, G., Lopez, J. A. & James, D. E. Rapid activation of Akt2 is sufficient to stimulate GLUT4 translocation in 3T3-L1 adipocytes. *Cell Metab.* **7**, 348–356 (2008).
84. Kohn, A. D., Summers, S. A., Birnbaum, M. J. & Roth, R. A. Expression of a constitutively active Akt Ser/Thr kinase in 3T3-L1 adipocytes stimulates glucose uptake and glucose transporter 4 translocation. *J. Biol. Chem.* **271**, 31372–31378 (1996).
85. Tucker, D. F. *et al.* Isolation of state-dependent monoclonal antibodies against the 12-transmembrane domain glucose transporter 4 using virus-like particles. *Proc. Natl. Acad. Sci. U. S. A.* **115**, E4990–E4999 (2018).
86. Diaz-Vegas, A. *et al.* A high-content endogenous GLUT4 trafficking assay reveals new aspects of adipocyte biology. *Life Sci. alliance* **6**, (2023).
87. DOI: https://zenodo.org/record/7805583#.ZC7C_exBxhE

Extended Data Figures

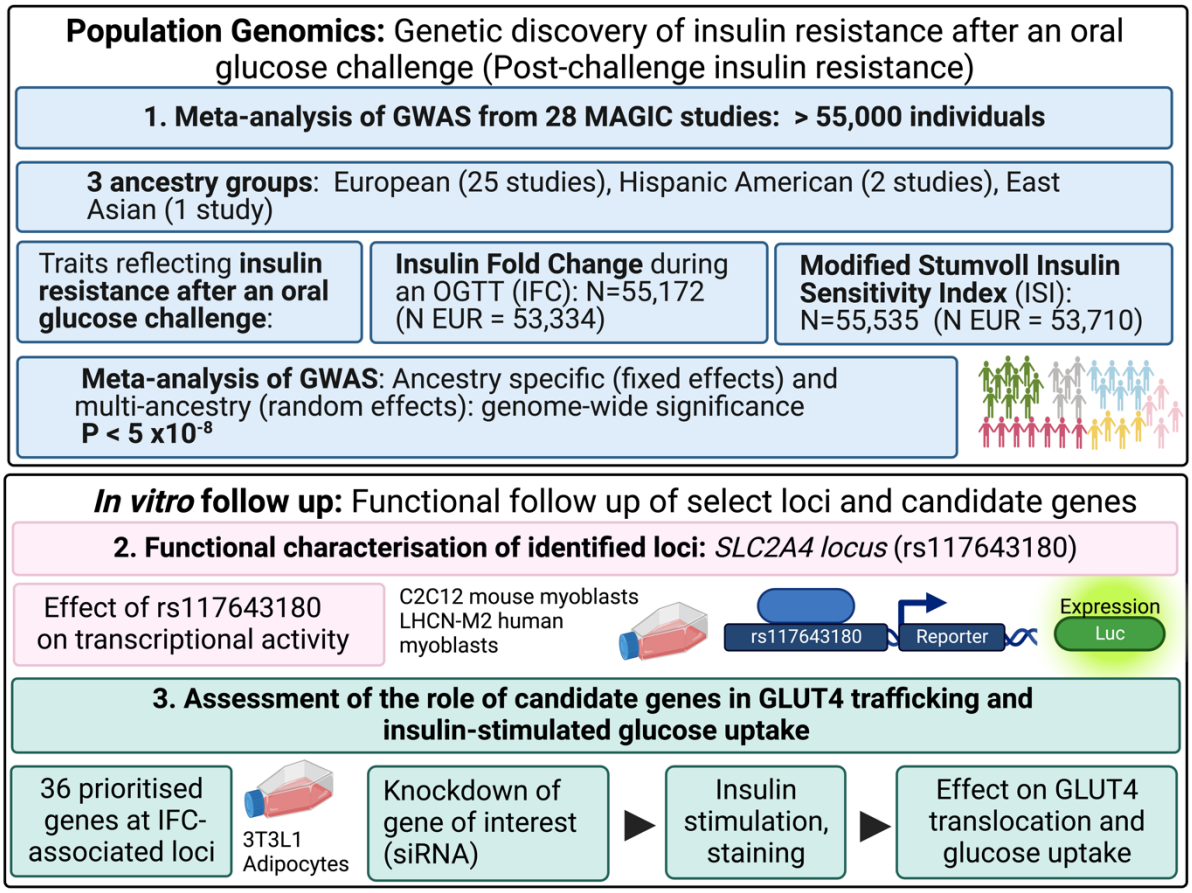

Extended Data Figure 1: Overview of genetic discovery for insulin fold change and Modified Stumvoll ISI, and downstream genetic and in vitro studies.
Created with BioRender.com.

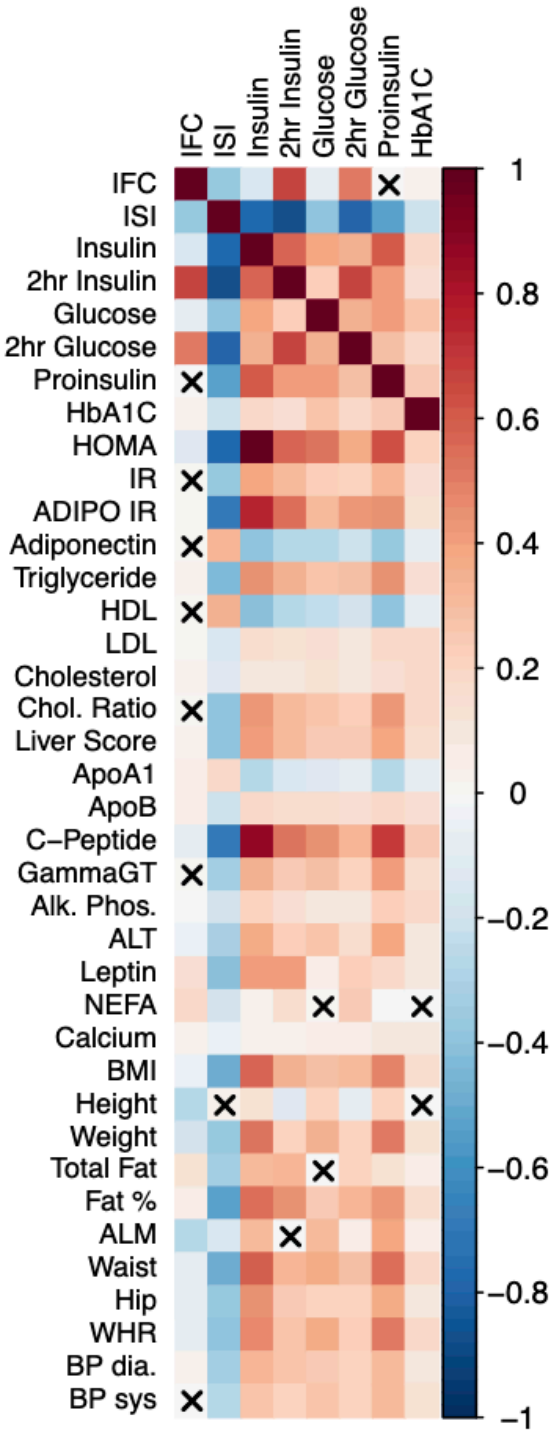

Extended Data Figure 2: Observational Correlation of Insulin Fold Change and Modified Stumvoll ISI with metabolic traits in the Fenland Study.

Pairwise Spearman's Rank correlation. Red shades denote positive correlation, blue shared denote negative correlation between trait pairs. X denotes no significant correlation ($P > 0.05$).

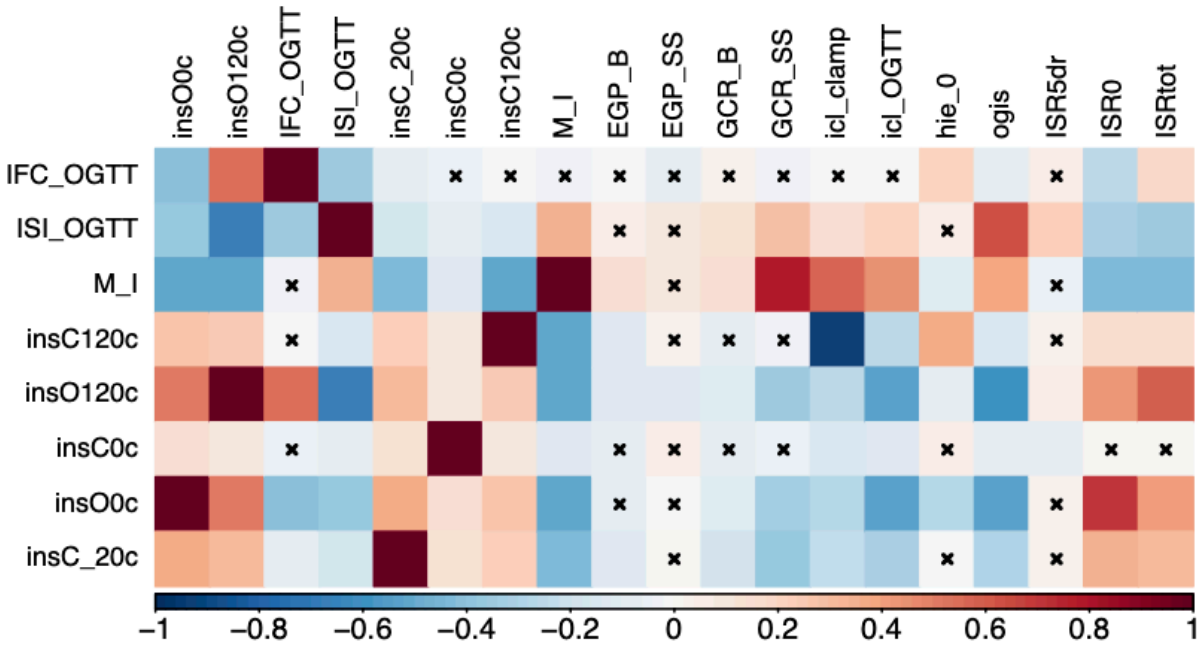

Extended Data Figure 3: Observational Correlation of insulin sensitivity and clearance related traits in the RISC study.

Pairwise Spearman's Rank correlation. Red shades denote positive correlation, blue shared denote negative correlation between trait pairs, legend along bottom of heatmap shows colour scale relative to rho value. X denotes no significant correlation ($P > 0.05$). Abbreviations denote: IFC_OGTT – IFC calculated using OGTT measures, ISI_OGTT – Modified Stumvoll ISI calculated using OGTT measures. M_I – M/I index of insulin sensitivity measured by clamp. InsC0c – insulin measured at 0min during clamp. InsO0c - insulin measured at 0min during OGTT. InsC120c – insulin measured at 120min during clamp. InsO120c - insulin measured at 120min during OGTT. InsC_20c – insulin measured at 20min before clamp. EGP_B -basal glucose production, EGP_SS - glucose production during clamp, GCR_B - basal glucose clearance, ml/min/kg lean body mass, GCR_SS - steady state glucose clearance, ml/min/kg lean body mass, icl_clamp - peripheral insulin clearance (1/min/m²), icl_OGTT - endogenous "pre-hepatic" clearance during the OGTT, hie_0 - hepatic insulin extraction during clamp, OGIS - oral glucose insulin sensitivity index (ml min-1 m-2). ISR5dr - insulin secretion 5 mM glucose, beta cell dose response (pmol min-1m-2). ISR0 basal insulin secretion (pmol min-1m-2). ISRtot - total insulin secretion (nmol m-2).

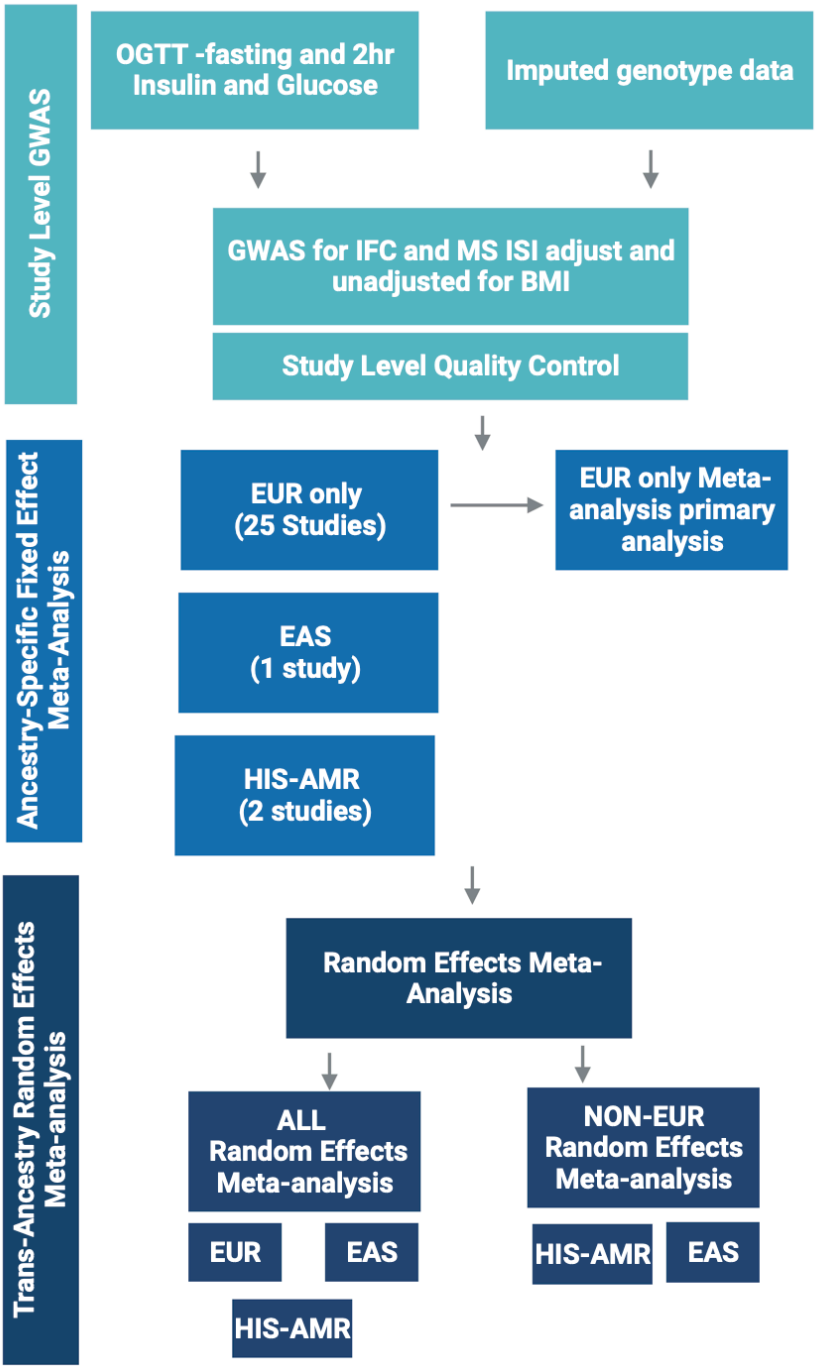

Extended Data Figure 4: Meta-analysis workflow for genetic discovery analyses
Analysis workflow for the meta-analysis of study-level GWAS results for Insulin fold change and Modified Stumvoll ISI. Created with BioRender.com

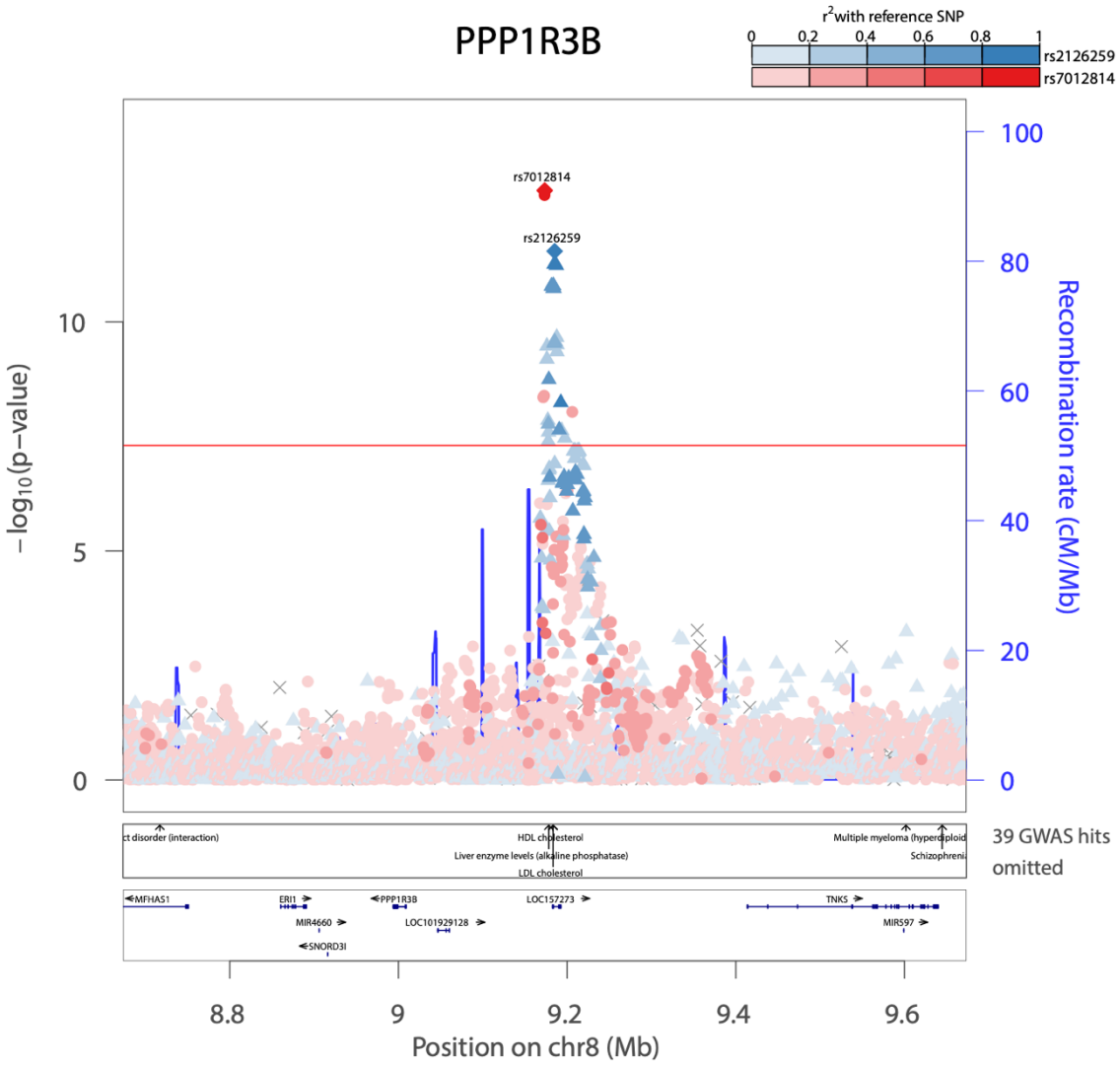

Extended Data Figure 5: Two independent signals were identified at *PPP1R3B* for insulin fold change

Conditional analyses identify a second independent signal at *PPP1R3B* for insulin fold change adjusted for BMI. The regional association plot shows the primary signal in red and the secondary signal in blue for marginal summary statistics for insulin fold change adjusted for BMI. Shade of point indicates pairwise LD (R^2) with indicated lead variant.

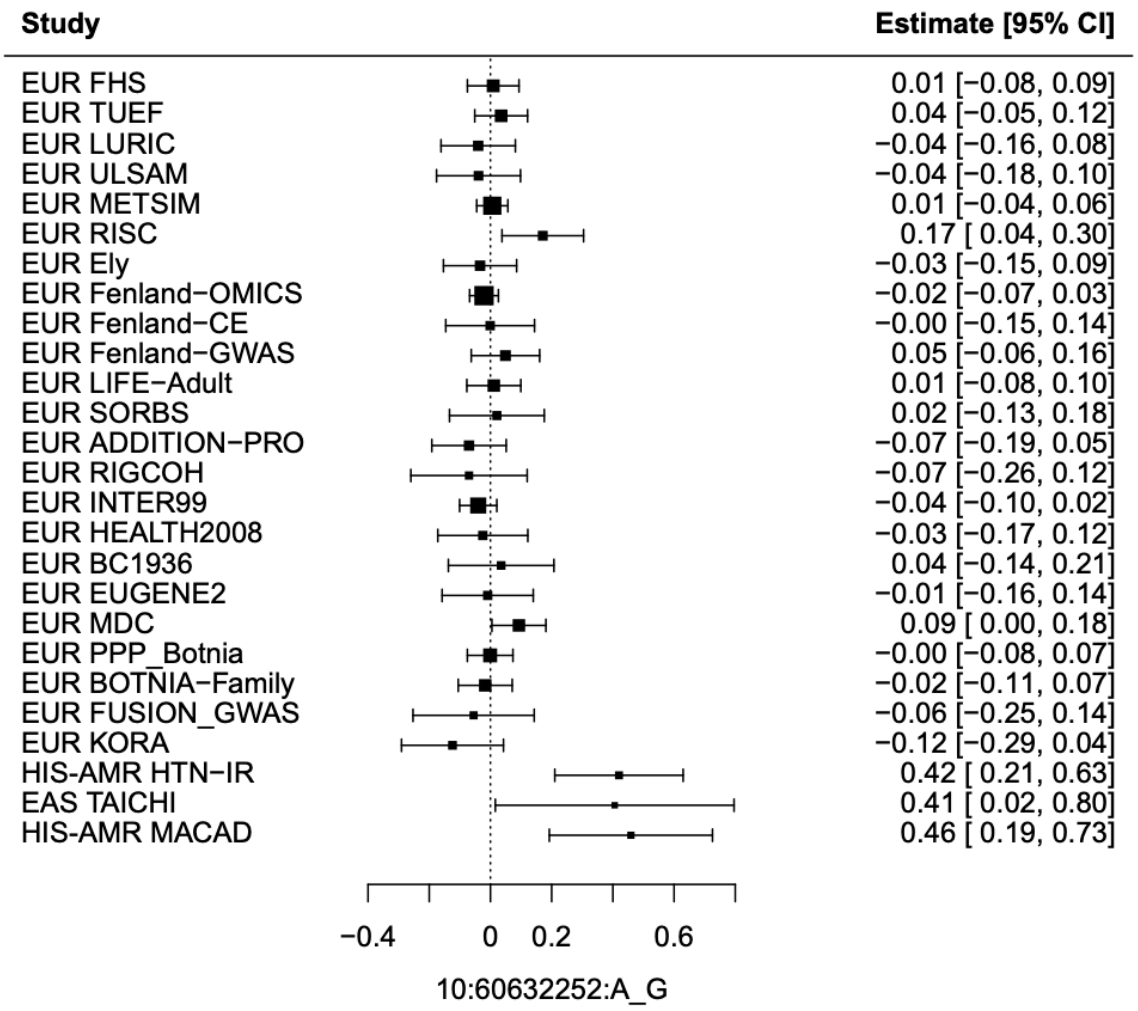

Extended Data Figure 6: Forest plot of beta estimates for the association of rs60453193 with insulin fold change in individual cohorts.

Labels on the right-hand side indicate the ancestry of the study and study name. EUR- European ancestry, HISAMR – Hispanic American ancestry, EAS – East Asian ancestry. Left-hand side values are beta estimate and 95% confidence interval. Error bars denote a 95% confidence interval. X-axis denotes the beta estimate of associations with insulin fold change in BMI adjusted analyses.

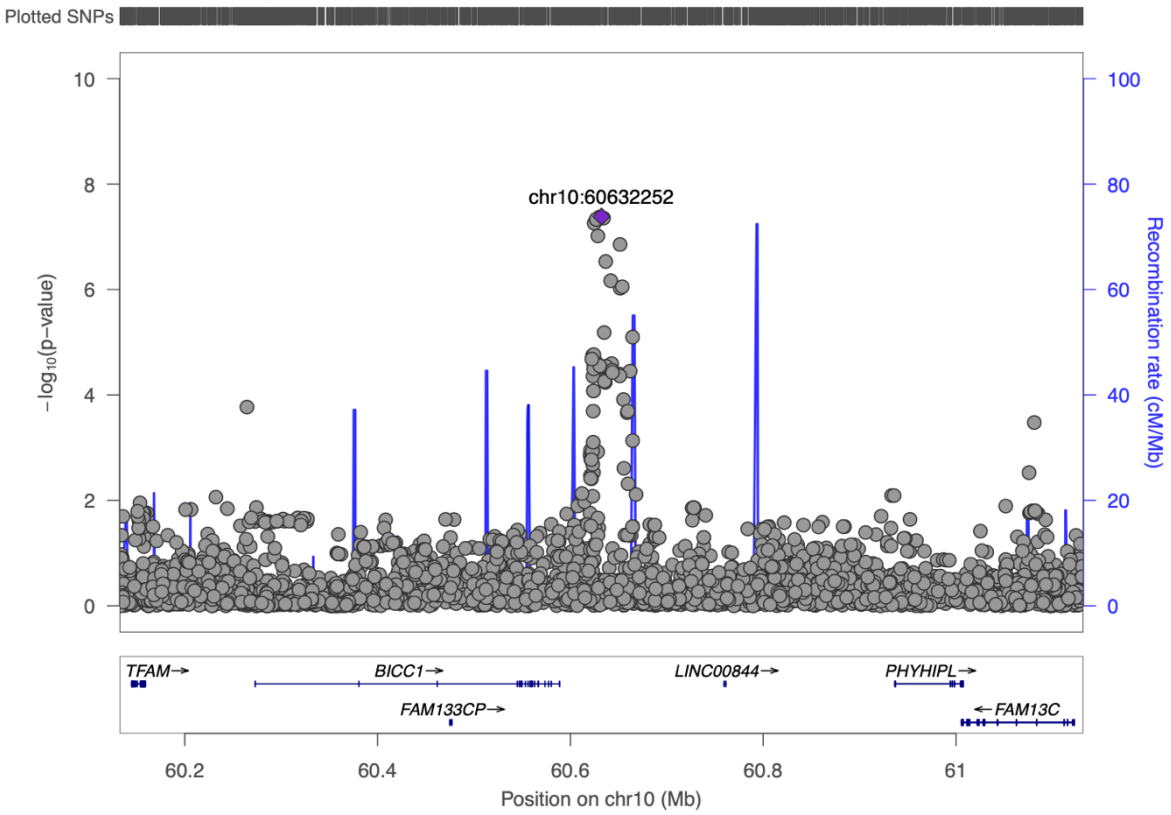

Extended Data Figure 7: Regional association plot at *BICC1* (rs60453193)for insulin fold change in meta-analysis of non-European cohorts.

Unadjusted -log10 p-values are indicated on the y axis. Lead variant indicated by purple diamond.

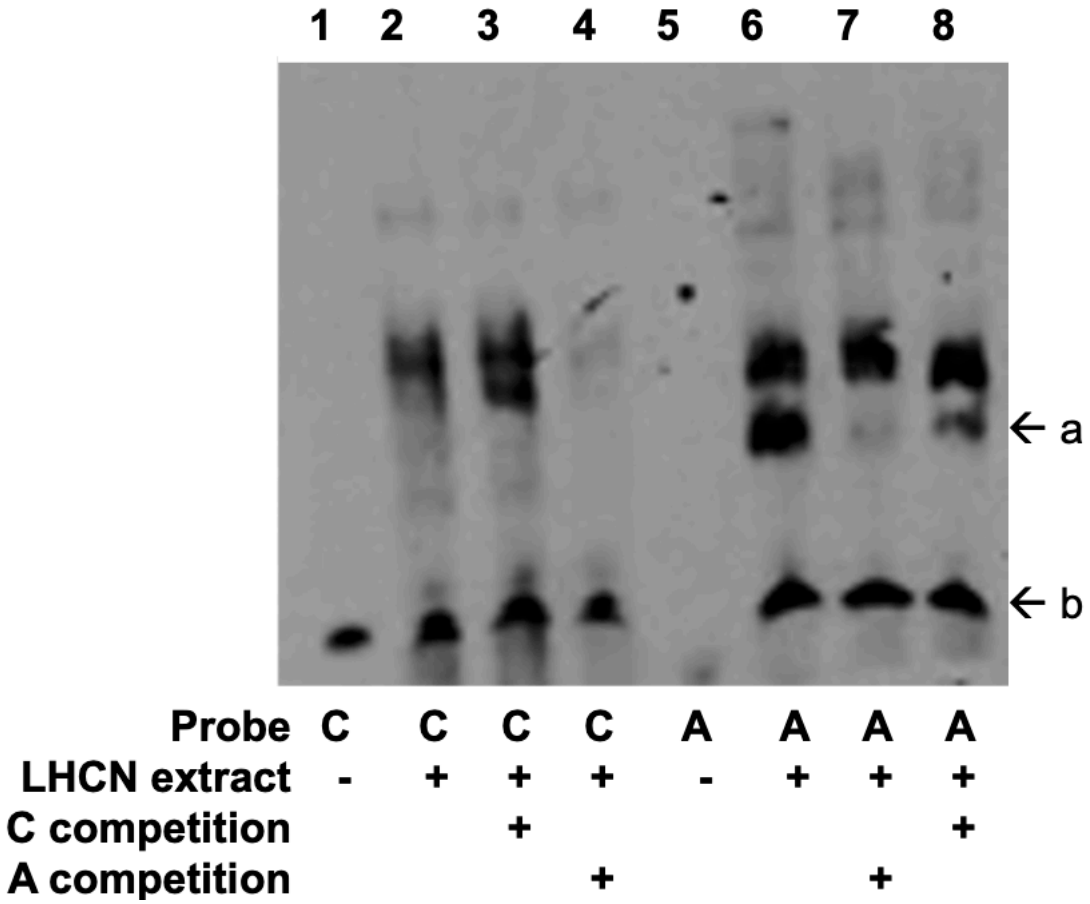

Extended Data Figure 8: rs117643180 exhibits allelic differences in transcription factor binding.

An EMSA using 6µg per lane of nuclear extract from undifferentiated LHCN-M2 cells shows protein-DNA interactions for probes centered around each both alleles of rs117643180. The probe containing rs117643180-A shows allele-specific protein binding (Arrow A, lane 6), relative to the probe containing rs117643180-C (lane 2). A 25-fold excess unlabeled probe containing the A allele competed away A-specific bands more effectively (lane 7) than 25-fold excess unlabeled probe containing the C allele (lane 8). Arrow B shows a biotinylated free probe (200 fmol per lane). Uncropped image is available in Source Data.

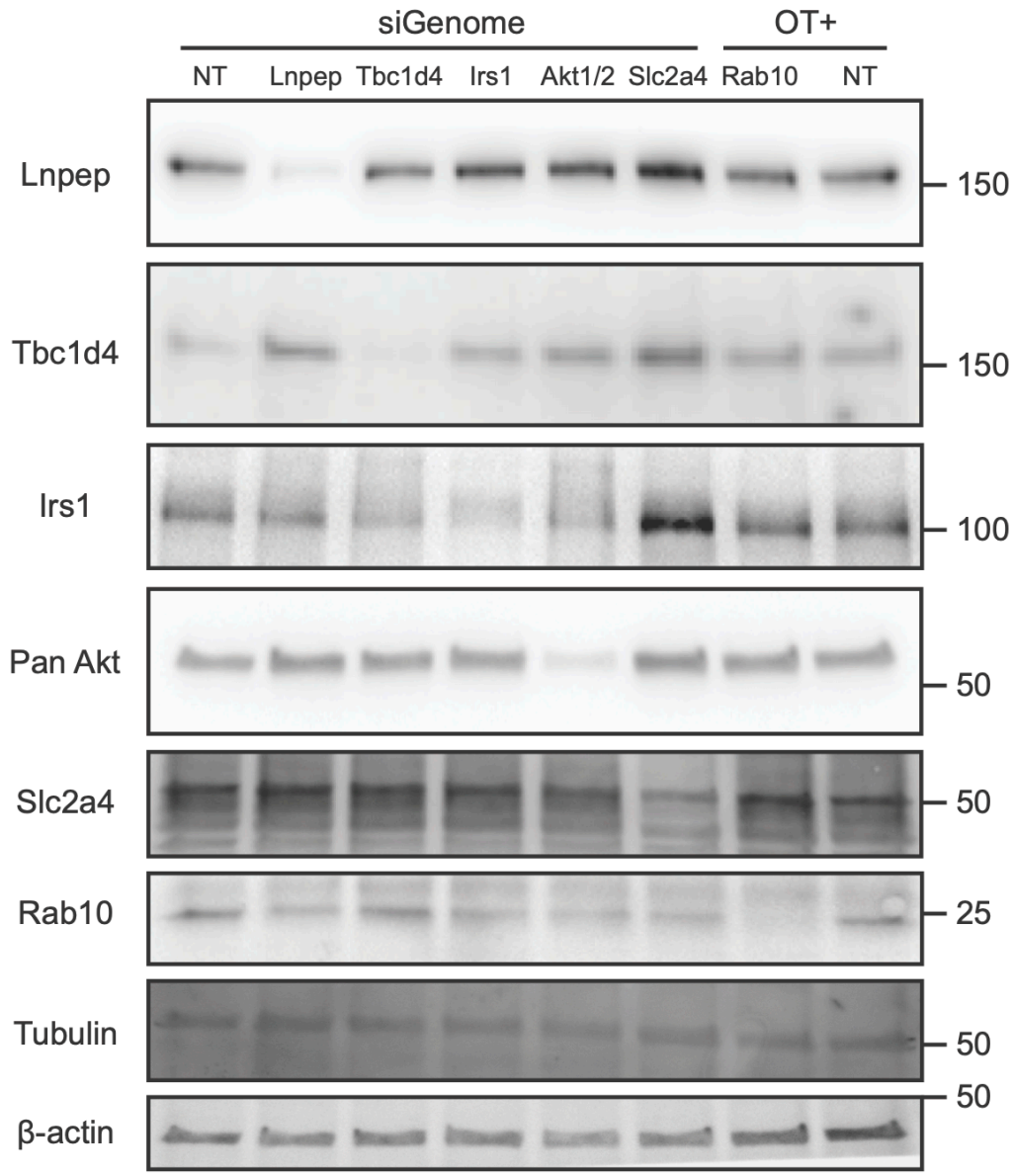

Extended Data Figure 9: Confirmation of knockdown of positive control genes in wildtype 3T3-L1 adipocytes by Western Blot.

Representative blot from N=2. Marker indicates protein size in kDa is outlined on the right-hand side of the blot. siGenome and OT+ represent siRNA pools with their corresponding targets indicated below (see methods) and NT denotes non-targeting control. Antibodies are outlined on the left-hand side of the blot with Tubulin and B-actin used as loading controls. Uncropped blots are provided in Source Data.

Supplementary Note:

Contents

Study Acknowledgements

Study	Acknowledgements
ADDITION-PRO	The ADDITION-PRO study was funded by an unrestricted grant from the European Foundation for the Study of Diabetes/Pfzer for Research into Cardiovascular Disease Risk Reduction in Patients with Diabetes (74550801), by the Danish Council for Strategic Research and by internal research and equipment funds from Steno Diabetes Center
Botnia Family Study	The Botnia Family Study and the PPP Botnia Study have been financially supported by grants from Folkhälsan Research Foundation, the Sigrid Juselius Foundation, The Academy of Finland (grants no. 263401, 267882, 312063 and 336822 to LG; 312072 and 336826 to TT), University of Helsinki, Nordic Center of Excellence in Disease Genetics, EU (EXGENESIS, MOSAIC FP7-600914), Ollqvist Foundation, Swedish Cultural Foundation in Finland, Finnish Diabetes Research Foundation, Foundation for Life and Health in Finland, Signe and Ane Gyllenberg Foundation, Finnish Medical Society, Paavo Nurmi Foundation, State Research Funding via the Helsinki University Hospital, Perklén Foundation, Närpes Health Care Foundation and Ahokas Foundation. The study has also been supported by the Ministry of Education in Finland, Municipal Heath Care Center and Hospital in Jakobstad and Health Care Centers in Vasa, Närpes and Korsholm. The research leading to these results has received funding from the European Research Council under the European Union's Seventh Framework Programme (FP7/2007-2013) / ERC grant agreement n° 269045. The skillful assistance of the Botnia Study Group is gratefully acknowledged.
Botnia PPP	The Botnia Family Study and the PPP Botnia Study have been financially supported by grants from Folkhälsan Research Foundation, the Sigrid Juselius Foundation, The Academy of Finland (grants no. 263401, 267882, 312063 and 336822 to LG; 312072 and 336826 to TT), University of Helsinki, Nordic Center of Excellence in Disease Genetics, EU (EXGENESIS, MOSAIC FP7-600914), Ollqvist Foundation, Swedish Cultural Foundation in Finland, Finnish Diabetes Research Foundation, Foundation for Life and Health in Finland, Signe and Ane Gyllenberg Foundation, Finnish Medical Society, Paavo Nurmi Foundation, State Research Funding via the Helsinki University Hospital, Perklén Foundation, Närpes Health Care Foundation and Ahokas Foundation. The study has also been supported by the Ministry of Education in Finland, Municipal Heath Care Center and Hospital in Jakobstad and Health Care Centers in Vasa, Närpes and Korsholm. The research leading to these results has received funding from the European Research Council under the European Union's Seventh Framework Programme (FP7/2007-2013) / ERC grant agreement n° 269045. The skillful assistance of the Botnia Study Group is gratefully acknowledged.
DIAGEN	The DIAGEN study was supported by the Commission of the European Communities, Directorate C -Public Health and Risk Assessment, Health & Consumer Protection, Grant Agreement number - 2004310 and by the Dresden University of Technology Funding Grant, Med Drive. We are grateful to all of the patients who cooperated in this study and to their referring physicians and diabetologists in Saxony.
DPS	The DPS has been financially supported by grants from the Academy of Finland (117844 and 40758, 211497, and 118590; The EVO funding of the Kuopio University Hospital from Ministry of Health and Social Affairs
DR's EXTRA Study	The DR's EXTRA study was supported by grants from Ministry of Education and Culture of Finland, Academy of Finland, European Commission FP6 Integrated Project (EXGENESIS), LSHM-CT-2004-005272, City of Kuopio, Juho Vainio Foundation, Finnish Diabetes Association, Finnish Foundation for Cardiovascular Research, Kuopio University Hospital, Päivikki and Sakari Sohlberg Foundation, Social Insurance Institution of Finland.
Ely	The Ely study was supported by the Medical Research Council (MC_UU_12015/1) and NHS Research and Development.
FHS	The Framingham Heart Study (FHS) was supported by the National Heart, Lung and Blood Institute's Framingham Heart Study Contract Nos. N01-HC-25195, HHSN268201500001I amd 75N92019D00031, and its contract with Affymetrix, Inc for genotyping services (Contract No. N02-HL-6-4278).
FUSION GWAS	The study was supported by the National Institutes of Health (R01 DK062370, DK072193, DK093757; ZIA HG000024)

FUSION2	The study was supported by the National Institutes of Health (R01 DK062370, DK072193; ZIA HG000024)
Health2008	Health2008 was supported by the Timber Merchant Vilhelm Bang's Foundation, the Danish Heart Foundation (Grant number 07-10-R61-A1754-B838-22392F), and the Health Insurance Foundation (Helsefonden) (Grant number 2012B233).
HTN-IR / MACAD	Supported in part by contacts HL-088457 (MACAD), HL-0697974 (HTN-IR), HL-055798 (NIDDM-Athero), and DK-079888. Andy by the National Center for Advancing Translational Sciences, CTSI grant UL1TR001881, and the National Institute of Diabetes and Digestive and Kidney Disease Diabetes Research Center (DRC) grant DK063491 to the Southern California Diabetes Endocrinology Research Center. Infrastructure for the CHARGE Consortium is supported in part by the National Heart, Lung, and Blood Institute (NHLBI) grant R01HL105756
Inter99	The study was financially supported by research grants from the Danish Research Council, the Danish Centre for Health Technology Assessment, Novo Nordisk Inc., Research Foundation of Copenhagen County, Ministry of Internal Affairs and Health, the Danish Heart Foundation, the Danish Pharmaceutical Association, the Augustinus Foundation, the Ib Henriksen Foundation, the Becket Foundation, and the Danish Diabetes Association.
KORA	The KORA study was initiated and financed by the Helmholtz Zentrum München – German Research Center for Environmental Health, which is funded by the German Federal Ministry of Education and Research (BMBF) and by the State of Bavaria.
LIFE-Adult	LIFE-Adult was funded by the Leipzig Research Center for Civilization Diseases (LIFE). LIFE was funded by means of the European Union, the European Regional Development Fund (ERDF, grant 713-24120) and by means of the Free State of Saxony within the framework of the excellence initiative (14505/2470).
LURIC	We thank all participants of the LURIC study, as well as the study teams who were either temporarily or permanently involved in patient recruitment as well as sample and data handling. We also thank the laboratory staff at the Ludwigshafen General Hospital and the Universities of Freiburg, Ulm, and Heidelberg in Germany. The genotyping of the LURIC participants was supported by the 7th Framework Programs AtheroRemo (grant agreement number 201668) and RiskyCAD (grant agreement number 305739) of the European Union. LURIC received further support by the H2020 Programs TO_AITION (grant agreement number 848146) and TIMELY (grant agreement number 101017424) of the European Union and the Competence Cluster of Nutrition and Cardiovascular Health (nutriCARD), which is funded by the German Federal Ministry of Education and Research (grant agreement number 01EA1808).
METSIM	The METSIM study was supported by the Academy of Finland (321428) and Sigrid Juselius Foundation.
RIGCOH	The RigCoh-study was supported by The Lundbeck Foundation, Civilingeniør H. C. Bechgaard's Foundation, The Danish Diabetes Association, The Danish Medical Research Council, the Gangsted Foundation, A. P. Moeller og Hustru Chastine Mc-Kinney Moeller's Foundation, Aase og Ejner Danielsen's Foundation, The Augustinus Foundation, and The Research Foundation of Rigshospitalet
RISC	The RISC study was supported by the EU 5th Framework (EU contract QLG1-CT-2001-01252) with additional funding from AstraZeneca.
TAICHI-G	The TAICHI-G study was supported by grants from the National Health Research Institutes, Taiwan (PH-099-PP-03, PH-100-PP-03, and PH-101-PP-03); the National Science Council, Taiwan (NSC 101-2314-B-075A-006-MY3, MOST 104-2314-B-075A-006-MY3, MOST 104-2314-B-075A-007, and MOST 105-2314-B-075A-003); and the Taichung Veterans General Hospital, Taiwan (TCVGH-1020101C, TCVGH-1020102D, TCVGH- 1023102B, TCVGH-1023107D, TCVGH-1030101C, TCVGH- 1030105D, TCVGH-1033503C, TCVGH-1033102B, TCVGH-1033108D, TCVGH-1040101C, TCVGH-1040102D, TCVGH-1043504C, and TCVGH-1043104B). The provision of genotyping data was supported in part by the National Center for Advancing Translational Sciences, CTSI grant UL1TR001881, and the National Institute of Diabetes and Digestive and Kidney Disease Diabetes Research (DRC) grant DK063491
The Fenland Study	The Fenland Study (10.22025/2017.10.101.00001) is funded by the Medical Research Council (MC UU 12015/1). We are grateful to all the volunteers and to the General

	Practitioners and practice staff for assistance with recruitment. We thank the Fenland Study Investigators, Fenland Study Co-ordination team and the Epidemiology Field, Data and Laboratory teams. We further acknowledge support for genomics from the Medical Research Council (MC PC 13046).
SORBS	This project was supported by grants from the Deutsche Forschungsgemeinschaft (DFG, German Research Foundation – Projektnummer 209933838 – SFB 1052 "Obesity mechanisms") and by the German Diabetes Association.
TUEF	This study was supported in parts by a grant (01GI0925) from the Federal Ministry of Education and Research to the German Center for Diabetes Research.
ULSAM	Genotyping in Swedish cohorts was performed by the SNP&SEQ Technology Platform in Uppsala.

Individual Acknowledgments

First	Middle	Last	Acknowledgement
Emma		*Ahlqvist*	Swedish Research Council (Grant.no 2020-02191)
Mette	*K*	*Andersen*	Novo Nordisk Foundation (grant.nr. NNF18CC0034900)
Inês		Barroso	IB was funded by an "Expanding excellence in England" award from Research England. This study was supported by the National Institute for Health and Care Research Exeter Biomedical Research Centre. The views expressed are those of the author(s) and not necessarily those of the NIHR or the Department of Health and Social Care.
Michael		Boehnke	US NIH R01 DK062370
Lori	L	Bonnycastle	National Institutes of Health, National Human Genome Research Institute, ZIA HG000024
K.	Alaine	Broadway	US National Institutes of Health (NIH) T32HL129982
Yii-Der Ida		Chen	The TAICHI-G study was supported by grants from the National Health Research Institutes, Taiwan (PH-099-PP-03, PH-100-PP-03, and PH-101-PP-03); the National Science Council, Taiwan (NSC 101-2314-B-075A-006-MY3, MOST 104-2314-B-075A-006-MY3, MOST 104-2314-B-075A-007, and MOST 105-2314-B-075A-003); and the Taichung Veterans General Hospital, Taiwan (TCVGH-1020101C, TCVGH-1020102D, TCVGH-1023102B, TCVGH-1023107D, TCVGH-1030101C, TCVGH- 1030105D, TCVGH-1033503C, TCVGH-1033102B, TCVGH-1033108D, TCVGH-1040101C, TCVGH-1040102D, TCVGH-1043504C, and TCVGH-1043104B). The provision of genotyping data was supported in part by the National Center for Advancing Translational Sciences, CTSI grant UL1TR001881, and the National Institute of Diabetes and Digestive and Kidney Disease Diabetes Research (DRC) grant DK063491
Francis	S	Collins	National Institutes of Health, National Human Genome Research Institute, ZIA HG000024
Josée		Dupuis	NIH R01DK078616, UM1DK078616, R01HL151855 Grants: NIH U01 DK078616; NIH R01 HL151855 Individuals supported: James B Meigs (PI of both of these grants), Josée Dupuis, Ching-Ti Liu, Peitao Wu
Michael	R	Erdos	National Institutes of Health, National Human Genome Research Institute, ZIA HG000024

Tove		Fall	T.F. was supported by Swedish Research Council grants (nos. 2015-03477 and 2018-02784), grant support from the Göran Gustafsson Foundation, and by a Starting Grant from the European Research Council (GUTSY - 801965).
Daniel	J	Fazakerley	D.J.F. was supported by an UKRI-MRC Career Development Award MR/S007091/1
Jose	C	Florez	NIH K24 DK110550
Andreas		Fritsche	Deutsche Forschungsgemeinschaft (DFG) Deutsches Zentrum für Diabetesforschung (DZD)
Mark	O	Goodarzi	M.O.G. was supported by the Eris M. Field Chair in Diabetes Research.
Niels		Grarup	Novo Nordisk Foundation (grant.nr. NNF18CC0034900), Independent Research Fund Denmark (grant. nr. 1030-00280B)
Xiuqing		Guo	Supported in part by the American Diabetes Association Distinguished Clinical Scientist Award (BetaGene), HL-088457 (MACAD), HL-0697974 (HTN-IR), HL-055798 (NIDDM-Athero), and DK-079888.(work related to insulin clearance in HTN-IR, MACAD, and NIDDM-Athero). Also supported by the National Center for Advancing Translational Sciences, CTSI grant UL1TR001881, and the National Institute of Diabetes and Digestive and Kidney Disease Diabetes Research Center (DRC) grant DK063491 to the Southern California Diabetes Endocrinology Research Center. Infrastructure for the CHARGE Consortium is supported in part by the National Heart, Lung, and Blood Institute (NHLBI) grant R01HL105756
Torben		*Hansen*	Novo Nordisk Foundation (grant.nr. NNF18CC0034900)
Kurt		Højlund	The RISC Study was supported by European Union grant QLG1-CT-2001-01252, and AstraZeneca and Merck & Co Inc.
Anna		*Jonsson*	Novo Nordisk Foundation (grant.nr. NNF18CC0034900)
Markku		*Laakso*	Grant from Academy of Finland
Timo	A	Lakka	Academy of Finland (211119)
Claudia		Langenberg	Medical Research Council (MC_UU_00006/1 - Etiology and Mechanisms)
Cecilia	M	Lindgren	C.M.L is supported by the Li Ka Shing Foundation, NIHR Oxford Biomedical Research Centre, Oxford, NIH (1P50HD104224-01), Gates Foundation (INV-024200), and a Wellcome Trust Investigator Award (221782/Z/20/Z).
Ching-Ti		Liu	NIH R01DK078616, UM1DK078616, R01HL151855
Jian'an		Luan	Medical Research Council MC_UU_00006/1 - Etiology and Mechanisms
James	B	Meigs	NIH R01DK078616, UM1DK078616, R01HL151855
Karen	L	Mohlke	US NIH R01 DK072193, R01 DK093757, UM1 DK126185
Narisu		Narisu	National Institutes of Health, National Human Genome Research Institute, ZIA HG000024
Stephen		O'Rahilly	S.O. is supported by a Wellcome Investigator award (WT 095515/Z/11/Z) and the NIHR Cambridge Biomedical Research Centre
Rashmi	B	Prasad	Swedish Research Council (2021-02623)

Rainer		Rauramaa	Personal; Ministry of Education and Culture of Finland (722 and 627; 2004-2010); Academy of Finland (102318, 104943, 123885); European Commission FP6 Integrated Project (EXGENESIS), LSHM-CT-2004-005272; Social Insurance Institution of Finland 4/26/2010; Päivikki and Sakari Sohlberg Foundation; Finnish Diabetes Association; Finnish Foundation for Cardiovascular Research. Groups; City of Kuopio; Juho Vainio Foundation; Kuopio University Hospital;
Carsten	*F*	*Rundsten*	Novo Nordisk Foundation (grant.nr. NNF18CC0034900)
Chloé		Sarnowski	NIH R01DK078616, R01HL15185, NIH K99AG066849-02
Kai	P	Savonen	No conflicts of interest. No financial support to declare.
Sara	*E*	*Stinson*	Novo Nordisk Foundation (grant.nr. NNF18CC0034900, NNF18CC0033668)
Michael		*Stumvoll*	This project was supported by grants from the Deutsche Forschungsgemeinschaft (DFG, German Research Foundation – Projektnummer 209933838 – SFB 1052 "Obesity mechanisms") and by the German Diabetes Association.
Sufyan		*Suleman*	Novo Nordisk Foundation (grant.nr. NNF18CC0034900)
Kent	D	Taylor	This study was supported in part by the National Institutes of Health, National Heart, Lung, and Blood Institute contract R01 HL0767711. Also supported by the National Center for Advancing Translational Sciences, CTSI grant UL1TR001881, and the National Institute of Diabetes and Digestive and Kidney Disease Diabetes Research Center (DRC) grant DK063491 to the Southern California Diabetes Endocrinology Research Center. Infrastructure for the CHARGE Consortium is supported in part by the National Heart, Lung, and Blood Institute (NHLBI) grant R01HL105756.
Robert		Wagner	Deutsche Forschungsgemeinschaft (DFG) Deutsches Zentrum für Diabetesforschung (DZD)
Mark		Walker	The RISC Study was supported by European Union grant QLG1-CT-2001-01252, and AstraZeneca and Merck & Co Inc.
Nicholas	J	Wareham	Medical Research Council (MC_UU_00006/1 - Etiology and Mechanisms
Eleanor		Wheeler	Medical Research Council (MC_UU_00006/1 - Etiology and Mechanisms
Alice		Williamson	Medical Research Council (MC_UU_00006/1) - Etiology and Mechanisms; AW holds a PhD studentship funded by the Wellcome Trust
Emma	P	Wilson	US NIH T32GM067553
Peitao		Wu	NIH R01DK078616, R01HL15185
Björn		Zethelius	No conflicts of interest. No financial support to declare.

Supplementary Methods

Genetic Risk Scores for ISI and IFC

We additionally constructed genetic risk scores (GRS) for IFC and ISI including lead variants at primary association signals in Europeans. GRS were constructed using the sum of allele scores for each individual where allele counts were weighted by the effect of this allele on IFC or ISI, adjusted or unadjusted for BMI as appropriate. Weights used in the construction of the GRS are outlined in **Supplementary Table 12**. Allele counts were discrete for genotyped variants (0 = reference, 1 = heterozygous, 2 = homozygous) and weights were aligned to the dosage coding allele prior to weighting of each variant. Weighted allele counts were summed for each individual to generate the GRS. GRS were constructed for ISI and IFC adjusted and unadjusted for BMI in unrelated individuals of European ancestry in UK Biobank[1] (N max = 351,987) and the OMICS subset Fenland Study[2] (N max = 8,925). Blood biochemistry measures in the Fenland Study and UK Biobank were natural log transformed prior to scaling. Phenotypes were prepared as has been previously described.[3–5]

Linear regression models were run for each genetic score and phenotype pair adjusting for age, sex and the 1st 10 genetic principal components to account for population structure. Phenotypes were scaled to a mean of 0 and SD of 1 to allow direct comparison across phenotypes. Significance was considered at a Bonferroni significance threshold in UKBB ($P < 4.5x10^{-4}$; N GRS = 4, N phenotypes = 28) and nominal significance threshold in the Fenland Study ($P < 0.05$).

LD Score Regression

We applied LD score regression[6] using python-based software LDSC (accessed at https://github.com/bulik/ldsc) to assess genome-wide genetic correlations between IFC and ISI with other cardiometabolic traits. We calculated LD scores for ISI, IFC using BMI adjusted summary statistics from our analyses in cohorts of European ancestry. We further calculated LD scores for additional T2D related traits from publicly available summary statistics for 2 h glucose[7], fasting insulin[7], T2D[8] and WHRadjBMI[9] in cohorts of European ancestry. Further pre-computed LD scores were obtained online for additional cardiometabolic traits of interest (https://data.broadinstitute.org/alkesgroup/LDSCORE/). The genetic correlations were

calculated restricting to HapMap3 SNPs with a MAF > 0.05, and we used the 1000G European LD Score reference[6].

Tissue specificity

To dissect the tissue of action of IFC and ISI loci, we used LDSC-SEG to assess the genome-wide enrichment of tissue-specific and cell type specific annotations[10]. In brief, LDSC-SEG employs stratified LD score regression to assess for genome-wide enrichment of sets of specifically expressed autosomal genes for a given trait of interest. We utilised LD scores available for a total of 205 specific tissue and cell types from GTEx (53 tissues; RNA-seq) and Franke Lab dataset which consists of expression data for 152 tissues of cell types in human, mouse, and rat[10]. In addition, we examined LD scores also generated by Finucane *et al* (2018)[10] from chromatin annotation from Roadmap[11] and ENTEx data from ENCODE[12]. Suggestive enrichment was considered at a nominal significance threshold of $P < 0.05$, with no result surviving multiple testing correction.

Confirmation of gene knockdown in 3T3-L1 adipocytes

RNA extraction

RNA was extracted from 3T3-L1 adipocytes cultured in 24-well plates 4 d after siRNA knockdown (see above). Cells were washed 2x in PBS and TRI reagent (Zymo Research) was added to each well. Cells were then flash frozen in the plate on dry ice and stored at -80°C. RNA extraction was conducted in an RNAse free environment using the Zymo Research Directzol RNA Extraction Kit following standard manufacture protocol. Briefly, plates were thawed on ice and cells were lysed by manual cell scraping and incubation at room temperature for 10 min. Samples were mixed with an equal volume of 100% ethanol and added directly to an RNA extraction column. RNA was eluted in 30 µL of RNAse and DNAse free water. All centrifugation steps were performed at room temperature at 12,000 x g.

Reverse transcription

RNA was diluted to a consistent concentration per biological replicate. Random primers (Promega) were annealed in a total volume of 30 µL at 70°C for 5 min, and immediately rapidly cooled on ice, in line with manufacturers' specifications. Reverse transcription was conducted in a total volume of 50 µL for each sample using MMLV Reverse Transcriptase (Promega) and

RNassin RNA inhibitor (Promega). Reverse transcription was conducted using BioRad Tetrad 2 Thermal Cycler at 25°C for 10 minutes, 37°C for 1 h and 85°C for 10 min before being stored at -20°C.

qPCR RNA quantification

Quantitative PCR was conducted using Thermo Fisher TaqMan gene expression assays following the standard manufacturer protocol. Probe specifications for targets of interest are outlined in **Supplementary Table 31**. These were added to master mix containing TaqMan 2x Universal PCR Master Mix (ThermoFisher) and nuclease-free water. Polymerase chain reaction was carried out using QuantStudio 7 or Quantstudio 5 Real-Time PCR system (Thermo Fisher Scientific). *ActB* (Mm04394036_g1) and *Canx* (Mm00500330_m1) were used as housekeeping controls for all samples. The standard pre-set cycling conditions for TaqMan reagents were used.

qPCR data analysis

Double delta CT values (ddCT) were calculated and the fold change relative to the NT control was used to assess knockdown efficiency. The geometric mean CT value of the housekeeping genes *ActB* and *Canx* were used for normalisation for a given sample. One-way ANOVA was used to compare delta CT (dCT) values for a given knockdown target compared to NT control, and significance was considered at FDR < 5%.

SDS-PAGE and immunoblotting

Typically, 10 µg of protein was resolved by SDS-PAGE and transferred to PVDF or nitrocellulose membranes. Membranes were blocked in 5% BSA or skim milk powder in TBS-T (0.1% v/v Tween-20 in Tris-buffered saline) for 1 h followed by overnight incubation at 4°C with specific primary antibodies (listed below). Following incubation with horseradish peroxidase (HRP)-conjugated anti-rabbit or mouse immunoglobulin G (IgG) or Alexa-647-conjugated anti-mouse IgG secondary antibodies for 1 h. Protein bands were visualised using ECL (Thermo Scientific) or 647-fluorescence intensity on the Chemidoc MP (Bio-Rad). The following antibodies were used: Lnpep/IRAP (Cell Signaling Technologies, #6918); TBC1D4 (Cell Signaling Technologies, #2670); IRS1 (Cell Signaling Technologies, #3407); PanAkt (Cell Signaling Technologies, #2920); GLUT4 (polyclonal antibody recognising the C-

terminus of GLUT4 provided by Professor David James, University of Sydney)[13]; Rab10 (Thermo Fisher; # MA5-15670); alpha-tubulin (Merck; #T9026) and beta-actin (Cell Signaling Technologies; #8457).

1. Correlation of post-challenge insulin traits with other metabolic traits in the Fenland Study and RISC cohort

To determine the traits correlated with insulin resistance in the fasted and fed state, we conducted observational correlation analyses for fasting insulin and dynamic insulin traits Modified Stumvoll Insulin Sensitivity Index (ISI) and Insulin Fold Change during an OGTT (IFC), with metabolic traits measured in the Fenland Study (pairwise N= 1454 (c-peptide)-11787). Fasting insulin was positively correlated with many metabolic traits including glycaemic traits fasting and 2hr glucose, proinsulin, HbA1C. Further fasting insulin is positively correlated with LDL triglycerides and liver biomarkers as well as BMI, WHR and blood pressure (**Extended Data Figure 2**).

We observed that both IFC and ISI show strong correlation with measures of insulin and glucose taken at 2hrs during a standard OGTT, however are poorly correlated with fasting measures, suggesting these are primarily capturing the post-challenge insulin response. ISI is additionally inversely correlated with liver-related traits, as seen with fasting insulin (hepatic steatosis score and measures of circulating alkaline phosphatase, gamma-glutamyl transferase, alanine aminotransferase), suggesting that ISI may additionally capture insulin action on the liver in the fasted state (**Extended Data Figure 2**). IFC was not correlated with any liver-related traits, suggesting that this potentially more specific to the post-prandial state. This is further evidenced by observations that ISI is more strongly correlated with HOMA-IR, an index of fasting insulin resistance (**Extended Data Figure 2**). Further, IFC was weakly correlated with ISI (rho = -0.35), compared to other insulin related traits e.g. 2 hour insulin, suggesting that a GWAS of this measure may capture variants that are distinct from those that are driving 2-hour insulin or alternatively that these traits are able to capture different aspects and pathways that contribute to the post-challenge insulin response.

We conducted similar analyses in participants without diabetes in the RISC cohort (N=1,138; methods) where hyperinsulinemic-euglycemic clamp and OGTT-derived measures of insulin sensitivity are available. We assessed and compared the correlation of clamp and OGTT-derived measures of insulin sensitivity with relevant traits, as was done in the Fenland Study above. We replicated the strong positive correlation of IFC with insulin at 120 min during an OGTT (rho = 0.725, P = 4.21e-177) and saw a weak negative correlation of IFC with fasting

insulin during an OGTT (rho = -0.165, P = 4.57e-8) as well as no correlation with insulin taken 20min before clamp (rho = 0.009, P =0.768). We additionally identified a significant inverse correlation between IFC and clamp-derived measure of insulin sensitivity M/I (rho = -0.180, P = 3.29e-9). For ISI we identify strong inverse correlation with insulin at fasting (rho = -0.68, P = 6.38e-149) and 120mins during an OGTT (rho = -0.869, P = 0), as seen in the Fenland Study **(Extended Data Figure 3).** We additionally identified a strong positive correlation of ISI with M/I (rho = 0.522, P = 5.10e-76). Overall correlations were similar and consistent in direction between RISC and Fenland studies for primary overlapping traits of interest.

2. Genetic Discovery of post-challenge insulin resistance: European-only meta-analyses

We performed fixed-effect meta-analyses within cohorts of European ancestry using METAL[14] for IFC and ISI. Manhattan and QQ plots summarising the results can be found in **Supplementary Figures 1-4** below. Unadjusted -log10 P-values are indicated on the y axis of the Manhattan plots. QQ plots show the observed (Y) vs expected (X) -log10 P value. Unadjusted P values are shown. In Manhattan plots on the left, the green points indicate those that meet genome wide significance. Red line indicates genome wide significance (P < 5e-8)_ and blue line represents suggestive significance (P < 1e-5).

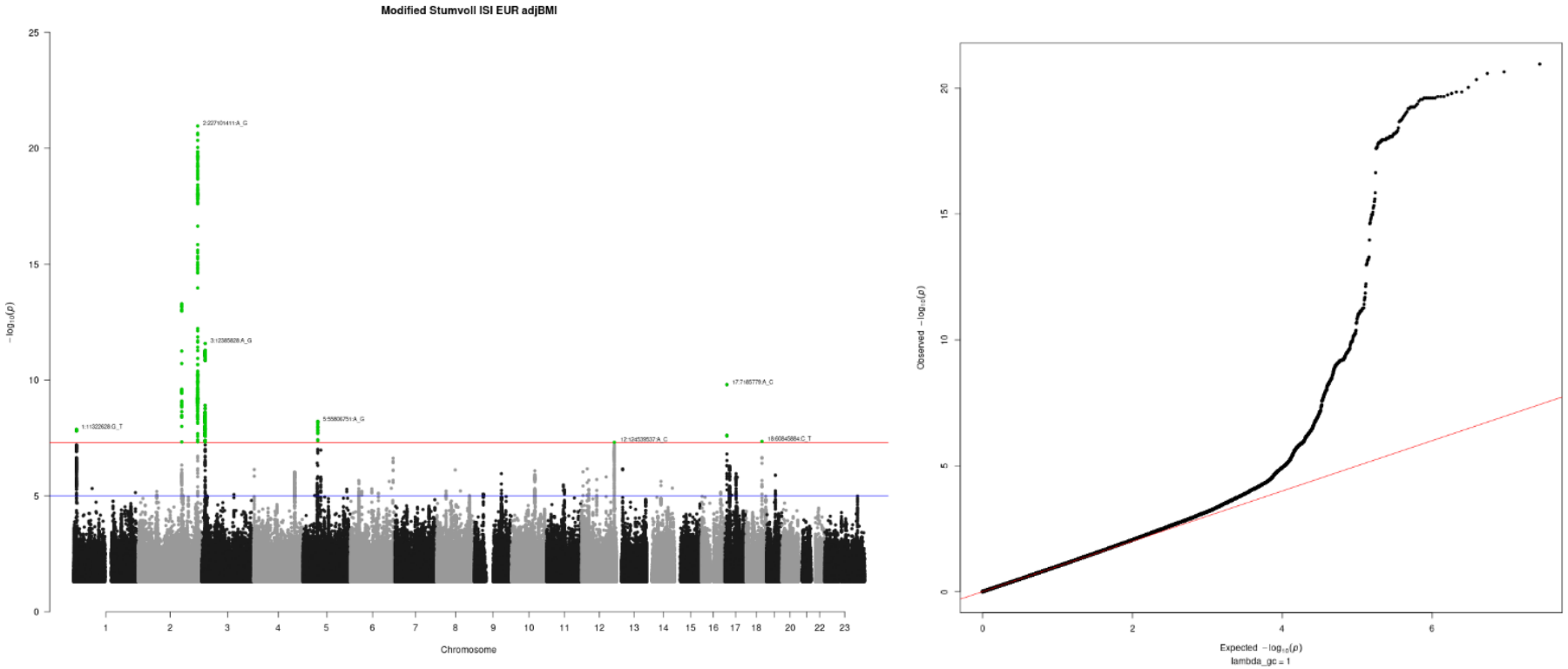

Supplementary Figure 1: Manhattan and QQ plots for European-only meta-analysis of Modified Stumvoll ISI adjusted for BMI

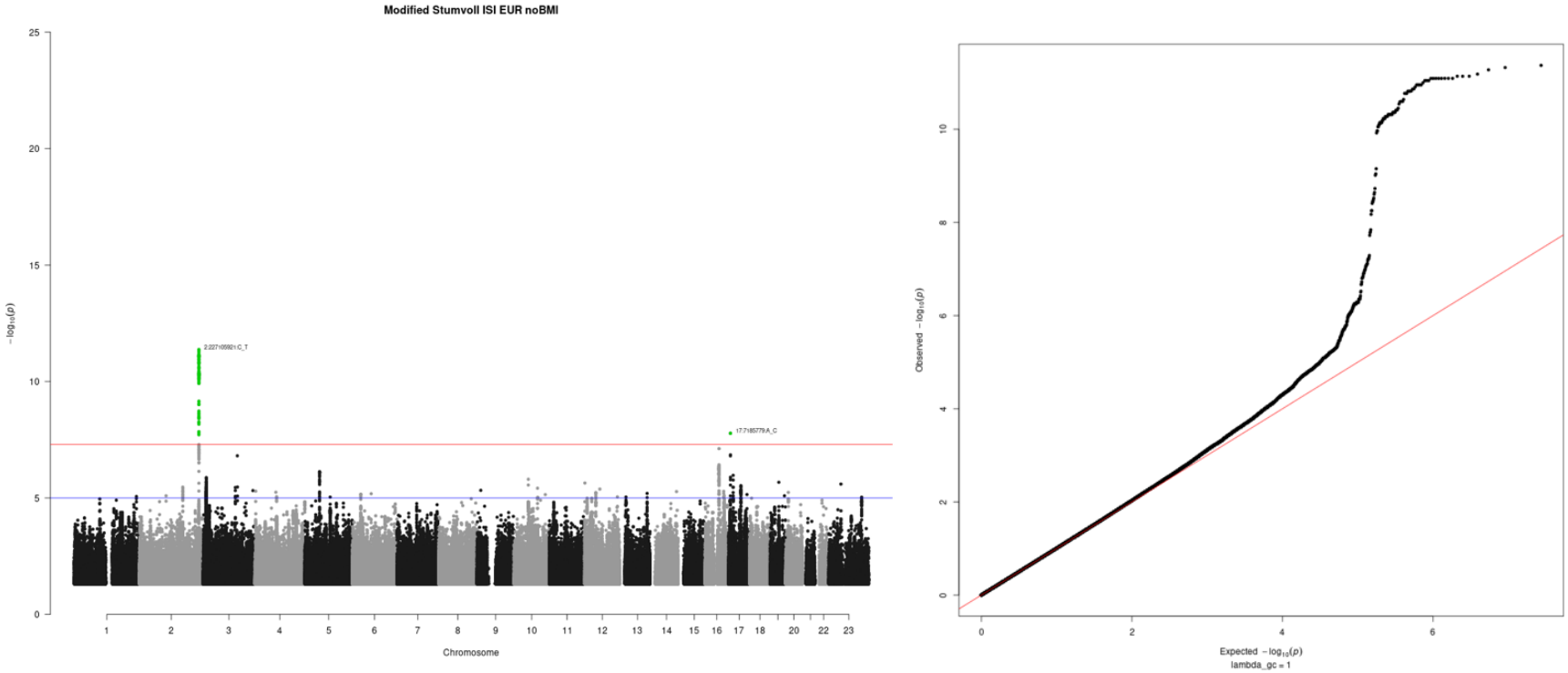

Supplementary Figure 2: Manhattan and QQ plots for European-only meta-analysis of Modified Stumvoll ISI unadjusted for BMI

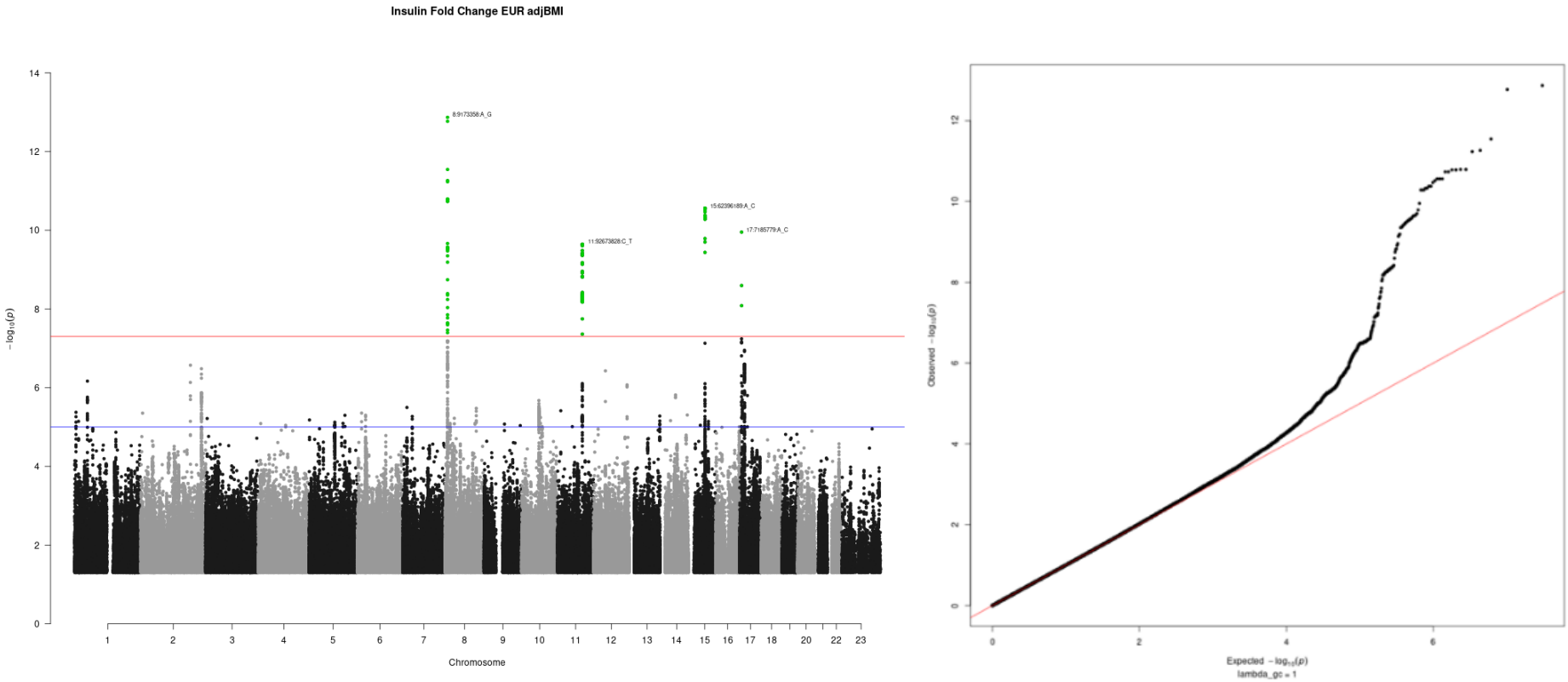

Supplementary Figure 3: Manhattan and QQ plots for European-only meta-analysis of insulin fold change adjusted for BMI

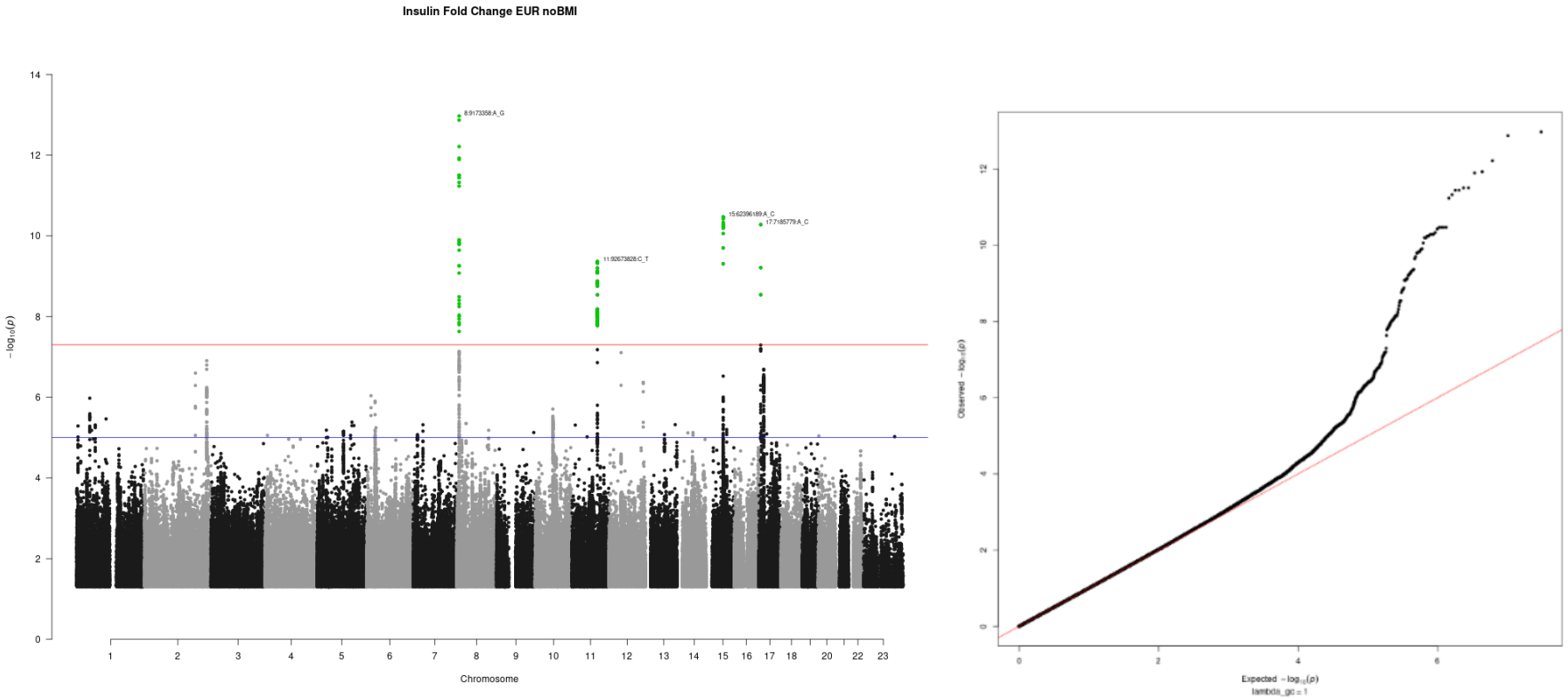

Supplementary Figure 4: Manhattan and QQ plots for European-only meta-analysis of insulin fold change unadjusted for BMI

3. Regional plots of genetic loci associated with Modified Stumvoll ISI adjBMI (Supplementary Figure 5)

Supplementary Figure 5: Regional association plots of genetic loci associated with Modified Stumvoll ISI adjBMI in European-only meta-analysis.

A locus was defined as ±500kb of the lead variant at a given locus. LD reference panel is 1000 Genomes CEU (European), the lead variant at a given locus is indicated by the purple triangle. Relative LD (R^2) of other variants with this lead variants is indicated by the colour scale shown in the legend on the left hand side of the plot. Unadjusted -log10 P-values are indicated on the y axis.

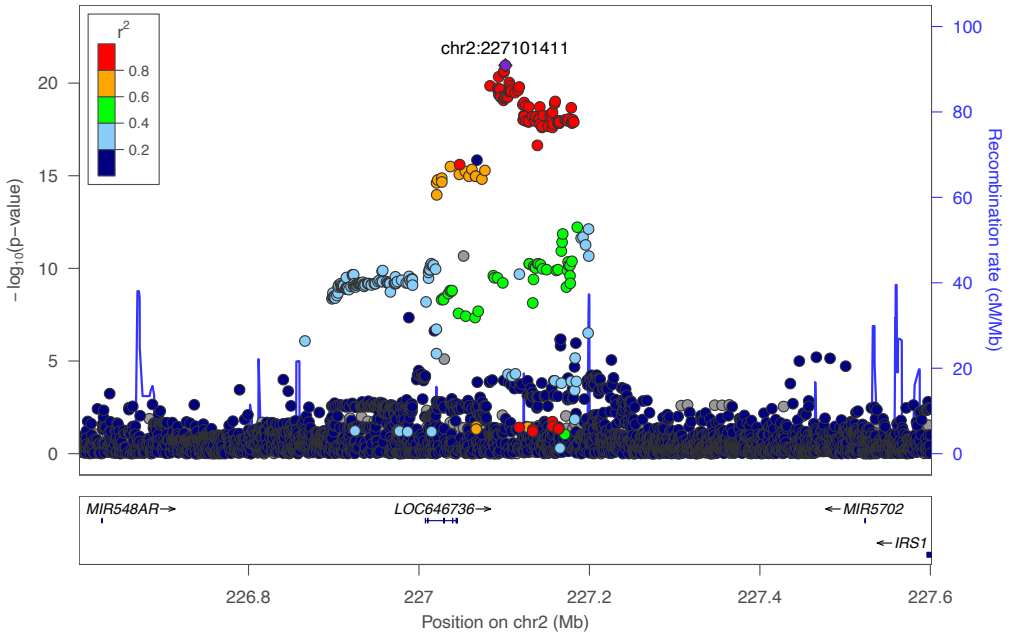

Supplementary Figure 5 a) IRS1

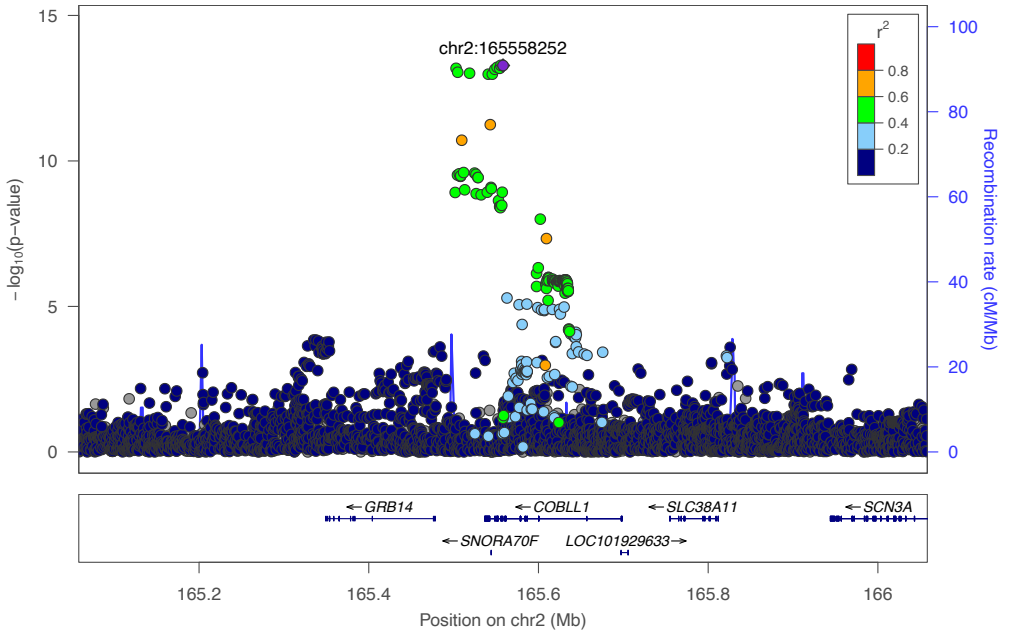

Supplementary Figure 5 b) COBLL1

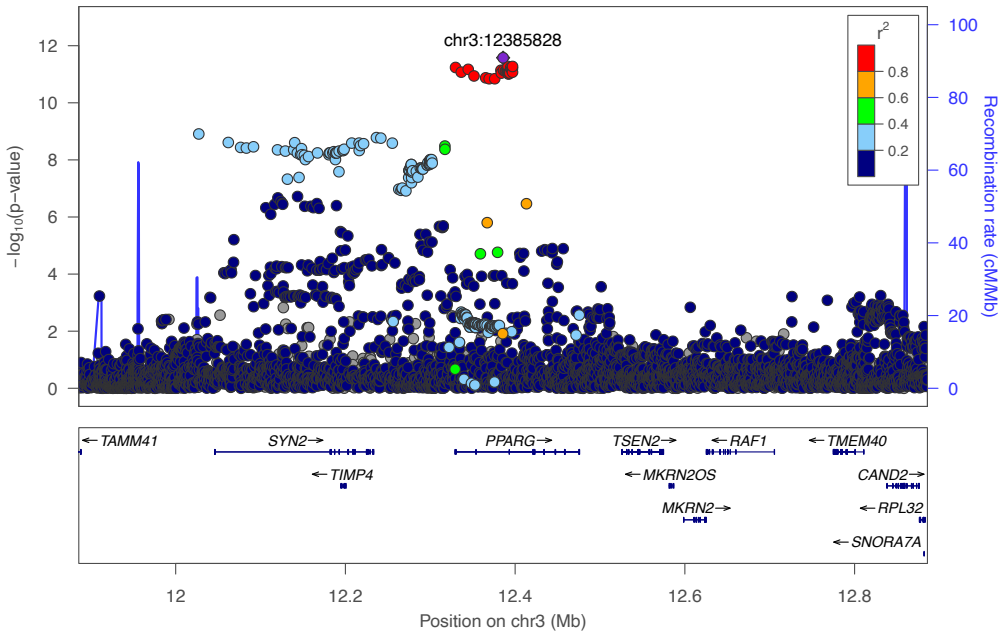

Supplementary Figure 5 c) PPARG

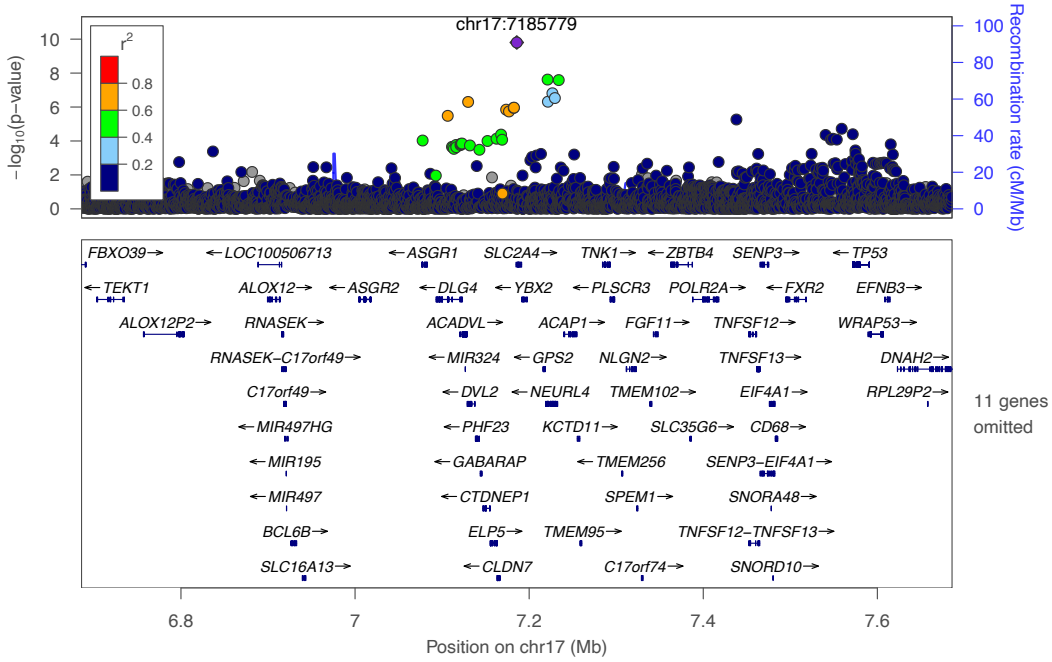

Supplementary Figure 5 d) SLC2A4

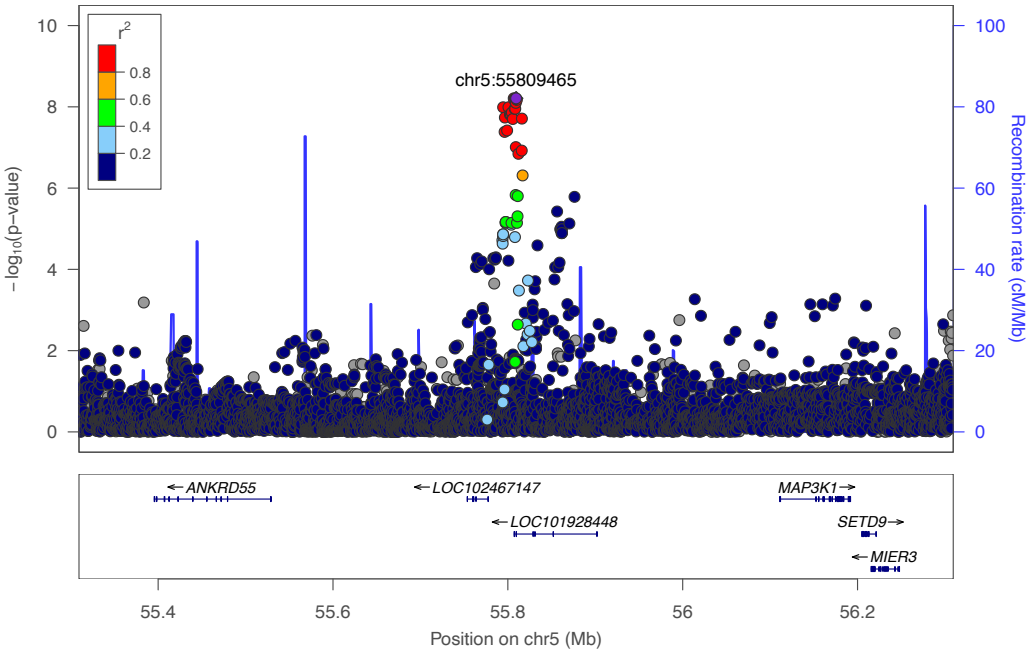

Supplementary Figure 5 e) C5orf67

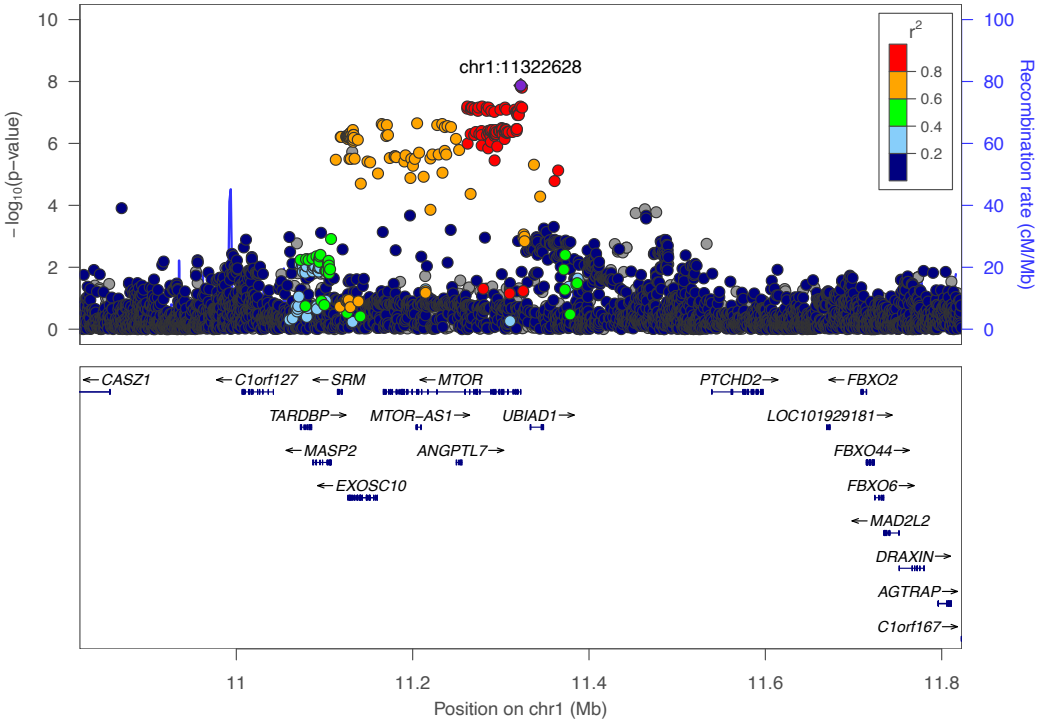

Supplementary Figure 5 f) MTOR

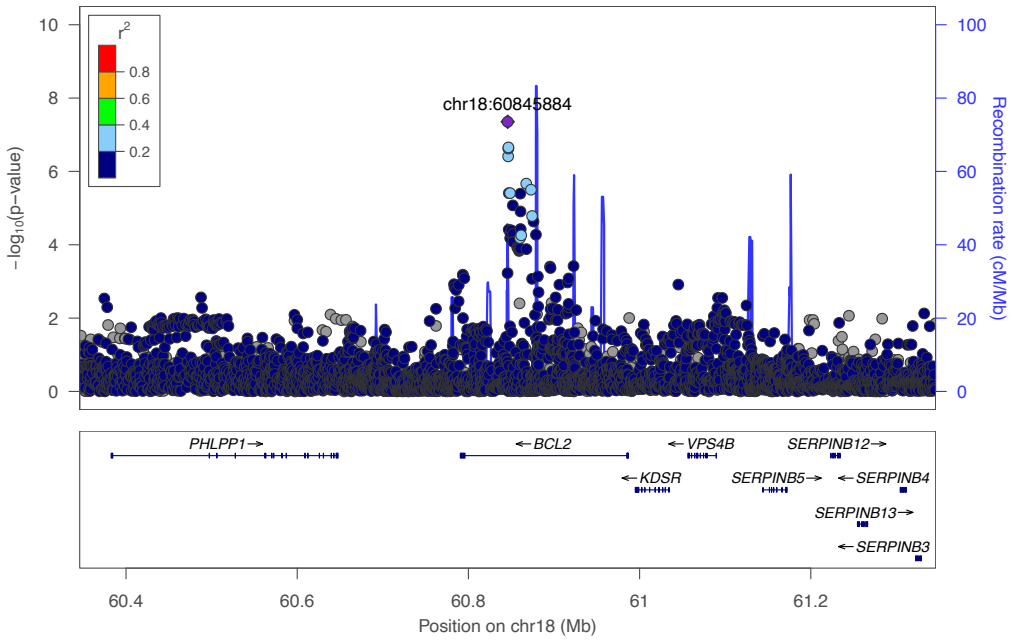

Supplementary Figure 5 g) BCL2

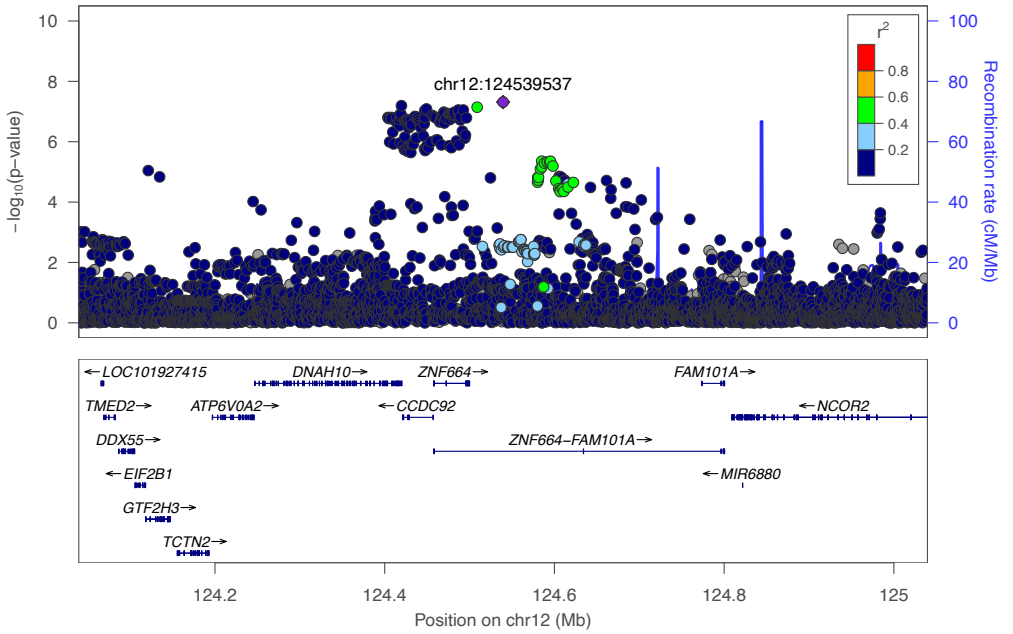

Supplementary Figure 5 h) FAM101A

4. Regional plots of genetic loci associated with Insulin Fold Change adjusted for BMI (Supplementary Figure 6)

Supplementary Figure 6: Regional association plots of genetic loci associated with insulin fold change adjBMI in European-only meta-analysis.

A locus was defined as ±500kb of the lead variant at a given, locus. LD reference panel is 1000 Genomes CEU (European), the lead variant at a given locus is indicated by the purple triangle. Relative LD (R^2) of other variants with this lead variants is indicated by the colour scale shown in the legend on the left hand side of the plot. Unadjusted -log10 P-values are indicated on the y axis. Unadjusted -log10 P-values are indicated on the y axis.

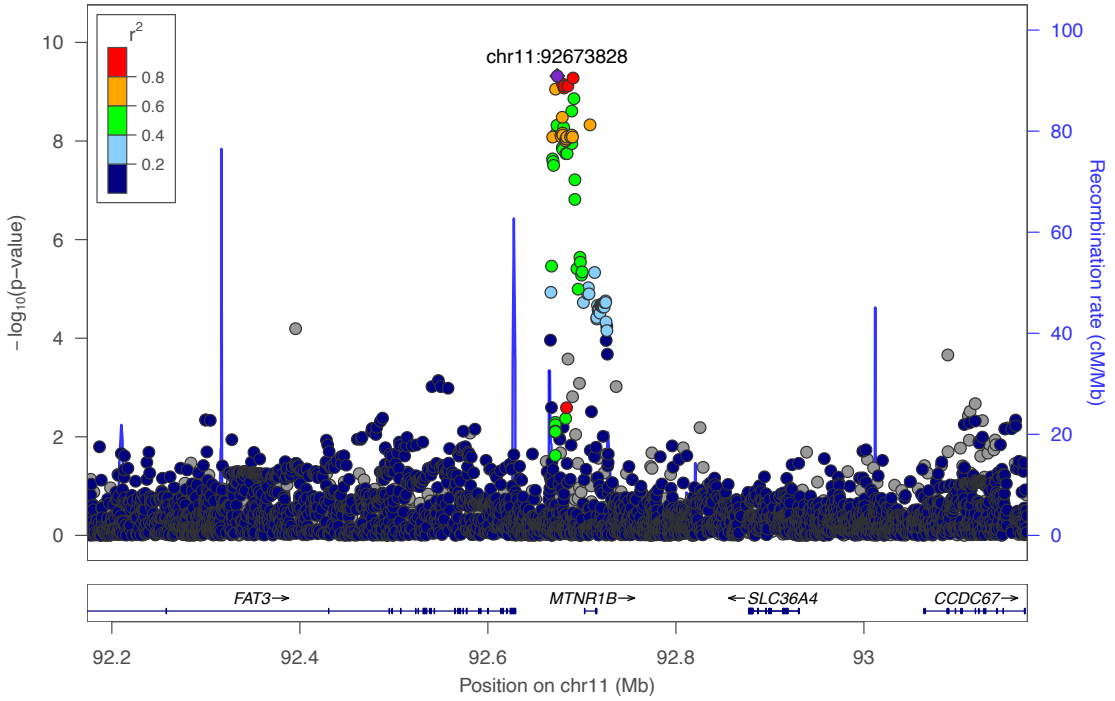

Supplementary Figure 6 a) MTN1RB

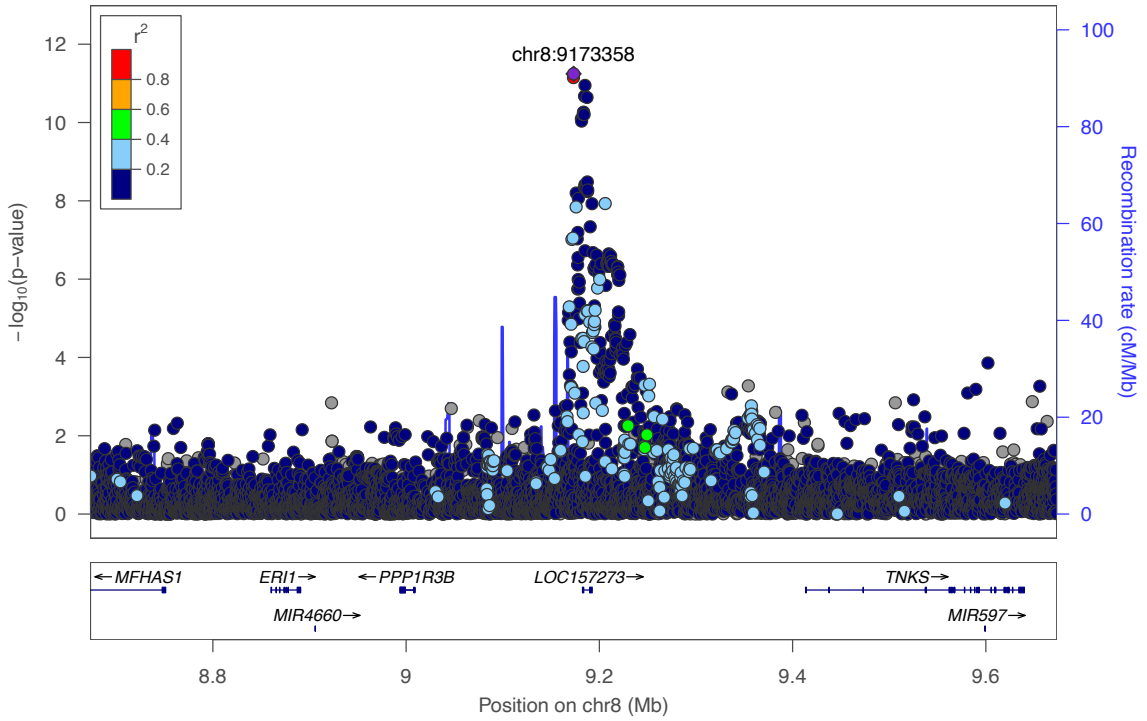

Supplementary Figure 6 b) PPP1R3B

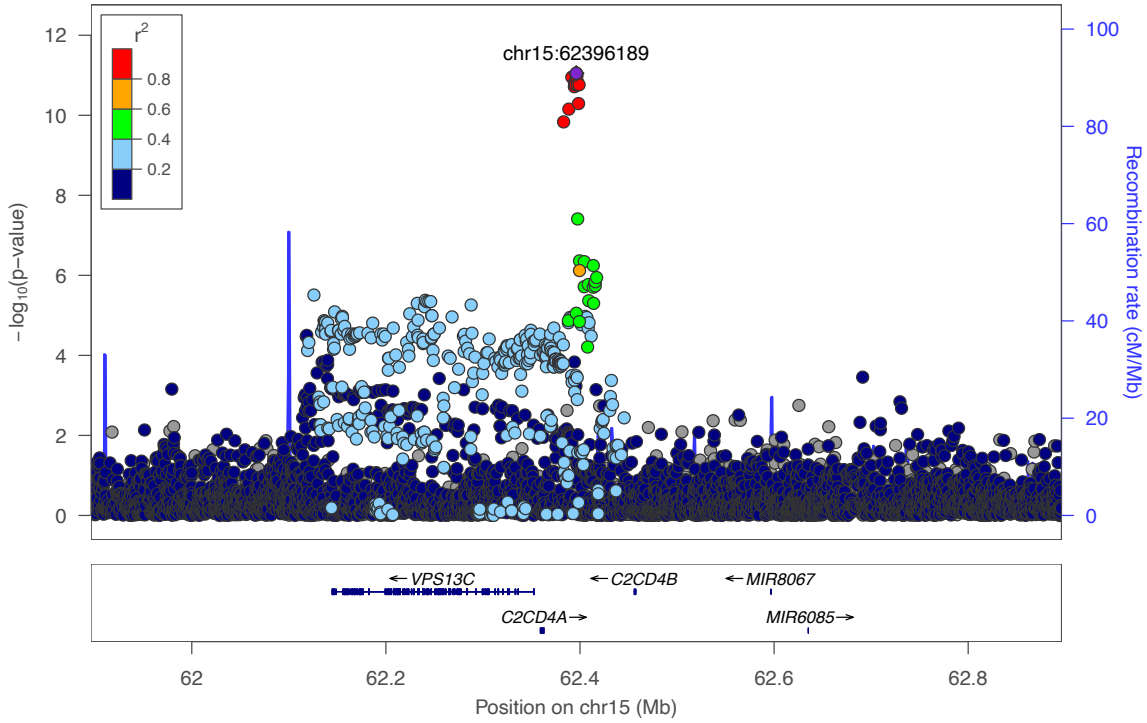

Supplementary Figure 6 c) C2CD4A

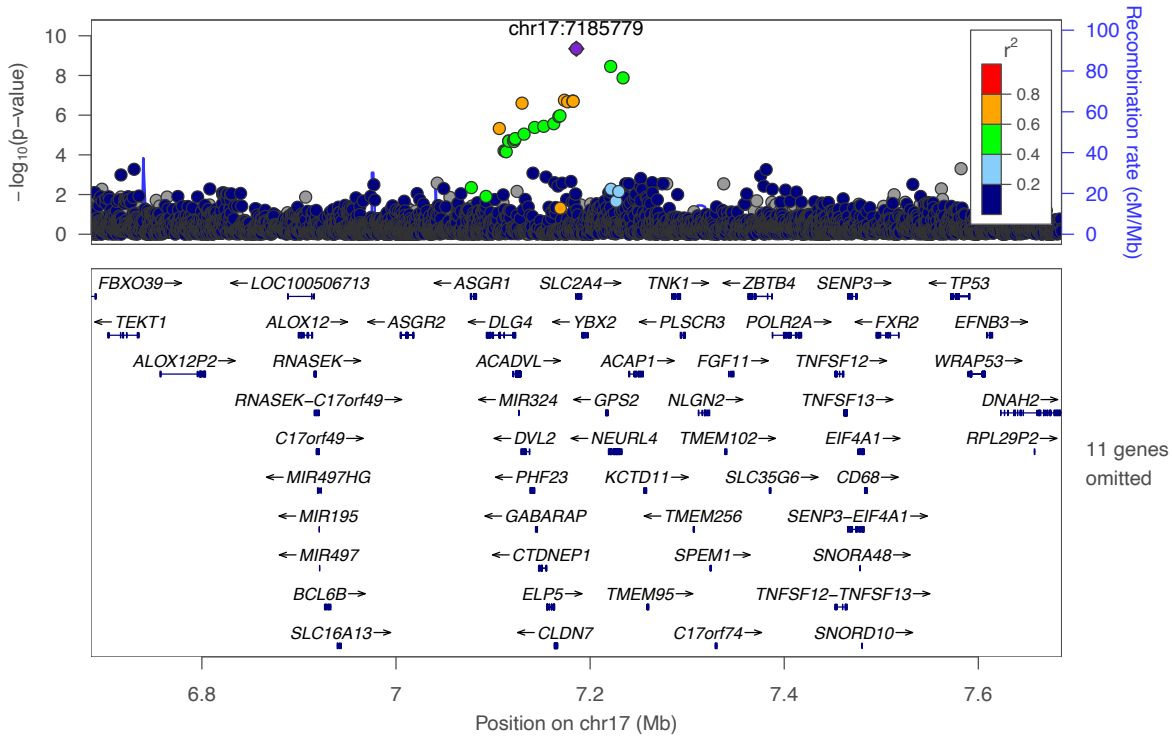

Supplementary Figure 6 d) SLC2A4

5. Genetic Discovery of post-challenge insulin resistance: non-European and multi-ancestry meta-analyses (Supplementary Figures 7-14)

We performed fixed-effect meta-analyses separately within cohorts of Hispanic American ancestry using METAL[14] for IFC and ISI. To examine trans-ancestry effects we conducted random effects meta-analyses of these ancestry-specific results (EUR, EAS, HISAMR) using METAL (**See methods**). Manhattan and QQ plots summarising the results can be found in **Supplementary Figures 7-14** below. Unadjusted -log10 P-values are indicated on the y axis of the Manhattan plots. QQ plots show the observed (Y) vs expected (X) -log10 P value. Unadjusted P values are shown. In Manhattan plots on the left, the green points indicate those that meet genome wide significance. Red line indicates genomewide significance (P < 5e-8)_ and blue line represents suggestive significance (P < 1e-5).

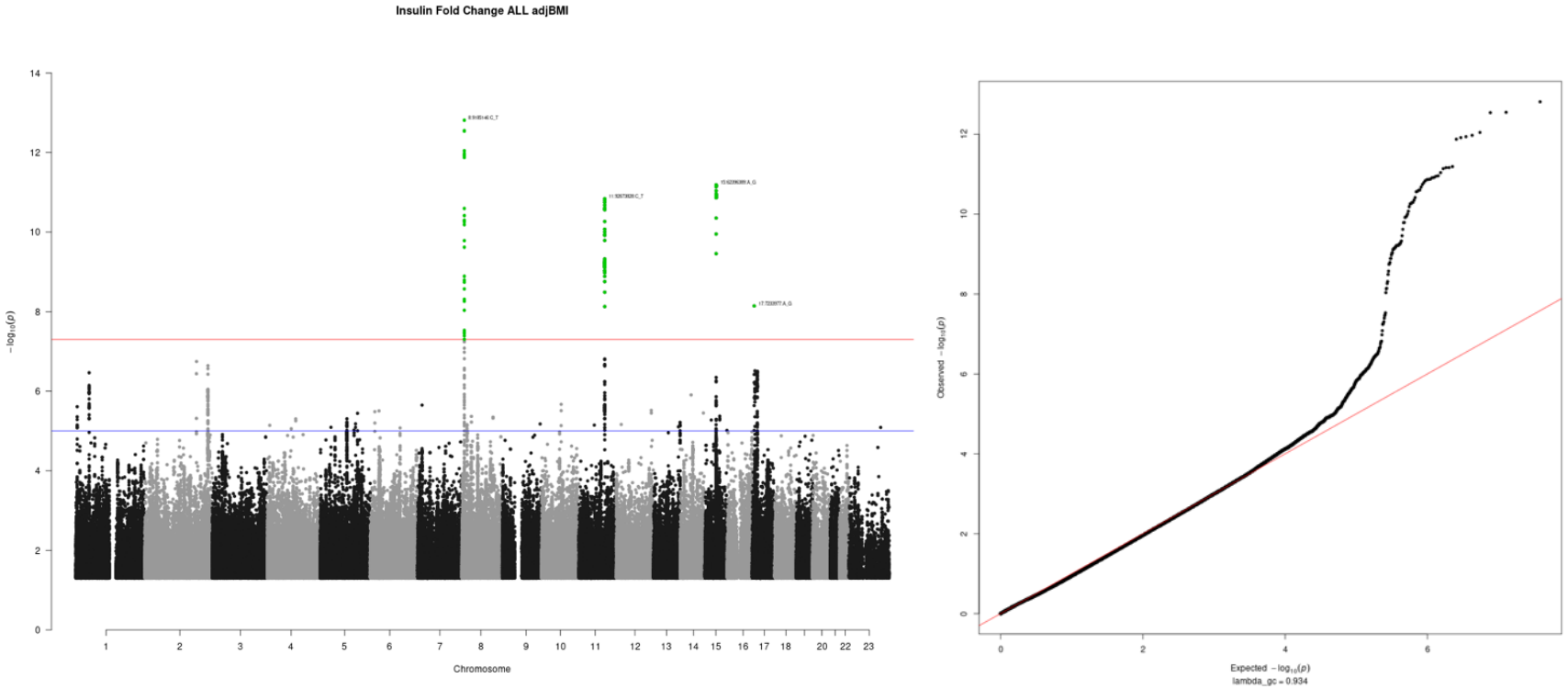

Supplementary Figure 7: Manhattan and QQ plots for multi-ancestry (EUR, HISAMR, EAS) meta-analysis Insulin Fold Change adjusted for BMI

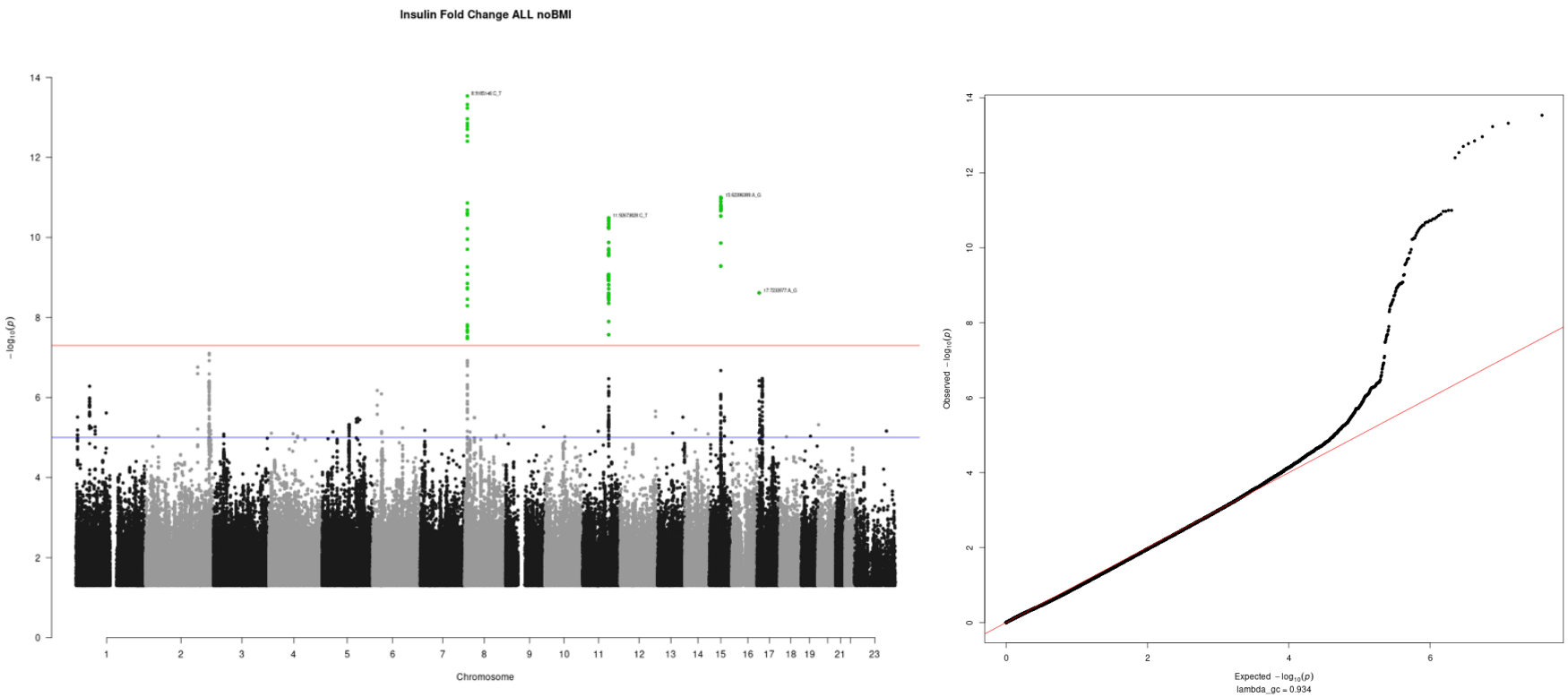

Supplementary Figure 8: Manhattan and QQ plots for multi-ancestry (EUR, HISAMR, EAS) meta-analysis Insulin Fold Change unadjusted for BMI

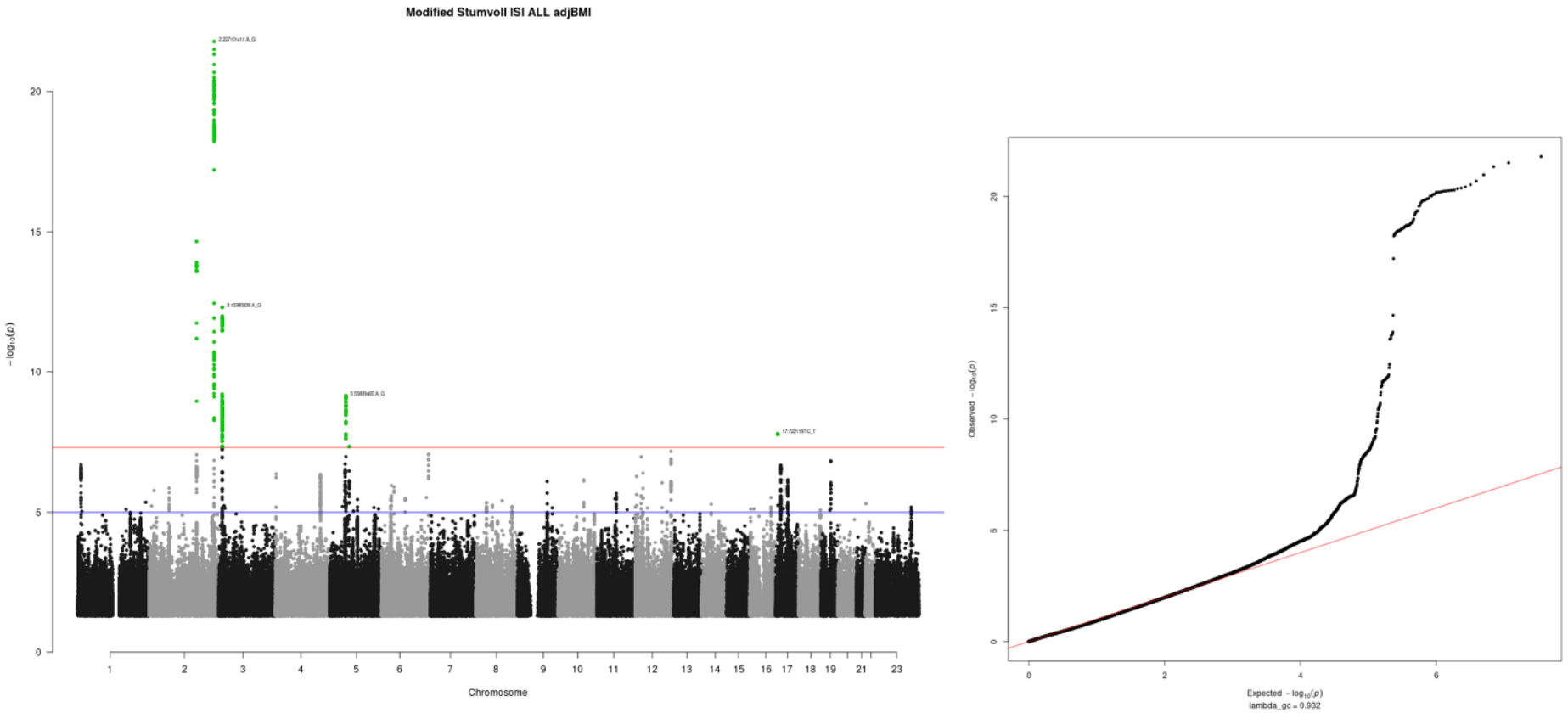

Supplementary Figure 9: Manhattan and QQ plots for multi-ancestry (EUR, HISAMR, EAS) meta-analysis Modified Stumvoll ISI adjusted for BMI

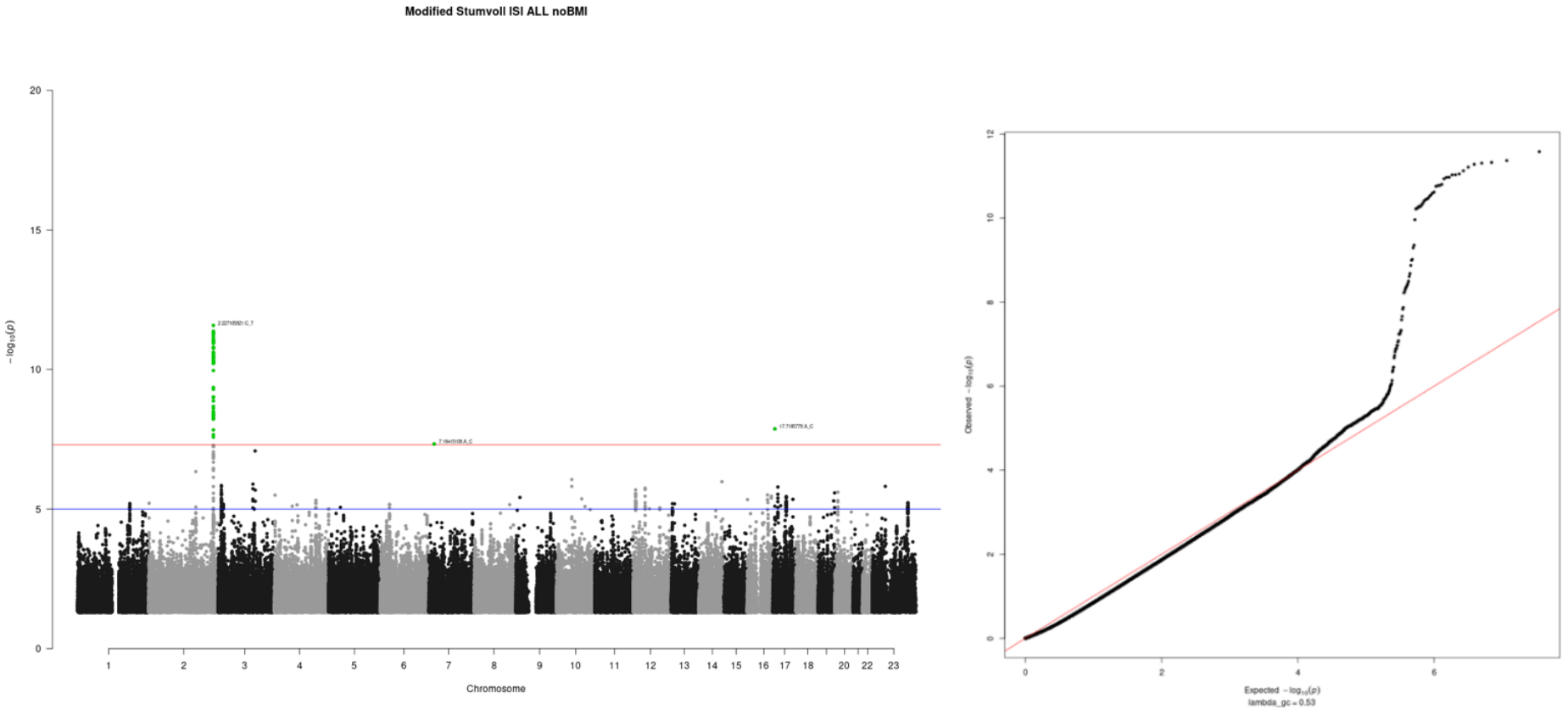

Supplementary Figure 10: Manhattan and QQ plots for multi-ancestry (EUR, HISAMR, EAS) meta-analysis Modified Stumvoll ISI adjusted for BMI

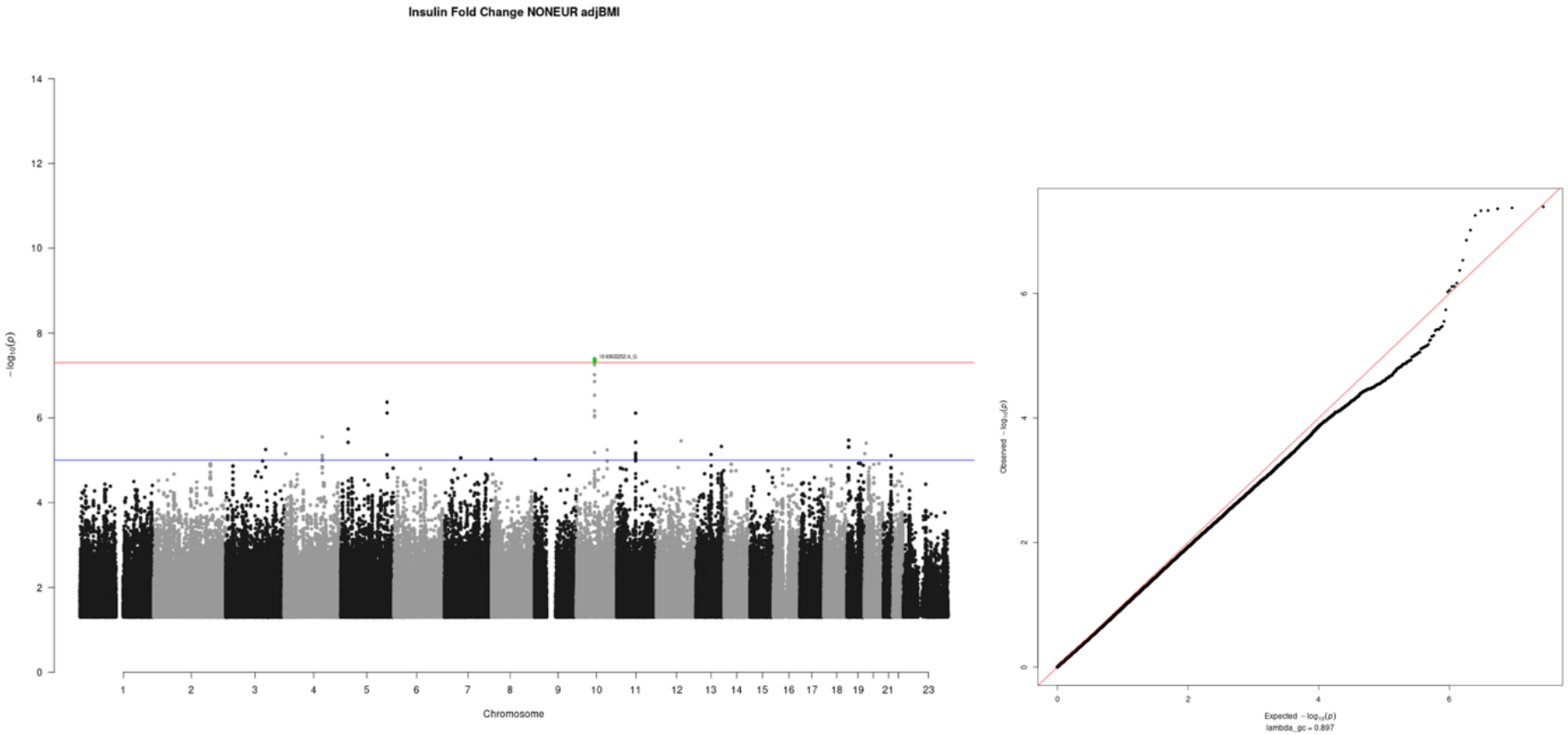

Supplementary Figure 11: Manhattan and QQ plots for non-European Ancestry (HISAMR, EAS) meta-analysis Insulin Fold Change adjusted for BMI

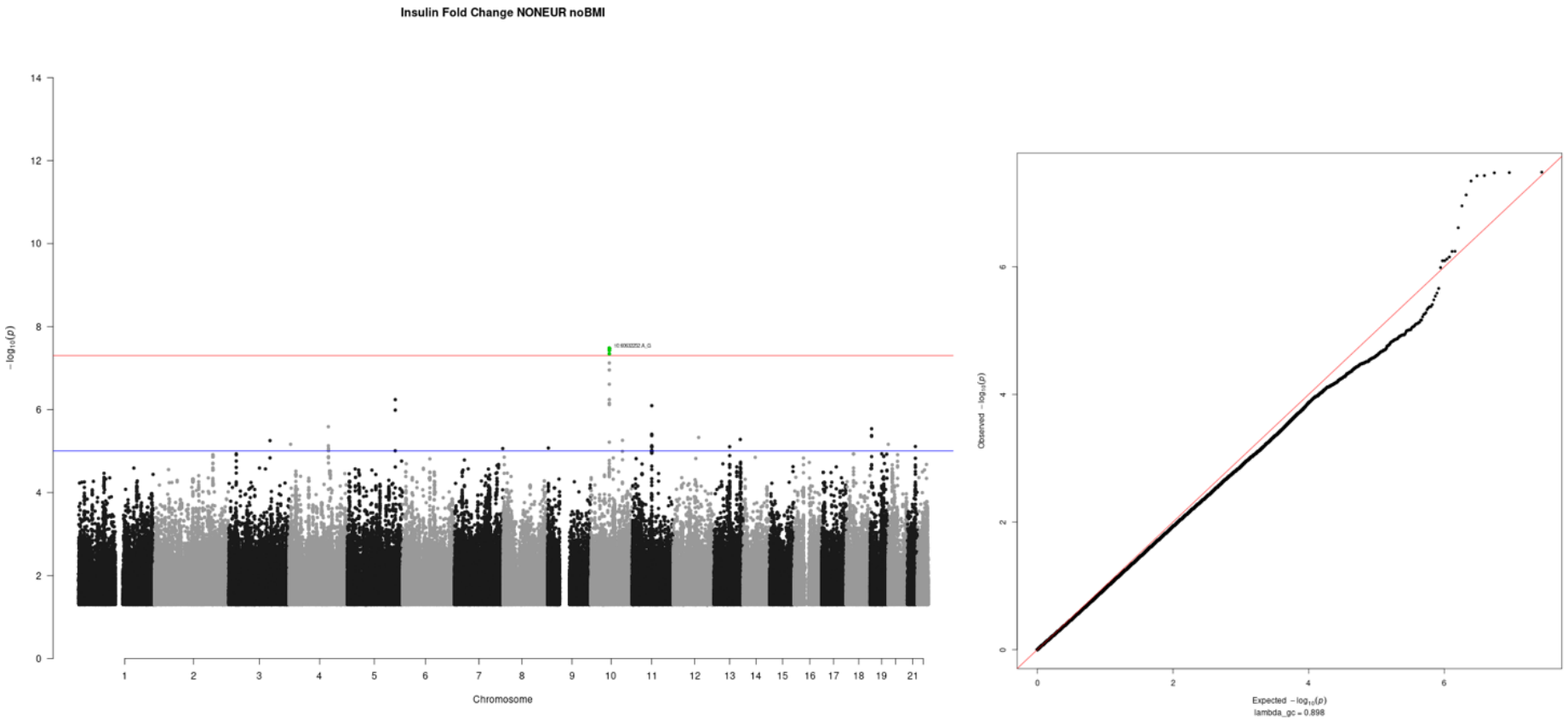

Supplementary Figure 12: Manhattan and QQ plots for non-European Ancestry (HISAMR, EAS) meta-analysis Insulin Fold Change unadjusted for BMI

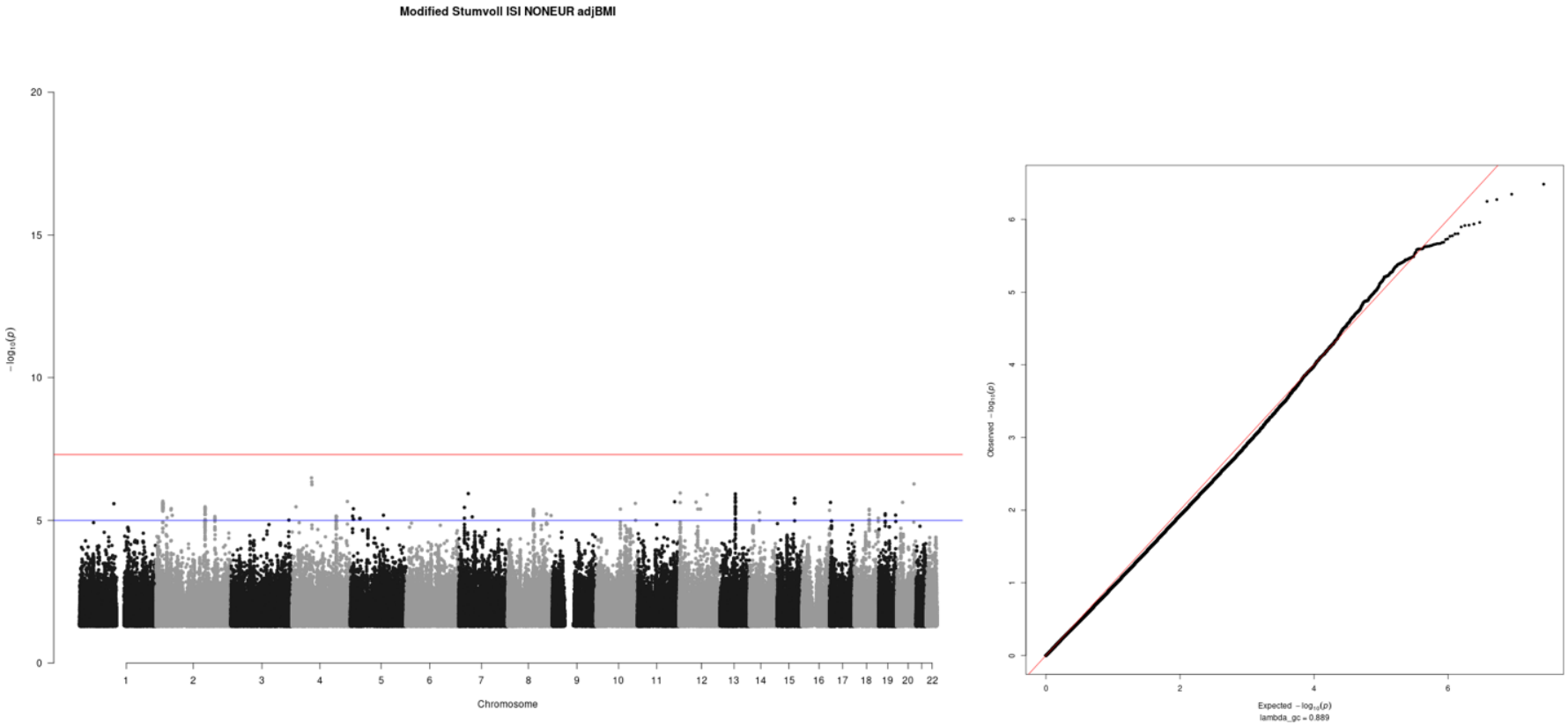

Supplementary Figure 13: Manhattan and QQ plots for non-European Ancestry (HISAMR, EAS) meta-analysis Modified Stumvoll ISI adjusted for BMI

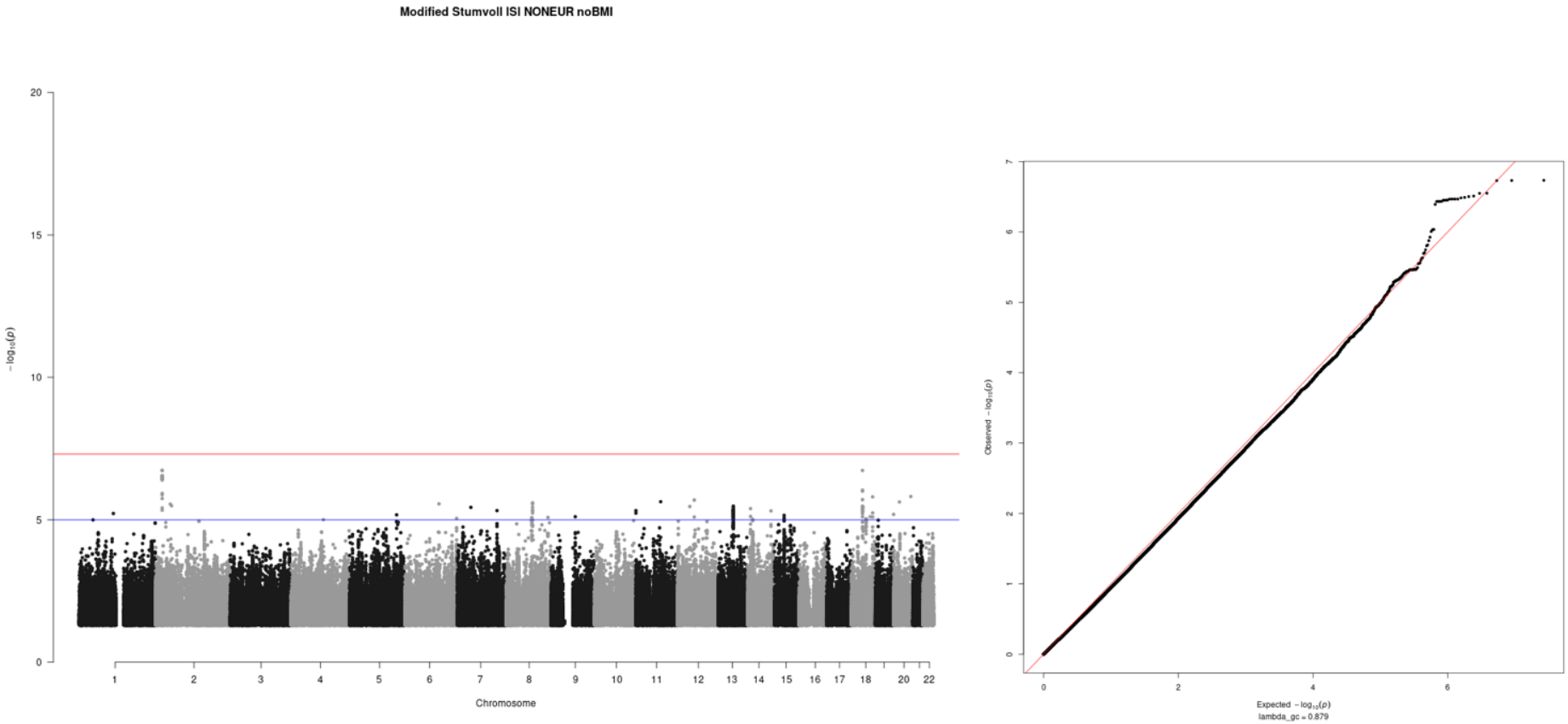

Supplementary Figure 14: Manhattan and QQ plots for non-European Ancestry (HISAMR, EAS) meta-analysis Modified Stumvoll ISI unadjusted for BMI

6. rs60453193 (chr10:60632252_A_G (b37)) at *BICC1* is associated with Insulin Fold Change specifically in Non-European Cohorts

We additionally identified *BICC1* (rs60453193, beta = 0.43, SE = 0.08, P = 4.06×10^{-8}, N = 1,837) as a signal associated with IFC **(see Methods).** This locus has not been implicated in post-challenge insulin resistance previously. The effects were consistent in meta-analyses of only East Asian (beta = 0.406, SE = 0.204, P = 0.046, N = 739) and Hispanic American ancestry studies (beta = 0.435, SE = 0.085, P = 3.15×10^{-7}, N = 1,098) (**Supplementary Tables 6 and 7; Extended Data 5-6**). *BICC1* was not associated with IFC in meta-analysis of studies only of European ancestry (beta = -0.0026, SE = 0.010, P = 0.791, N = 50,671; **Supplementary Table 6**); despite being common in all ancestry groups (MAF European = 12%, Hispanic American =7.8%, East Asian = 4.2%). Further, *BICC1* was not statistically significant in the multi-ancestry analyses of IFC, including all cohorts (beta = 0.26, SE = 0.18, P = 0.16, N = 52,508; **Supplementary Tables 6 and 7**), likely due to cohorts of European ancestry dominating the overall sample size (97%). Variants within this locus (±500kb of rs60453193) have been reported to be associated with T2D at suggestive significance in multi-ancestry analyses[8] (Minimum P = $1.0 \times 10^{-4.7}$), however rs60453193 itself is not associated (MVP multi-ancestry T2D: beta = 0.0079, SE = 0.0062, P = 0.020) [8]. Rare, damaging variants in *BICC1* have been reported to be nominally associated with T2D in individuals of European ancestry.[15]

7. SLC2A4 is in perfect D' with variants reported to be associated with type 2 diabetes in Hispanic American and East Asian ancestries.

SLC2A4 locus and T2D risk

The lack of evidence of a shared signal between post-challenge insulin resistance and T2D at SLC2A4 in cohorts of European ancestry is surprising, since lead variant rs117643180 is located in the first intron of *SLC2A4*, encoding GLUT4, a key player in post-prandial glucose uptake. rs117643180 is also associated with higher 2 h glucose (**Supplementary Table 6**), one of the diagnostic criteria for T2D[7,16]. There are several reasons which may explain this. First the true causal variant for T2D may not be captured. *SLC2A4* lead variant rs117643180 is in perfect linkage disequilibrium (LD; D' = 1) with lead SNPs at T2D loci identified in East Asian and Hispanic American ancestries (**Supplementary Figures 15- 17, Supplementary Table 18**).[17,18] The respective lead variants at this locus in each ancestry are too rare in other ancestries, such as European descent, to be included in previous efforts (**Supplementary Table 18)**[19]. The small sample size of non-European ancestries for post-challenge insulin resistance traits, unfortunately does not allow formal statistical colocalisation testing.

Finally, it is possible that epistatic effects may play a role and the A risk allele of rs117643180 for post-challenge insulin resistance co-segregates with the established nearby protective T2D C allele of rs858519 (T2D association at rs858519: Beta = -0.025, SE = 0.004, P = 1.28e-9 , EA = C EAF = 0.505)[8]. For instance in 1000 genomes[20], the rs117643180-A risk allele is present at a frequency of 3.1% in European ancestry, and when present, this co-segregates on the same haplotype with the T2D protective C allele at rs858519 approximately 42% of the time[21].

Finally our analyses focus on variants with MAF > 0.5% and there is suggestive evidence of rare predicted damaging missense variants (**see methods**) in *SLC2A4* being associated with T2D (MAF < 0.005%, N SNPs = 68) in ~450,000 European ancestry participants from the UK Biobank with whole exome sequencing[15]. These variants have been reported to be nominally associated with increased diabetes risk (UK Biobank field 20002 #1220, OR = 1.79 [1.25-2.68], P = 5.5×10^{-3}), increased random glucose (Beta = 0.11, SE = 0.05, P =0.03) and increased HbA1c (Beta = 0.13, SE = 0.06, P = 0.018).[15]

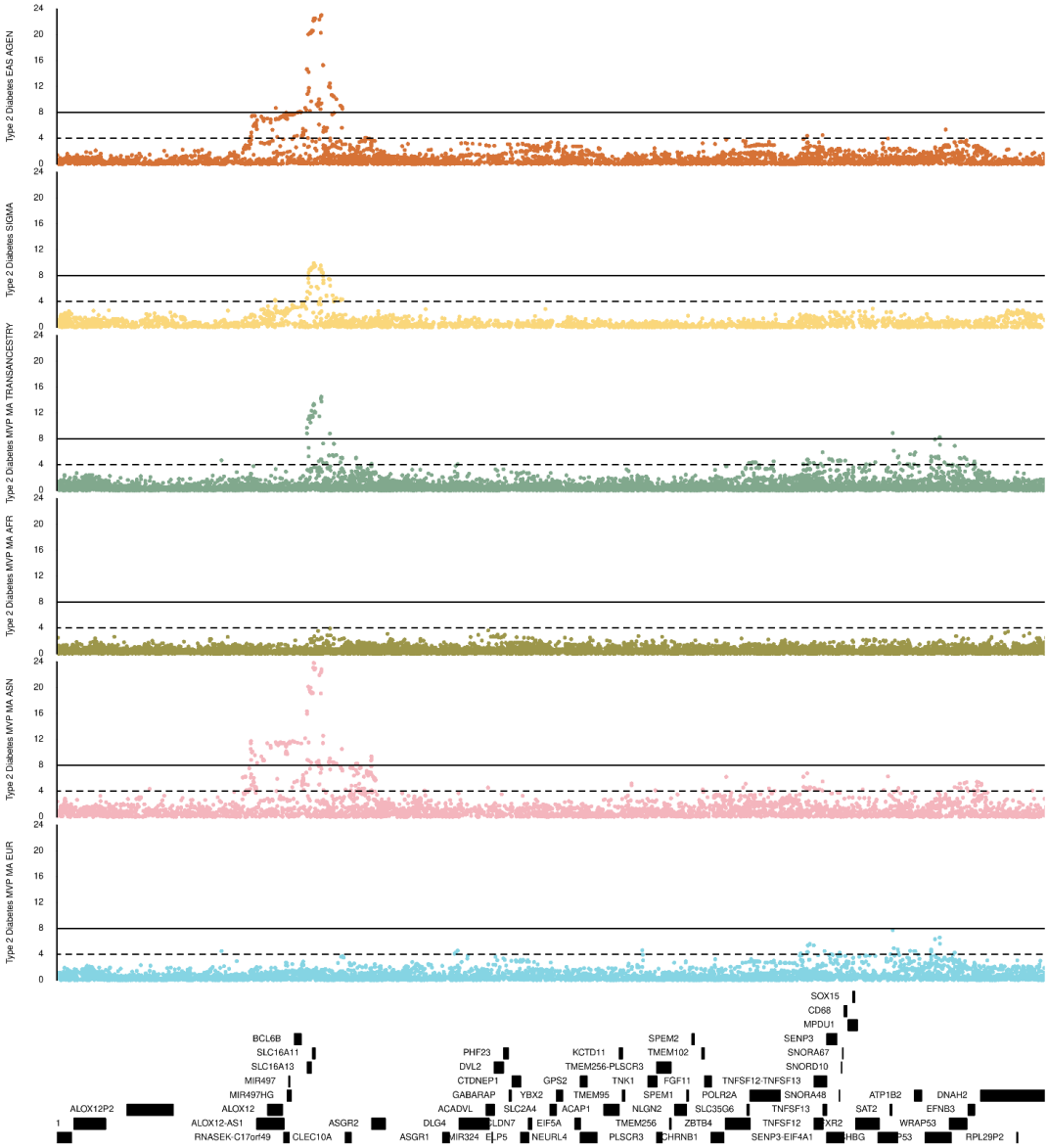

Supplementary Figure 15: SLC2A4 locus regional association plot for Type 2 Diabetes across studies in different ancestry groups.

Locus is defined as ±500kb from lead ISI and IFC SNP rs117643180. From top to bottom the tracks denote the following publicly available Type 2 Diabetes meta-analysis results: Track 1: East Asian Ancestry (AGEN; Spracklen et al; 2021)[17]. Track 2: Hispanic American ancestry, SIGMA consortium (Wiliams et al 2013)[18]. Track 3: MVP meta-analysis (Vujkovic et al; 2020)[8] trans-ancestry. Track 4: MVP meta-analysis (Vujkovic et al; 2020) African ancestry. Track 5: MVP meta-analysis (Vujkovic et al; 2020) Asian ancestry. Track 6: MVP meta-analysis (Vujkovic et al; 2020) European ancestry. Track 7: genes located at this locus. Y axis represents the –log10(p-value) of association. (unadjusted p-value). The solid line refers to genome-wide significance threshold of P = 5e-8, and the dashed line denotes to suggestive significance threshold of p= 1e-5.

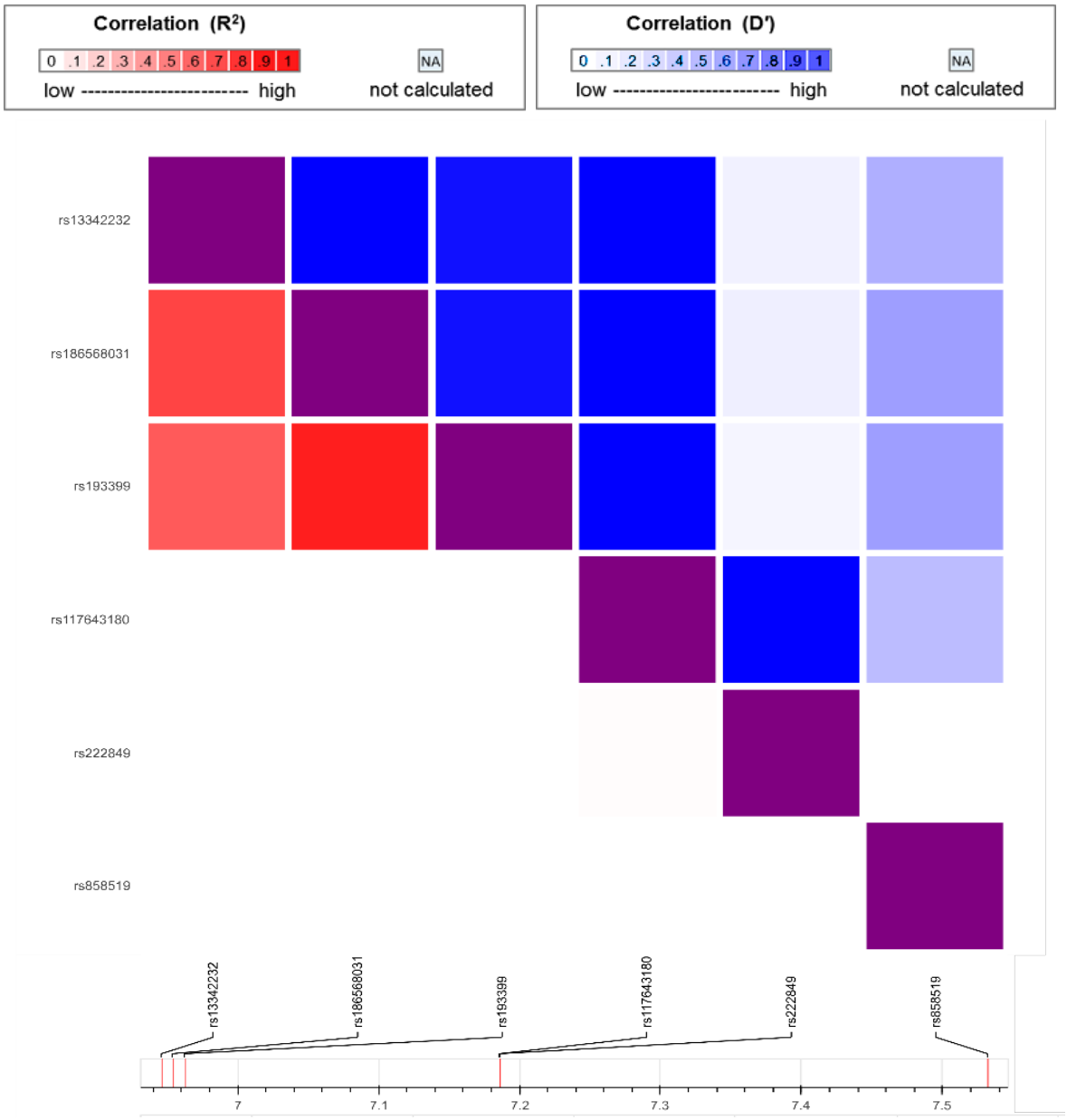

Supplementary Figure 16: LD matrix for lead SNPs in IFC, ISI and T2D GWAS at SLC2A4 locus in European ancestry

LD matrix generated for individuals of European ancestry using LDLink[21]. LD as denoted by R^2 is shown in red, and D' in blue. The colour scales are indicated at the top of the plot.

8. Genetic associations of IFC and ISI with other cardiometabolic traits

We further assessed the associations of increased genetic risk for post-challenge insulin resistance, represented by genetic risk scores (GRS; **see methods**) for ISI and IFC, with T2D related traits in unrelated European ancestry participants in UK Biobank (UKBB). We identified highly significant associations between both the ISI and IFC GRS with type 2 diabetes, with directions of associations consistent with post-challenge insulin resistance and increased risk of T2D (ISIadjBMI: beta = -0.28, SE = 0.020, P = 1.97×10^{-43}; IFCadjBMI: beta = 0.17, SE = 0.027, P = 1.40×10^{-10}). Directionally consistent effects were also seen for GRS for ISI and IFC with HbA1C, random glucose, WHR adjusted for BMI, which were all increased with increased genetic risk of post-challenge insulin resistance (**Supplementary Table 13**). We further assessed the associations between GRS for ISI and IFC and glycaemic traits not available in UKBB in a subset of the Fenland Study. In this much smaller study (N max = 8,925), the IFC and ISI GRS were still nominally (P < 0.5) associated with dynamic glycaemic traits and with associations being directionally consistent with post-challenge insulin resistance (**Supplementary Table 14**).

However, it should be noted that the Fenland Study is 1 of 28 studies that contributed to the GWAS meta-analyses from which these scores were constructed, reflecting 19% of the total sample size included in the discovery.

We used LD score regression analyses to assess genome-wide genetic correlations of ISI and IFC with a wider range of related biochemical and cardiometabolic traits. We identified strong genetic correlations of both ISI and IFC with 2h glucose, consistent with insulin resistance and the observational correlations in the Fenland Study (IFC and 2 h glucose: genetic correlation (rg) = 0.713, SE = 0.089, P = 2.63×10^{-22}; ISI and 2 h glucose: rg = -0.820, SE = 0.048, P = 2.12×10^{-22}; **Supplementary Tables 4, 15 and 16**). In contrast to ISI, which was strongly correlated with fasting insulin levels, IFC showed only a weak correlation, highlighting greater specificity as an indicator of post-challenge insulin resistance. Both ISI and IFC showed only moderate genetic correlations with T2D, consistent with the fact that multiple pathways contribute to its genetic architecture, with postprandial insulin resistance being only one of several aetiologies (**Supplementary Table 15 and 16**)

9. Colocalisation of post-challenge insulin resistance and eQTL for SLC2A4 in skeletal muscle at the SLC2A4 locus

The *SLC2A4* locus was the only locus where we did not see evidence of colocalisation of IFC/ISI with marginal statistics for the identified eQTL signal. This is due to two independent eQTL signals in skeletal muscle having been identified for *SLC2A4* at the *SLC2A4* locus (rs117643180)[22]. We ran conditional analyses using GCTA-cojo to generate conditional summary statistics conditioning on the primary (rs117643180) and secondary (rs222849) signals at this locus. Genetic of IFC/ISI and this eQTL signal were identified only when conditioning on the secondary signal (rs222849) showing that rs117643180 is the primary signal implicating both post-challenge insulin resistance and expression of SLC2A4 at this locus (**Supplementary Table 17**).

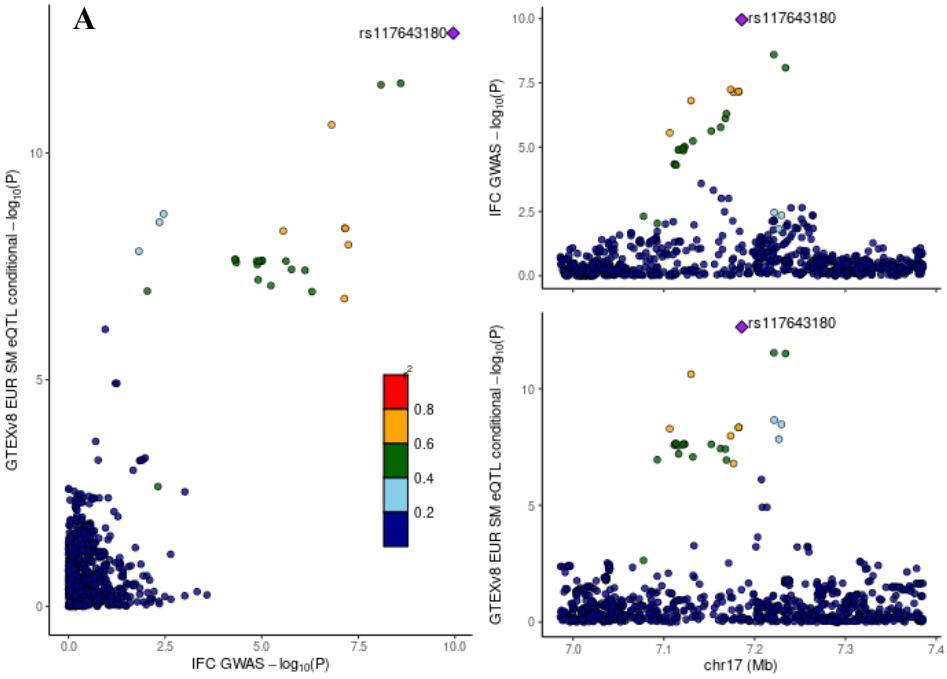

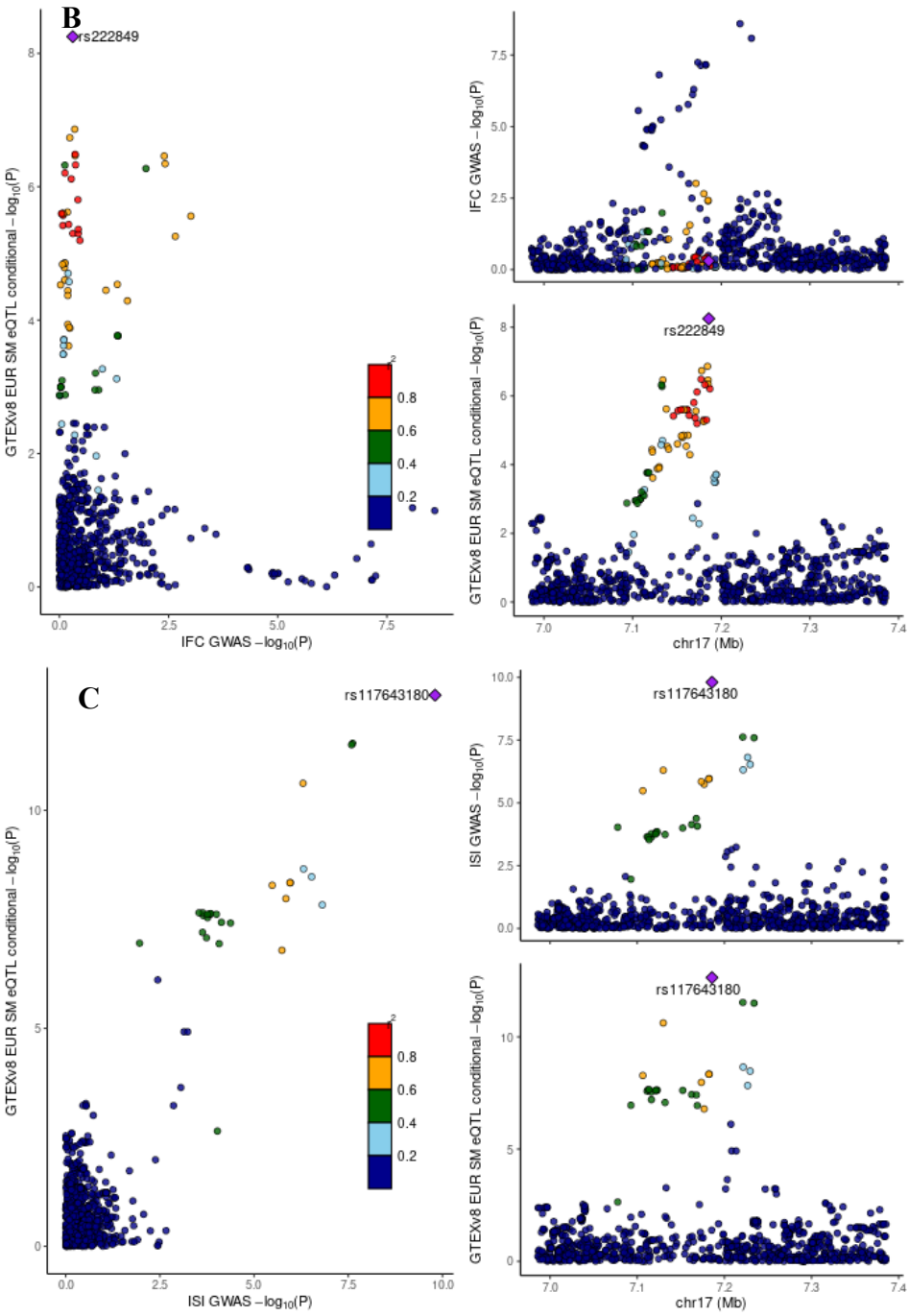
B
rs222849
GTEXv8 EUR SM eQTL conditional – log10(P)
IFC GWAS – log10(P)
IFC GWAS – log10(P)
rs222849
GTEXv8 EUR SM eQTL conditional – log10(P)
chr17 (Mb)
C
rs117643180
GTEXv8 EUR SM eQTL conditional – log10(P)
ISI GWAS – log10(P)
ISI GWAS – log10(P)
rs117643180
GTEXv8 EUR SM eQTL conditional – log10(P)
chr17 (Mb)

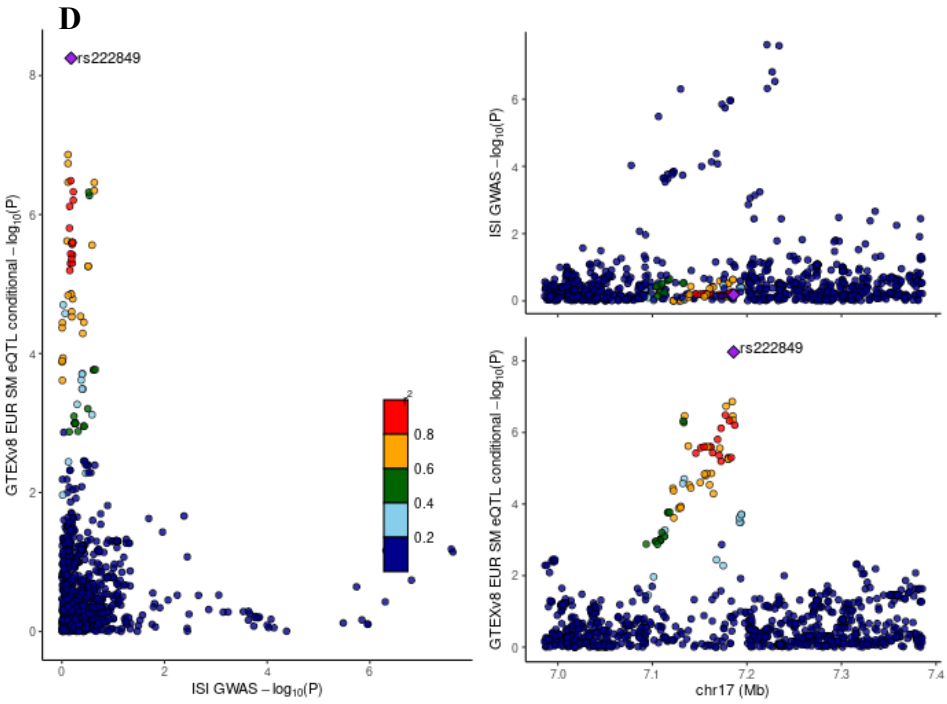

Supplementary Figure 17: statistical colocalisation of ISI/IFC with conditional summary statistics for eQTL in skeletal muscle at the SLC2A4 locus.

A) IFC and SLC2A4 eQTL statistics conditioned on the secondary signal rs222849. B) IFC and SLC2A4 eQTL statistics conditioned on the primary signal rs117643180. C) ISIand SLC2A4 eQTL statistics conditioned on the secondary signal rs222849. D) ISI and SLC2A4 eQTL statistics conditioned on the primary signal rs117643180. Locus was defined as ±200kb of rs117643180 for colocalisation analyses. The colour of points, as indicated in the legend, represent R^2 values compared to the lead SNP (1000 genomes European LD reference) for each signal annotated with a purple diamond. Unadjusted -log10 p-values are displayed.

10. rs117643180 (*SLC2A4*) affects expression of GLUT4 in skeletal muscle through changes in transcriptional regulation

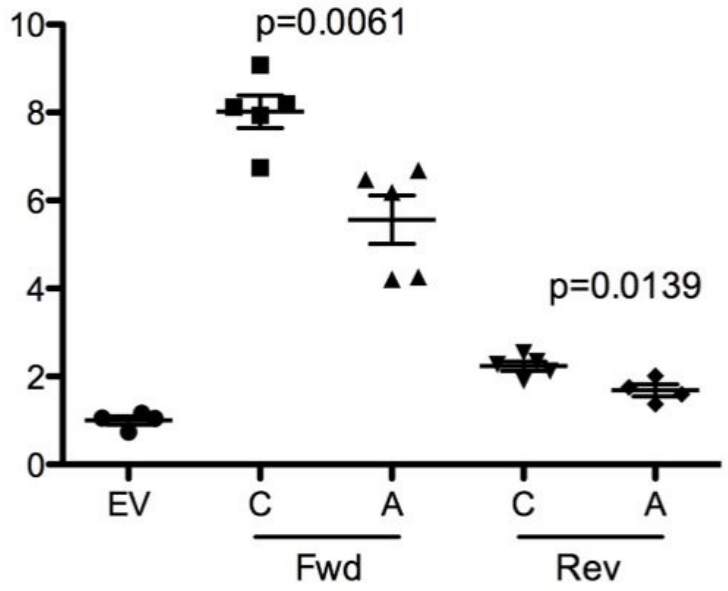

Supplementary Figure 18: rs117643180 exhibits allelic differences in transcriptional activity.
229-bp fragments flanking rs117643180-C or rs117643180-A were cloned upstream of a minimal promoter driving luciferase expression in the forward and reverse orientations with respect to the promoter. Values represent fold-change of firefly luciferase/*Renilla* activity normalized to empty pGL4.23 vector in undifferentiated LHCN-M2 myoblasts. Error bars represent the SEM of four or five independent clones tested in duplicate wells, individual points represent independent clones. P-values are calculated from two-sided t-tests.

11. Tissue of Action at post-challenge insulin reflects loci reflect tissues implicated in post-prandial insulin action.

To delineate potential tissue of action for post-challenge loci we employed LDSC-SEG to identify if the heritability of IFC or Modified Stumvoll ISI is enriched in regions surrounding genes with the highest specific tissue or cell type expression.

Modified Stumvoll ISI showed nominal genome-wide enrichment of active chromatin state in adipose, liver, skeletal muscle and pancreatic tissues, as well as nominal enrichment in tissue-specific gene expression in liver, muscle tissues and other T2D unspecific tissues (**Supplementary Tables 24 and 25**). Insulin fold change showed nominal enrichment in active chromatin marks in the liver, pancreas, and other tissues, as well as nominal enrichment in liver-specific gene expression. However, none of these annotations survives multiple testing corrections (**Supplementary Tables 22 and 23**).

12. Integration of additional phenotypic layers identifies additional loci implicated in post-challenge insulin action

Previous research has shown the utility of integrating information on associations with related traits when prioritising genetic loci associated with insulin resistance.[23] Here, we employed this approach to ISI and IFC with the aim to identify biologically relevant loci, with a post-challenge specific insulin resistance association pattern, which do not yet reach genome wide significance. This approach allowed us to identify additional loci of interest without sufficient sample size to detect these at a stringent genome wide significance threshold. To do this we prioritised variants that were suggestively associated with IFC and/or ISI ($P < 5x10^{-5}$). We next further filtered these variants based on their association with 2 h plasma glucose levels[7] ($P < 5x10^{-4}$) to prioritise those variants with additional evidence of being associated with post-challenge insulin resistance state. We additionally employed a second strategy where we filtered the variants suggestively associated with ISI and/or IFC based on their lack ($P < 0.05$) of association with fasting insulin, to remove those likely associated with insulin resistance in the fasting state, implicating the liver. These variants were further filtered based on evidence of being eQTLs in skeletal muscle ($P < 5x10^{-4}$).[24] This allowed us to prioritise those variants with evidence of regulating expression in skeletal muscle, a tissue of high biological relevance to postprandial insulin action. Loci which met both prioritisation criteria were considered to have a post-challenge insulin resistance specific association signature, with further evidence of regulatory effects in skeletal muscle, the key tissue in post-prandial glucose uptake.

Through this strategy we prioritised 10 loci, including 6 loci that were not identified at genome wide significance for either IFC and ISI; **Supplementary Table 19**).

The *ERAP2* locus (rs1216570) was associated with higher IFC and 2 h glucose[7], and lower ISI, suggestive of post-challenge insulin resistance (**Supplementary Figure 19a-b**. rs1216570 is an eQTL associated with higher *ERAP2* expression in skeletal muscle (GTEX v8 EUR: NES = 1.01, SE= 0.029, $P = 4.15x10^{-138}$). This eQTL in both muscle and adipose tissues, as well as 2hr glucose association has also been identified in other populations including in a cohort of African American ancestry[25], as well as a cohort from Sweden.[26] A muscle *ERAP2* eQTL at this

locus has additionally identified in the Pima Indian population.[27] However, we identified limited evidence of a shared genetic signal for this eQTL signal (GTEX v8 EUR) and IFC (posterior probability of colocalisation = 0.32).

The lead variant at this locus, rs1216570, is additionally an eQTL in skeletal muscle for *LNPEP (*GTEx v8 EUR: NES = -0.13, SE = 0.026, P = 3.92×10^{-7})[22] and there is strong evidence of colocalisation of this eQTL and IFC signal (posterior probability colocalisation = 0.85). *LNPEP* encodes IRAP, an insulin responsive amino peptidase that collocates with GLUT4 on GLUT4 secretory vesicles, and is well established to be involved in GLUT4 trafficking.[28] This demonstrates that this integrated approach identifies loci that are biologically relevant to post-challenge insulin resistance.

SHMT1 (rs7212808) was associated with a favourable glycaemic signature (**Supplementary Figure 19c-d**) and is additionally an eQTL for increased *LLGL1* expression in skeletal muscle (GTEx v8 EUR: NES = 0.15, SE = 0.028, P = 1.00×10^{-7} ; posterior probability of colocalisation IFC and LLGL1 eQTL = 0.91[22]). LLGL1 is a Rab GTPase activating protein that interacts with Rab10, a key player in insulin-stimulated GLUT4 translocation.[29] Although LLGL1 has not previously been implicated in post-challenge insulin response, it is plausible that this may play a role in regulating glucose uptake in the postprandial state.

All phenotypic signatures were additionally assessed using formal statistical colocalisation method hyprcoloc[30] (**Supplementary Figure 20**). We additionally tested for pairwise colocalisation of IFC and ISI signals with eQTLs in diabetes relevant tissues using coloc[31] (skeletal muscle, adipose, liver, and pancreatic islet; **see methods; Supplementary Table 20**). Further insight into tissue specificity of the genetic architecture of ISI and IFC was gained using LDSC-SEG, which leverages cell and tissue specific gene expression profiles to assess tissue specific enrichment of trait heritability (**see above; Supplementary Tables 21 to 25**).

By going below, the stringent genome wide significance level we identified evidence of loci directly implicating the biology of GLUT4 translocation in post-challenge insulin resistance comes from our findings at the *ERAP2* locus (rs1216570), suggestively associated (P = $1.01 \times 10^{-}$

^{5}) with increased IFC and reduced ISI (P = 2.4x10^{-4}), and suggestively associated with 2 h glucose (P = 2.64x10^{-5}) but not fasting glycaemic measures. We identified evidence of a shared genetic signal for IFC and eQTL in skeletal muscle for *LNPEP* which encodes IRAP, the insulin responsive amino peptidase. IRAP is found on GLUT4 secretory vesicles and binds TBC1D4, to prevent translocation of GLUT4 to the plasma membrane in the fasting state (low insulin).[32] In line with previous reports that IRAP is a negative regulator of plasma membrane GLUT4[28], depletion of *LNPEP* in 3T3-L1 adipocytes increased GLUT4 translocation to the cell surface. The lead variant at this locus is further in perfect LD (R^2=1) in Europeans with a previously reported missense variant significantly associated with 2hr glucose (rs2549782)[33]. However, colocalisation of our lead variant rs1216570 with an *LNPEP* skeletal muscle eQTL, no evidence of an impact of *ERAP2* knockdown on GLUT4 trafficking in vitro, and in silico algorithms including SIFT[34], PolyPhen2[35] and CADD[36] predicting the missense variant to be benign and to be unlikely to have an impact on the function of the encoding protein, suggest that *LNPEP* rather than *ERAP2* may be the causal gene at this locus.

We further assessed potential tissue of action at individual associated loci by assessing colocalization of loci identified to be associated with IFC and Modified Stumvoll ISI in either the genetic discovery or integrated analyses with eQTLs in T2D relevant tissues – adipose, liver, pancreatic islets and skeletal muscle. We identified colocalization (posterior probability of colocalization > 0.7) at 3 loci associated with IFC at ERAP1/ERAP2, SHMT1 and IRS1 with eQTLs identified in skeletal muscle and subcutaneous and visceral adipose tissues, key tissues in the post-prandial insulin response (**Supplementary Table 20**).

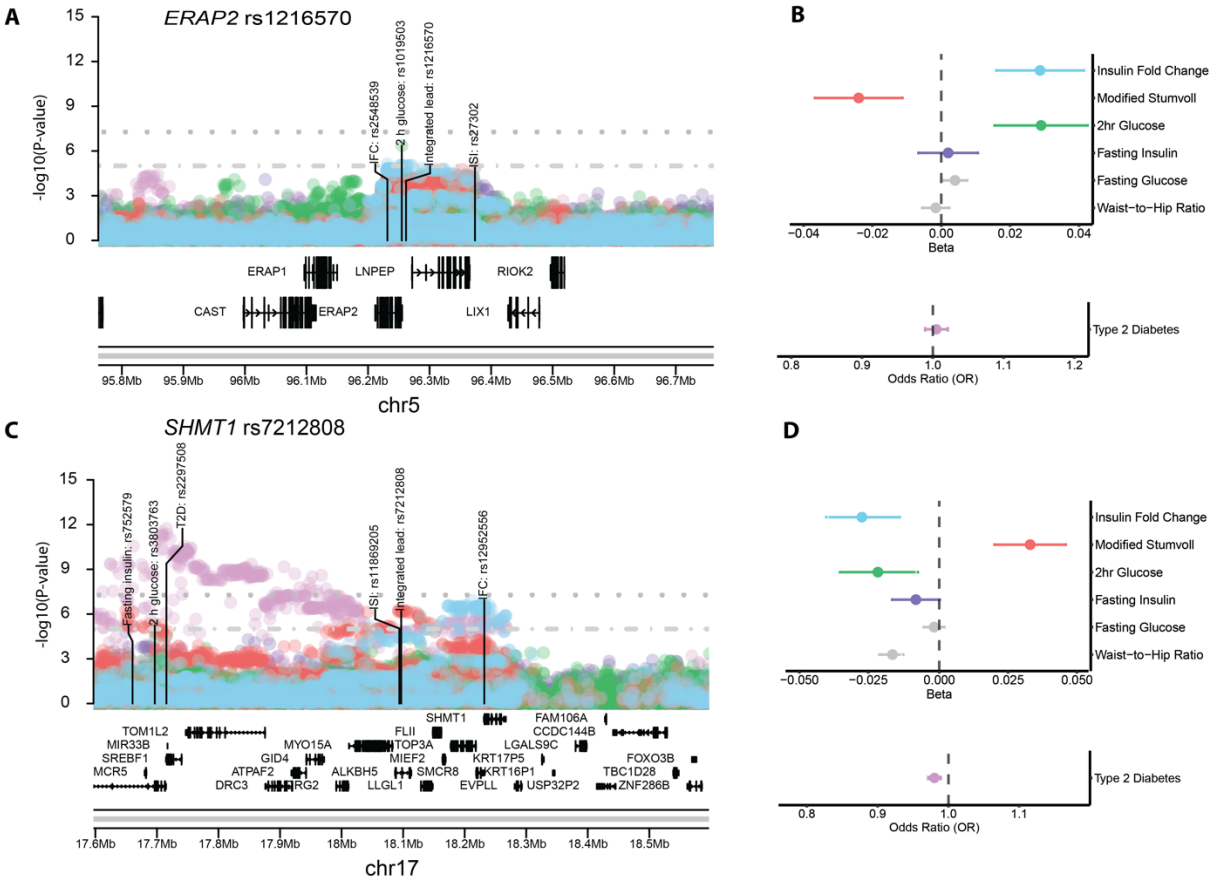

Supplementary Figure 19: Integrated GWAS approach highlights additional loci including those implicating glucose transport.

A) *ERAP2* locus: regional association plot for relevant traits. B) *ERAP2* locus: association of rs1216570 with relevant traits. **C)** *SHMT1* locus: regional association plot for relevant traits, with colours of points indicating traits of interest. **D**) *SHMT1* locus: association of rs7212808 with relevant traits. **A and C)** Regional association plot showing ± 500kb around the lead IFC-associated variant, with points indicating the association and location of individual variants. Colours of points indicating traits of interest: insulin fold change (IFC) - blue, Modified Stumvoll (ISI) – red, and 2 h glucose[7] – green, fasting insulin[7] – purple, type 2 diabetes[8] – pink . Y-axis denotes the unadjusted $-\log_{10}$(p-value) of association. The dashed lines and dotted line indicate genome-wide ($P = 5\times10^{-8}$) and suggestive ($P = 1\times10^{-5}$) significance threshold, respectively. X-axis denotes the genomic position. All association statistics are from BMI adjusted analyses in studies of European ancestry, except T2D which is unadjusted for BMI**.** The dashed lines indicate suggestive ($P = 1\times10^{-5}$) significance threshold and dotted line indicates genome-wide significance ($P = 5\times10^{-8}$), respectively. Labels indicate the lead variant for each trait, with location indicating position. Integrated lead is the lead variant defined for this locus using the integrated GWAS approach. **B and D)** Plot shows beta estimate or odds ratio of association for lead variant with insulin fold change (IFC) - blue, Modified Stumvoll (ISI) – red, and 2 h glucose[7] – green, fasting insulin[7] – purple, type 2 diabetes[8] – pink, all included in a) as well as fasting glucose[7] and waist-to-hip ratio[9] plotted in grey. All association statistics

are from BMI adjusted analyses in studies of European ancestry. Error bars indicate 95% CI of the effect size. Sample size is outlined in **Methods**.

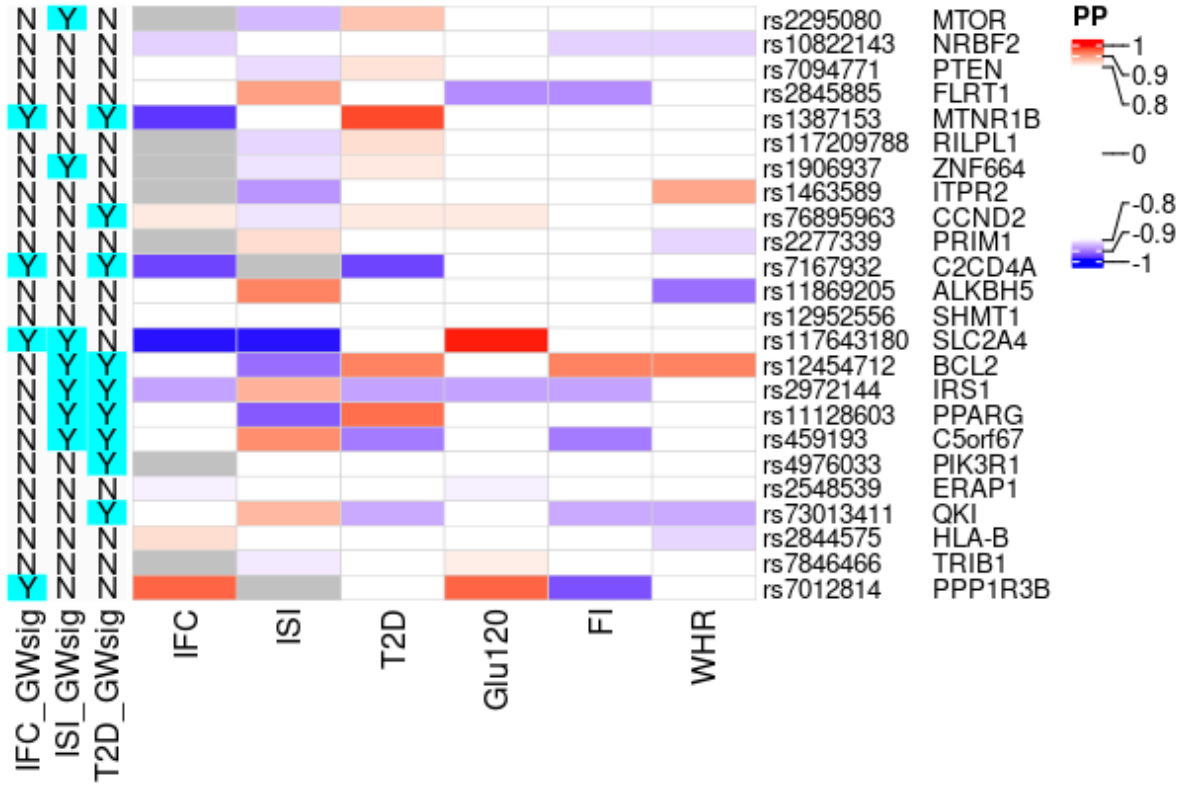

Supplementary Figure 20: Assessment of colocalisation at loci associated with IFC or ISI with related traits

Fasting insulin (FI), 2hr glucose (Glu120) type 2 diabetes (T2D) and waist-to-hip ratio (WHR). All summary statistics used as input are from European ancestry individuals and adjusted for BMI, except for T2D which is unadjusted for BMI (Methods). GWsig denotes whether the IFC/ISI lead SNP at a locus (indicated by the rsid) meets genome-wide significance for the indicated trait (unadjusted P < 5e-8). White denotes posterior probability < 0.8, with no evidence of colocalisation. Red positive beta for the indicated trait, the blue negative beta for the trait. Shade denotes the posterior probability of colocalisation between 0.8 and 1. Grey denotes that the trait was not included in hyprcoloc due to the locus (lead SNP +/- 500kb) not meeting the inclusion threshold of P < 5e-4 for that trait. All effects are aligned to the IFC effect allele.

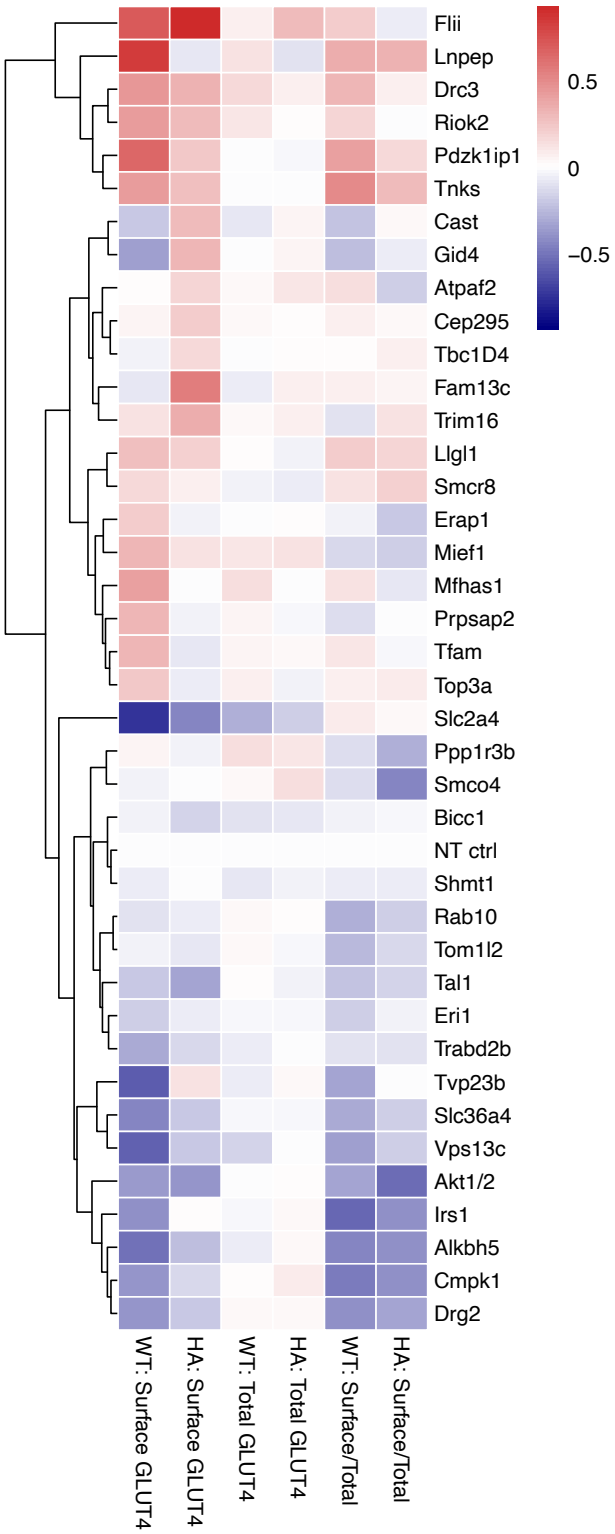

Supplementary Figure 21: GLUT4 screen results for 3T3L1 WT and 3T3L1 HA-GLUT4-mRuby 3T3-L1 adipocytes for all targets

All values are normalised to non-targeting control (NT) for the relevant measure/cell line combination. Targets with values lower than NT control are shown in blue and those with higher values in red. Clustering of targets was done using hierarchical clustering. Values are those measured at 0.5nM insulin. WT N = 3 biological replicates, with 2 technical replicates per N. HA – N = 5 biological replicates, with 2 technical replicates per N.

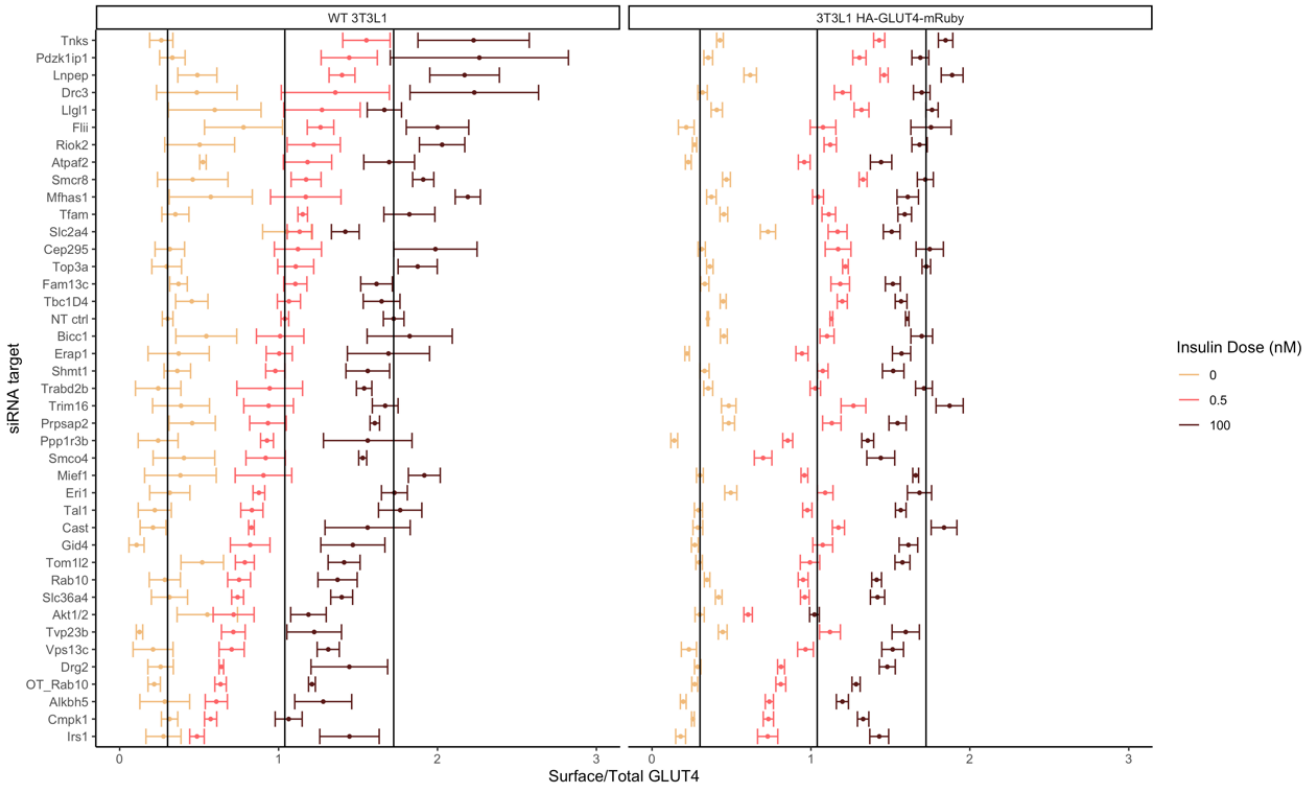

Supplementary Figure 22: Overall screen surface/total GLUT4 comparison for HA-GLUT4-mRuby and WT 3T3-L1 adipocytes.

Lines denote NT ctrl response at each dose line for WT 3T3L1 adipocytes. WT N = 3 biological replicates, with 2 technical replicates per N. HA-GLUT4-mRuby – N = 5 biological replicates, with 2 technical replicates per N. Insulin dose is indicated by colours in legend in nM. Error bar represents mean +/- SE.

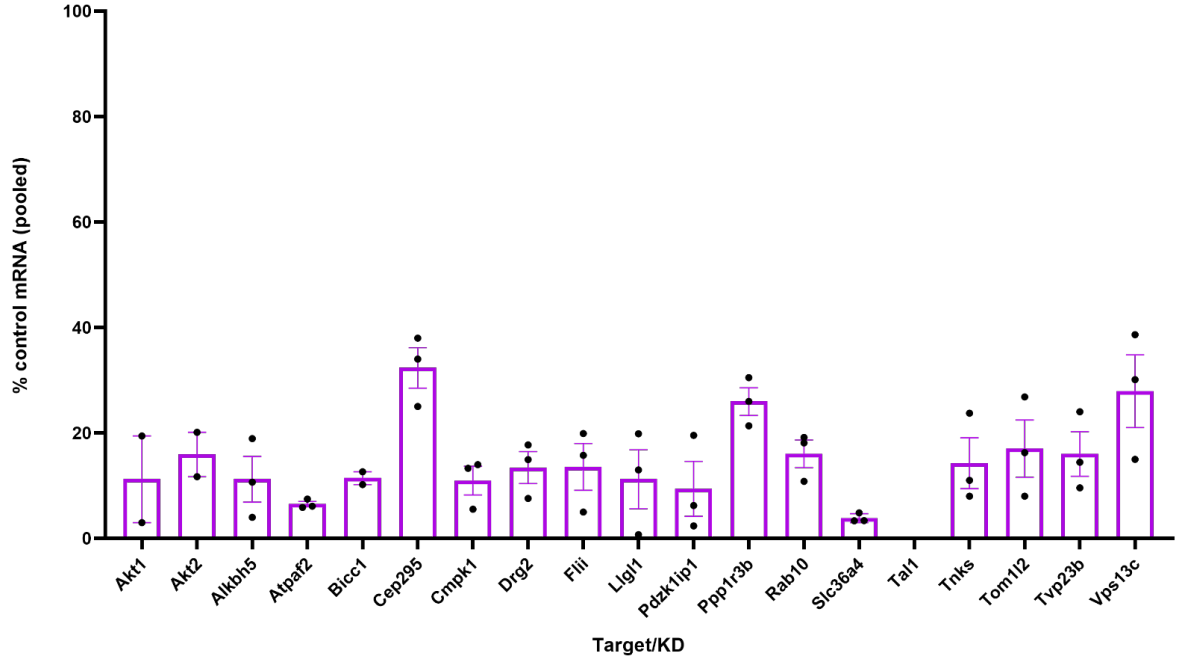

Supplementary Figure 23: Average percentage of mRNA detected in knockdown samples compared to NT control.

N = 2-3 independent biological replicates per gene, points represent independent samples. Error bar represents +/- standard error of mean.

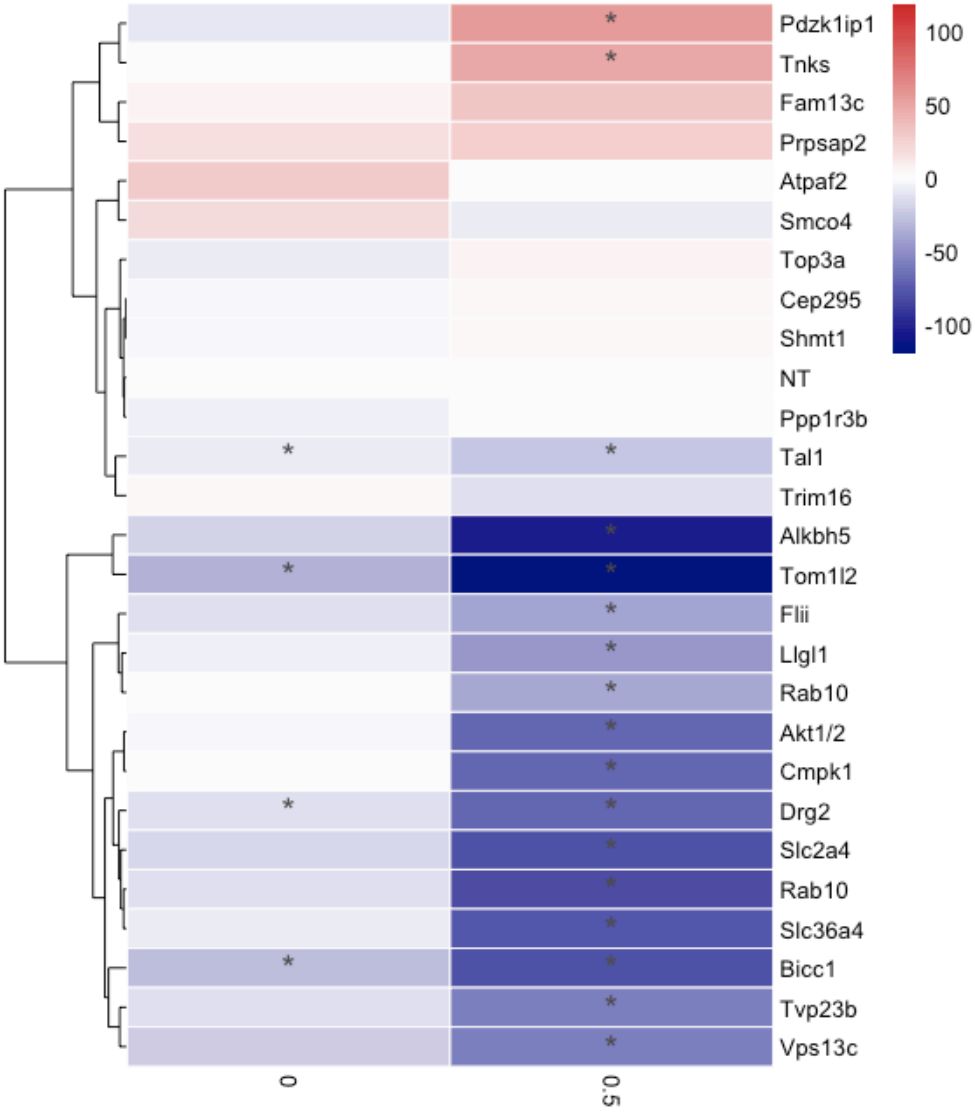

Supplementary Figure 24: Glucose Transport relative to NT control

Values are normalised glucose response to non-targeting control (NT; 0) per dose of insulin (nM), and scaled to the absolute maximal response expressed as percentage . * Indicates targets that are significantly different from the NT control at each dose (unadjusted P < 0.05; two-tailed t-test). N = 3 biological replicates per condition, except NT N = 6; Akt1/2 N = 6, Rab10 N = 6, Tvp23b N = 4. All replicates were successful.

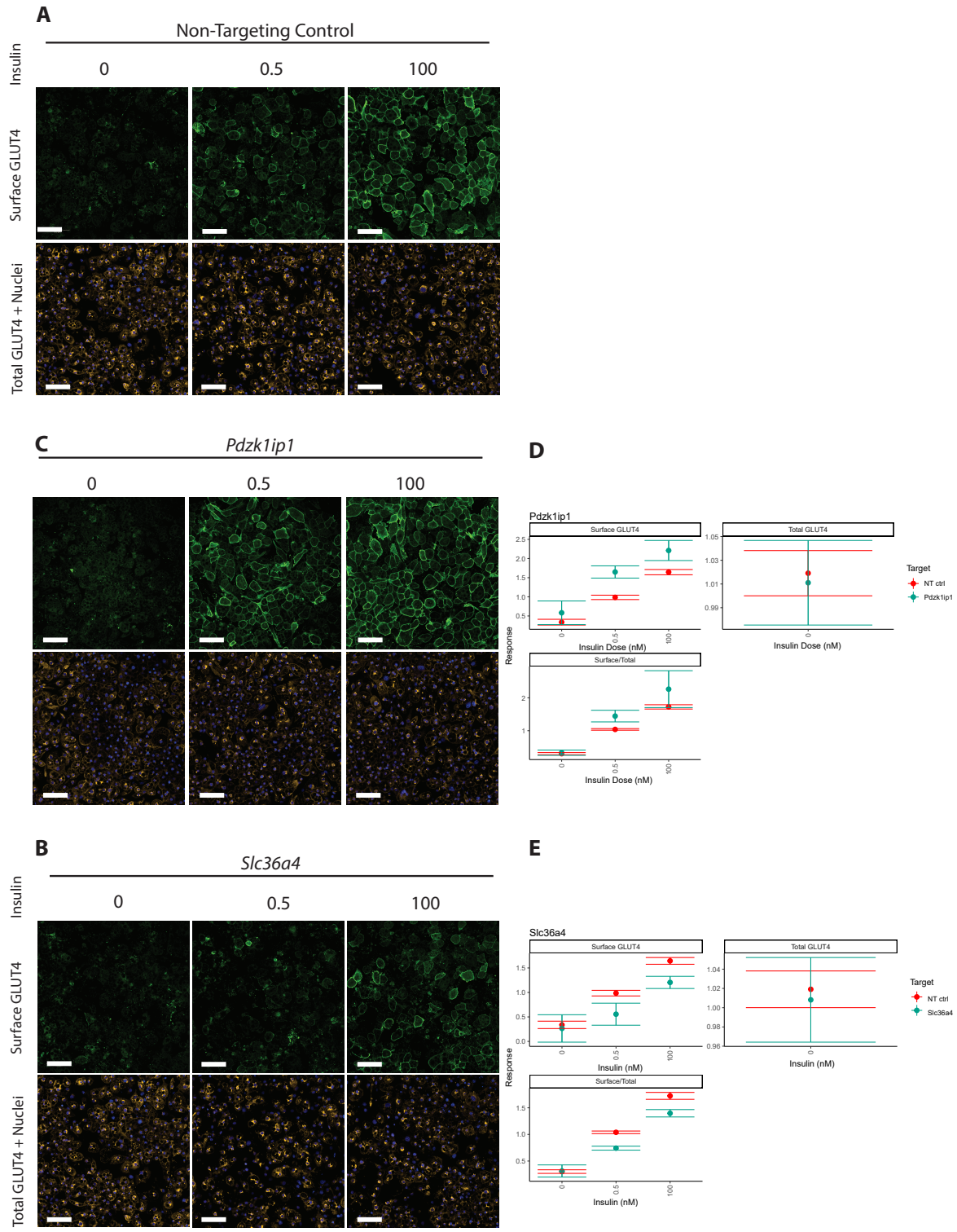

Supplementary Figure 25: Visualisation and quantification of impact on parameters of interest of knockdown Slc36a4 and Pdzk1ip1 in 3T3-L1 adipocytes.

A) Representative microscopy images of non-targeting control (NT ctrl) at 0,0.5 and 100nM insulin stimulation. Surface GLUT4 in green, total GLUT4 in orange, and nuclei in blue. The scale bar on each image represents 100μm. B) Representative microscopy images of Pdzk1ip1 knockdown. As outlined in a). C) Representative microscopy images of Slc36a4 knockdown. As outlined in a). D and E) quantification of the effect of knockdown on parameters of interest, normalised to background control. Response is relative to NT at a given insulin concentration, as indicated on X axis. Green – target, red- NT control. Error bars represent mean +/- SE.

References for Supplementary Note:

1. Bycroft, C. *et al.* The UK Biobank resource with deep phenotyping and genomic data. *Nature* **562**, 203–209 (2018).
2. Lindsay, T. *et al.* Descriptive epidemiology of physical activity energy expenditure in UK adults (The Fenland study). *Int. J. Behav. Nutr. Phys. Act.* **16**, (2019).
3. Pietzner, M. *et al.* Genetic architecture of host proteins involved in SARS-CoV-2 infection. *Nat. Commun. 2020 111* **11**, 1–14 (2020).
4. Powell, R. *et al.* Development and validation of total and regional body composition prediction equations from anthropometry and single frequency segmental bioelectrical impedance with DEXA. *medRxiv* 2020.12.16.20248330 (2020) doi:10.1101/2020.12.16.20248330.
5. Lam, B. Y. H. *et al.* MC3R links nutritional state to childhood growth and the timing of puberty. *Nat. 2021 5997885* **599**, 436–441 (2021).
6. Bulik-Sullivan, B. *et al.* LD Score regression distinguishes confounding from polygenicity in genome-wide association studies. *Nat. Genet. 2015 473* **47**, 291–295 (2015).
7. Chen, J. *et al.* The trans-ancestral genomic architecture of glycemic traits. *Nat. Genet. 2021 536* **53**, 840–860 (2021).
8. Vujkovic, M. *et al.* Discovery of 318 new risk loci for type 2 diabetes and related vascular outcomes among 1.4 million participants in a multi-ancestry meta-analysis. *Nat. Genet. 2020 527* **52**, 680–691 (2020).
9. Pulit, S. L. *et al.* Meta-analysis of genome-wide association studies for body fat distribution in 694 649 individuals of European ancestry. *Hum. Mol. Genet.* **28**, 166–174 (2019).
10. Finucane, H. K. *et al.* Heritability enrichment of specifically expressed genes identifies disease-relevant tissues and cell types. *Nat. Genet.* **50**, 621 (2018).
11. Roadmap Epigenomics Consortium *et al.* Integrative analysis of 111 reference human epigenomes. *Nature* **518**, 317–329 (2015).
12. Dunham, I. *et al.* An integrated encyclopedia of DNA elements in the human genome. *Nature* **489**, 57–74 (2012).
13. Diaz-Vegas, A. *et al.* A high-content endogenous GLUT4 trafficking assay reveals new aspects of adipocyte biology. *Life Sci. alliance* **6**, (2023).
14. Willer, C. J., Li, Y. & Abecasis, G. R. METAL: Fast and efficient meta-analysis of genomewide association scans. *Bioinformatics* **26**, 2190–2191 (2010).
15. Wang, Q. *et al.* Rare variant contribution to human disease in 281,104 UK Biobank exomes. *Nat. 2021 5977877* **597**, 527–532 (2021).
16. American Diabetes Association. 2. Classification and diagnosis of diabetes: Standards of medical care in diabetes-2021. *Diabetes Care* **44**, S15–S33 (2021).
17. Spracklen, C. N. *et al.* Identification of type 2 diabetes loci in 433,540 East Asianindividuals. *Nature* **582**, 240 (2020).
18. Williams, A. L. *et al.* Sequence variants in SLC16A11 are a common risk factor for type 2 diabetes in Mexico. *Nature* **506**, 97–101 (2014).
19. Karczewski, K. J. *et al.* The mutational constraint spectrum quantified from variation in 141,456 humans. *Nature* **581**, 434–443 (2020).
20. Auton, A. *et al.* A global reference for human genetic variation. *Nature* **526**, 68–74 (2015).
21. Machiela, M. J. & Chanock, S. J. LDlink: a web-based application for exploring

population-specific haplotype structure and linking correlated alleles of possible functional variants. *Bioinformatics* **31**, 3555–3557 (2015).
22. Aguet, F. *et al.* The GTEx Consortium atlas of genetic regulatory effects across human tissues. *Science (80-.).* **369**, 1318–1330 (2020).
23. Lotta, L. A. *et al.* Integrative genomic analysis implicates limited peripheral adipose storage capacity in the pathogenesis of human insulin resistance. *Nat Genet* **49**, 17–26 (2017).
24. Lonsdale, J. *et al.* The Genotype-Tissue Expression (GTEx) project. *Nature Genetics* vol. 45 580–585 (2013).
25. Sajuthi, S. P. *et al.* Mapping adipose and muscle tissue expression quantitative trait loci in African Americans to identify genes for type 2 diabetes and obesity. *Hum. Genet.* **135**, 869–880 (2016).
26. Keildson, S. *et al.* Expression of Phosphofructokinase in Skeletal Muscle Is Influenced by Genetic Variation and Associated With Insulin Sensitivity. *Diabetes* **63**, 1154–1165 (2014).
27. Mason, C. C. *et al.* Bimodal distribution of RNA expression levels in human skeletal muscle tissue. *BMC Genomics* **12**, (2011).
28. Jordens, I., Molle, D., Xiong, W., Keller, S. R. & McGraw, T. E. Insulin-regulated aminopeptidase is a key regulator of GLUT4 trafficking by controlling the sorting of GLUT4 from endosomes to specialized insulin-regulated vesicles. *Mol. Biol. Cell* **21**, 2034–2044 (2010).
29. Sano, H. *et al.* Rab10, a target of the AS160 Rab GAP, is required for insulin-stimulated translocation of GLUT4 to the adipocyte plasma membrane. *Cell Metab.* **5**, 293–303 (2007).
30. Foley, C. N. *et al.* A fast and efficient colocalization algorithm for identifying shared genetic risk factors across multiple traits. *Nat. Commun. 2021 121* **12**, 1–18 (2021).
31. Giambartolomei, C. *et al.* Bayesian Test for Colocalisation between Pairs of Genetic Association Studies Using Summary Statistics. *PLOS Genet.* **10**, e1004383 (2014).
32. Rubio-Sastre, P., Scheer, F. A. J. L., Gómez-Abellán, P., Madrid, J. A. & Garaulet, M. Acute melatonin administration in humans impairs glucose tolerance in both the morning and evening. *Sleep* **37**, 1715-1719B (2014).
33. Ng, N. H. J. *et al.* Tissue-Specific Alteration of Metabolic Pathways Influences Glycemic Regulation. *bioRxiv* **29**, 790618 (2019).
34. Sim, N.-L. *et al.* SIFT web server: predicting effects of amino acid substitutions on proteins. *Nucleic Acids Res.* **40**, W452–W457 (2012).
35. Adzhubei, I. A. *et al.* A method and server for predicting damaging missense mutations. *Nat. Methods* **7**, 248–249 (2010).
36. Rentzsch, P., Witten, D., Cooper, G. M., Shendure, J. & Kircher, M. CADD: predicting the deleteriousness of variants throughout the human genome. *Nucleic Acids Res.* **47**, D886–D894 (2019).